A CONCEPTUAL MODEL OF SHALLOW GROUNDWATER FLOW WITHIN THE LOWER EAST RIFT ZONE OF KILAUEA VOLCANO, HAWAII

A THESIS SUBMITTED TO THE GRADUATE DIVISION OF THE UNIVERSITY OF HAWAII IN PARTIAL FULFILLMENT OF THE REQUIREMENTS FOR THE DEGREE OF

MASTER OF SCIENCE

IN

GEOLOGY AND GEOPHYSICS

MAY 1995

By

Elizabeth A. Novak

Thesis Committee:
Donald M. Thomas, Chairperson
Frank Peterson
Aly El-Kadi

We certify that we have read this thesis and that, in our opinion, it is satisfactory in scope and quality as a thesis for the degree of Master of Science in Geology and Geophysics.

THESIS COMMITTEE

Chairperson

ACKNOWLEDGMENTS

First of all, I would like to thank Gary Delanoy for allowing me to use his water chemistry analyses data, without which this thesis could not have been written. I would like to thank the personnel of Puna Geothermal Venture, especially Greg Davidson, for their generous assistance with manpower, equipment, and data. I would like to thank Robert Kochy for his field support services and for imparting to me the benefit of his years of wellfield management experience. I would like to thank Joaquim Born for supplying the hourly precipitation data. I would like to thank Steve Gingerich for supplying the hourly recorded tide data and providing ideas for manipulating my hourly hydrological data. Most of all, I would like to thank Donald Thomas for his material support and enduring patience.

TABLE OF CONTENTS

LIST OF TABLES

LIST OF FIGURES

CHAPTER I.

INTRODUCTION

The discovery, development, and production of geothermal energy within the lower east rift zone (LERZ) of Kilauea volcano has been the impetus for development of models of shallow groundwater flow within the LERZ. During the last twenty years several models have been proposed. Each has drawn upon the preceding model, and has refined and improved upon it as new data became available.

The purpose of this thesis research is to again refine the conceptual model of LERZ shallow groundwater flow using data from newly drilled wells and a data set acquired through continuous well monitoring, an approach which has not previously been used in the LERZ.

The objectives of this research are twofold; first, the conceptual model will characterize the shallow unconfined aquifer present within the LERZ and lower south flank (LSF) in its natural state of dynamic equilibrium. Second, with commercial geothermal production beginning in this area, the data contained in this thesis will be used as a baseline to asses the impact, if any, of production and reinjection of geothermal fluids on the shallow LERZ groundwater aquifer.

This research utilizes geochemical analyses from several recently drilled LERZ wells, as well as temperature, pressure, and conductivity data acquired through continuous monitoring of five wells on the lower north flank (LNF), LERZ, and the LSF of Kilauea. These data are used to characterize water level, temperature, and chlorinity responses to recharge events; develop transmissivity and hydraulic conductivity values for the LNF,

LERZ, and LSF; delineate groundwater flow paths within the LERZ; establish the percentage of geothermal fluid mixed with groundwater in various LERZ wells; estimate the temperature of the reservoir or reservoirs from which this geothermal fluid is derived; and identify the origin of their thermal fluids as either fresh or salt water.

CHAPTER II.

GEOLOGICAL AND HYDROLOGICAL SETTING

Geology

The island of Hawaii currently overlies the Hawaiian hot spot at the southeastern end of the Hawaiian Ridge (Clague and Dalrymple, 1987). It is composed of five Quaternary shield volcanoes; Kohala, Mauna Kea, Hualalai, Mauna Loa, and Kilauea (Figure 1).

Kohala volcano, at the northern tip of the island, was formed more than 700 ka ago (Macdonald and Abbott, 1970). It has been dormant the longest and its windward slope has been deeply incised by stream erosion. Post erosional cinder cones, which stud the upper part of the shield, were formed at about 60 ka (McDougall and Swanson, 1972).

Mauna Kea, whose summit is the highest point on the island (4206 m), adjoins Kohala to the southeast; it is believed to have formed over the last 500 ka (Macdonald and Abbott, 1970). The summit and upper flanks of Mauna Kea are covered by a thin alkalic cap and a number of small cinder cones which were active as recently as 3.6 ka (Porter, 1979).

Hualalai lies to the west of Mauna Kea and is less than 400 ka old (Macdonald and Abbott, 1970). Hualalai's surface is entirely covered by an alkalic cap, although tholeiites have been found offshore and in drill holes (Moore, et al., 1987). Seven eruptions have occurred on the NW rift in the last 2,100 years with the most recent occurring in 1800-1801 (Walker, 1990).

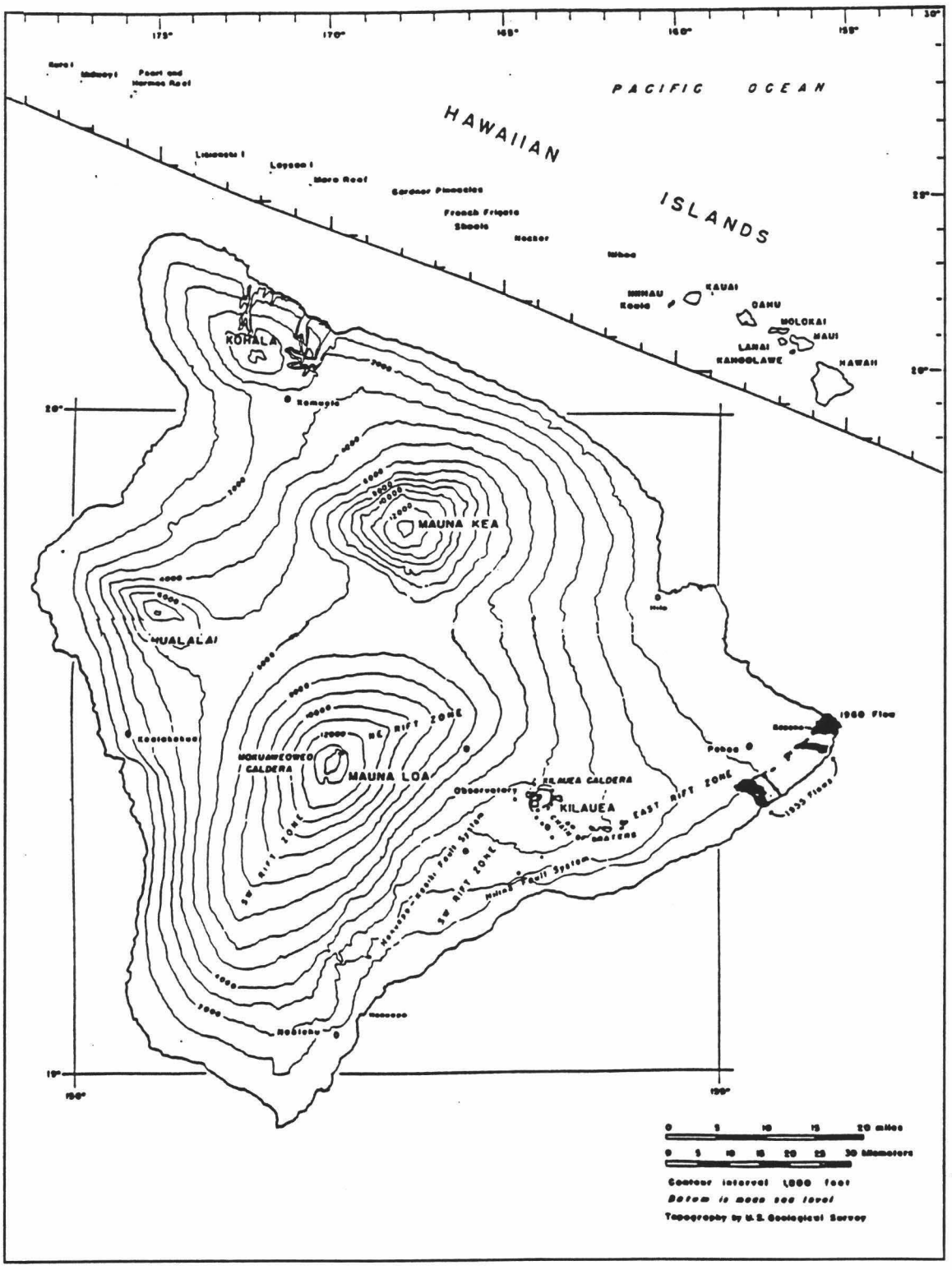

Figure 1. Hawaii location map after Eaton and Murata 1972.

Mauna Loa forms most of the southern half of the island of Hawaii. It has been constructed over a period of at least 100 ka (Macdonald and Abbott, 1970). This huge tholeiitic shield volcano is largely uneroded. It has a summit caldera and well defined northeast and southwest rift zones. Mauna Loa has erupted thirty two times since 1843 (Walker, 1990), and most recently in 1984.

Kilauea abuts Mauna Loa to the southeast, and is the youngest and most active of Hawaii's volcanoes. Over 90% of its surface is younger than 1.1 ka (Holcomb, 1987). Like Mauna Loa, it is an undissected tholeiitic shield with a summit caldera and well defined east and southwest rift zones. Kilauea has been in constant eruption on its upper east rift zone since 1983.

Kilauea's east rift zone (ERZ) initially trends southeast for 6 km from the summit caldera then turns east and extends another 45 km to Cape Kumukahi where it enters the sea and continues another 70 km as a submarine ridge (Moore and Reed, 1963). The ERZ has historically been Kilauea's most active rift. Its surface expression is characterized by pit craters and small lava shields on the upper and middle east rift zone (UERZ and MERZ), and cinder cones and occasional tuff cones on the middle and lower east rift zone (LERZ). Large fissures and grabens are common along the entire length of the east rift, and subsurface thermal activity is evidenced by numerous steam and gas vents which discharge at atmospheric pressure.

The present study has focused on the Kilauea LERZ from the area around Puu Honuaula to Cape Kumukahi and the north and south flanks of Kilauea which are adjacent to this part of the LERZ. This area is located within the district of Puna (Figure 2).

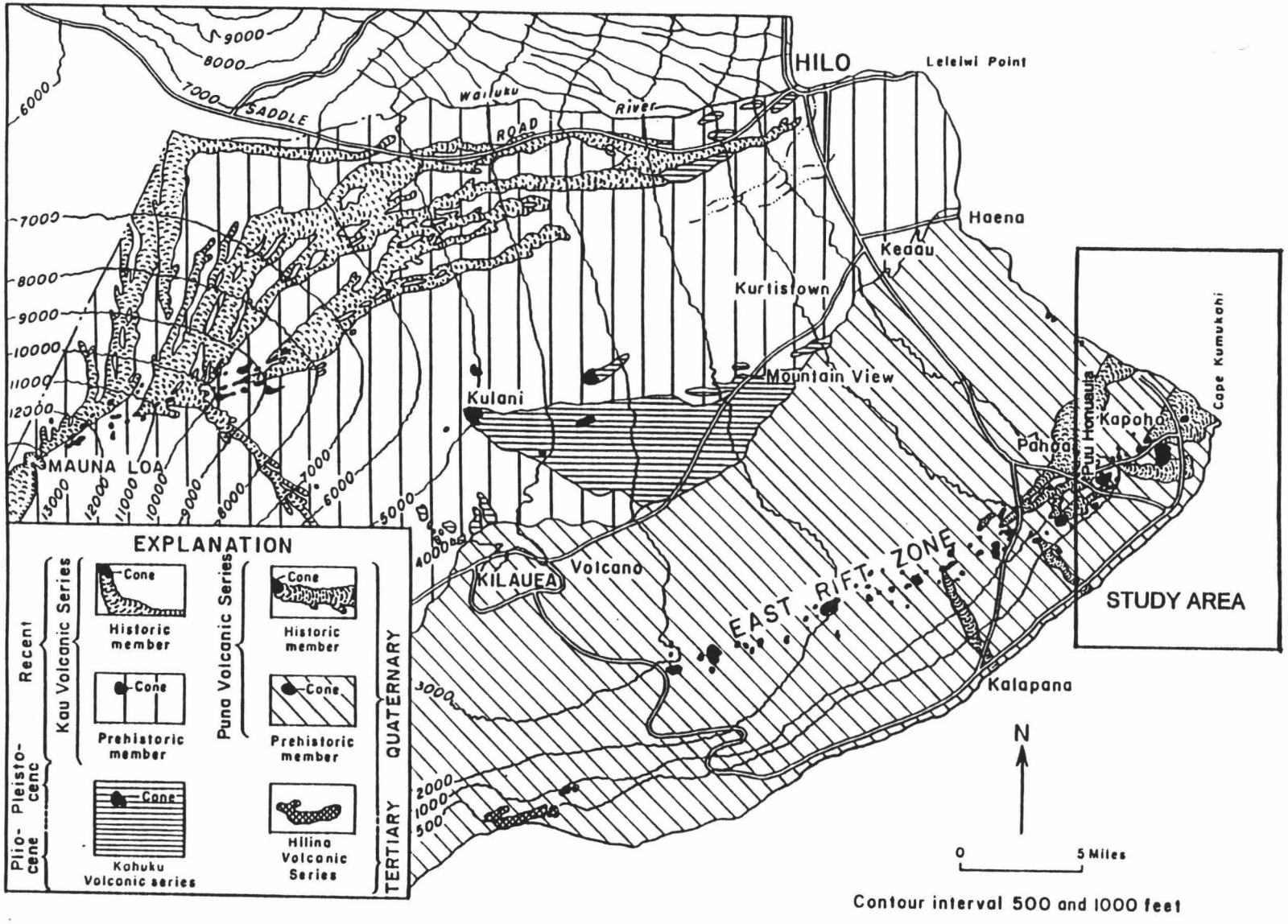

Figure 2. Lower Puna study area map from Macdonald et al (1983).

The region is covered by lavas of the Puna volcanic series which range in age from 1,500 ybp to 1960 (Holcomb, 1987). These consist of numerous thin aa and pahoehoe flows which are extremely permeable due to their high vesicularity, cooling joints, interflow joints, aa clinker layers, and lava tubes.

The dominant structural feature in the study area is the LERZ which forms a topographical high 4 to 6 km wide (Holcomb, 1987) studded by six major cinder cones and a large tuff ring near its eastern terminus at Cape Kumukahi. There are also numerous minor eruptive vents, fissures, and grabens aligned parallel to the strike of the rift. Southwest of Puu Honuaula a northwest trending strike-slip fault intersects the LERZ at approximately a right angle (Zablocki, 1977; Holcomb, 1987; Flanigan and Long, 1987; Iovenitti, 1990).

Eruptive vents formed within the study area during Kilauea's 1955 and 1960 eruptions. The 1955 vents south of Puu Honuaula and the 1960 vents in Kapoho were the sites of violent phreatic explosions when the eruption of lava from them had ceased (Macdonald and Abbot, 1970). Kapoho Crater, a large tuff ring near Cape Kumukahi, and Puu Lena, a large tuff crater southwest of Puu Honuaula, are evidence of large prehistoric phreatomagmatic eruptions.

Intrusive bodies are common throughout the subsurface of the ERZ, where they have broken the surface in eruption, they form the cinder cones and vents of the rift. However, a far greater percentage remain below the surface where they solidify as tabulate dikes with strikes generally parallel to the ERZ and dips which average 60^0 to 80^0 from horizontal (Novak et al, 1991). These bodies form the coherent dike complex which

is the subsurface expression of the ERZ. Gravity mapping indicates that the LERZ dike complex widens with depth to form a high density mass which extends 4 km south to 10 km north of the rift zone, with a depth of 2 km on its southern edge to almost 4 km on its northern boundary (Furumoto, 1978; Broyles, et al., 1979). Evidence from deep drill holes also indicates that the entire length of the core of the LERZ is hot at this depth, with temperatures of at least 350^0 C (Novak and Evans, 1991).

Since dikes solidify under high lithostatic pressure, they are almost always avesicular and do not develop the cooling joints found in surface lavas (Novak et al, 1991). Therefore, their permeability is much less than the highly vesicular, densely jointed lava flows that they intrude. This difference in morphology and the discordant orientation of dikes effectively allows them to partition the ERZ into compartments of highly permeable lava flows (Novak, et al, 1991) separated by relatively impermeable dikes. Deposition of secondary minerals and alteration of basalts to clay minerals by hydrothermal fluids also contribute to a reduction in permeability within the LERZ by sealing fractures and voids. The retrograde solubility of anhydrite and gypsum, the high concentrations of calcium and sulfate ions in seawater, and laboratory seawater-basalt reactions (Mottl and Holland, 1978; Mottl and Seyfried, 1980; Seyfried and Mottl, 1982) suggest these minerals would be precipitated from seawater heated within the rift zone. Anhydrite and gypsum are the most abundant secondary minerals found in Scientific Observation Hole cores (Novak et al, 1991), and are common in cuttings from other deep wells drilled on the LERZ (Thomas, 1987). Smectite clay is an ubiquitous alteration product in the high temperature seawater-basalt experiments performed by the workers

cited above, and has been noted in cores from the high temperature seawater-basalt Rekjanes geothermal field (Tomasson and Kristmannsdottir, 1972). Smectite is also the most common alteration mineral in Scientific Observation Hole cores (Novak, et al, 1991).

Data from a deep core hole, SOH#1, has shown that the subsurface structure of the LERZ in the study area near Puu Honuaula consists of numerous extrusive lava flows as well as intrusive dikes. Thin aa and pahoehoe flows interbed to a depth of approximately 750 m below sea level. Below them lies a 500 m thick transition zone of mixed hyaloclastites and pillow lavas which grade into a basement of deep submarine pillow lavas (Novak et al, 1991). The upper 750 m of the section is extremely permeable; but the change in morphology at the transition zone, increasing lithostatic load, and increasing secondary mineral precipitation and alteration from increasingly hot fluid circulation rapidly decrease permeability below the transition zone. Permeability below the transition zone is fracture dominated secondary permeability which has developed as the result of forceful injection of dikes into the rift zone and the seaward slippage of Kilauea's unbuttressed south flank (Walker, 1990).

LERZ permeability may increase from west to east along the rift. The slope of Mauna Loa buttresses Kilauea to the north, however, the slope of Mauna Loa and the pre-Kilauea sea floor may intersect beneath Puu Honuaula (Epp, et al., 1983). West of this intersection Kilauea can expand only to the south, while to the east, in the study area, the volcano can expand to both the north and south. This reduction in stress may result in higher permeabilities in the LERZ to the east of Puu Honuaula than to the west.

The permeability structure of Kilauea within the study area may also be inferred from sparse field data and numerical modeling results. The validity of permeability measurements is highly scale dependent because more diverse permeabilities, which result from near well geological structures (e. g. lava tubes, fissures, and dikes) must be averaged to obtain large scale regional permeabilities. Permeability measured from well test field data can confidently be applied to an area of approximately 100 m diameter around the well (Ingebritsen and Scholl, 1993). Regional permeability estimates developed from numerical modeling can be applied to much larger areas, but may vary considerably from individual well test permeability measurements. Druecker and Fan (1976) estimated average permeabilities of Puna lavas from well tests to range between 4,000 and 5,000 darcys (3.95×10^{-9} m^2 and 4.93×10^{-9} m^2). Using a numerical model, Imada (1984) simulated fluid flow and solute transport within the study area. Her best match of water table elevations was obtained by assigning permeability values of 5×10^{-9} m^2 to rocks outside of the LERZ, 1×10^{-9} m^2 to LERZ rocks within 10 km of Cape Kumukahi, and 1×10^{-11} m^2 to LERZ rocks more than 10 km from Cape Kumukahi. Since these two data sources are in close agreement for rocks outside the LERZ, 5×10^{-9} m^2 appears to be a valid estimate of horizontal permeability of dike free, unaltered Puna lavas. This model also appears to corroborate the west to east increase in shallow permeability in the LERZ.

Climate

Hawaiian climate is characterized by a two season year consisting of a relatively rainy seven month winter season lasting from October through April and a relatively dry summer season lasting from May through September (Ruffner, 1980). However, variations in monthly and annual rainfall can be very large. Climate in the LERZ and on the lower flanks of Kilauea is controlled by elevation and the direction of the tradewinds, which blow from the northeast most of the year.

Rainfall ranges from 381 cm per year at 200 m, on the crest of the LERZ, the highest windward point in the study area, to 127 cm per year at sea level on the leeward south flank (Druecker and Fan, 1976). Average yearly rainfall for the LERZ and north flank study area is 250 cm, and 150 cm for the south flank (Juvik, 1978). Groundwater recharge, computed by averaging mean annual precipitation over mean annual potential evapo-transpiration, generally follows the same pattern. The north flank and upper part of the LERZ receive a surplus greater than 100 cm, while the south flank and lower LERZ receive a 0 to 100 cm surplus (Juvik, 1978).

Hydrology

The youthful age of Kilauea volcano has directly affected its hydrology. Deep soils and valleys have not had time to develop and extremely porous lavas remain at or very near its surface. Consequently, there is no runoff from the high precipitation which falls on the volcano and Kilauea supports no perennial streams. Rainfall is returned to the atmosphere as evapo-transpiration or infiltrates to groundwater. Groundwater flow

generally follows surface topography, moving down gradient to eventually exit as coastal springs and diffuse seeps (Stearns and Macdonald, 1946). The average volume of ground water discharged from these basal springs between Hilo and Kalapana has been estimated to be approximately 215 billion liters per year (Stearns and Macdonald, 1946). Because of high permeabilities and extremely high recharge rates, groundwater residence times are short. A recent tritium dating study (Scholl et al, 1992) yields residence times for well and spring waters within the study area of 10 to 18 years or 15 to 20 years, depending on whether a well mixed or piston flow model is used.

Three types of groundwater are present within Kilauea. First, there is a minor component of water which is perched on less permeable material. In the study area, perched water occurs in the tuff underlying Kapoho Crater and in the Green Lake within the crater (Stearns and Macdonald, 1946). Other perched water bodies are present on ash layers which underlie areas on the higher slopes of Kilauea, but they are thin and of small areal extent (Swain, 1973).

Dike impounded water is present under the summit of Kilauea (Keller, et al., 1979; Kauahikaua, 1993) and within the ERZ where the relatively impermeable dikes dam water which infiltrates the permeable lavas. Wells drilled in the LERZ study area show large fluctuations in static water level over small areas (PGV, 1990; Deymonaz, 1991) but heads are generally higher than heads in wells located outside the rift zone at the same distance from the coast (Swain, 1973) (Figure 3).

The largest component of Kilauea's groundwater is basal groundwater which exists as a lens shaped fresh water body floating on the salt water that permeates the island

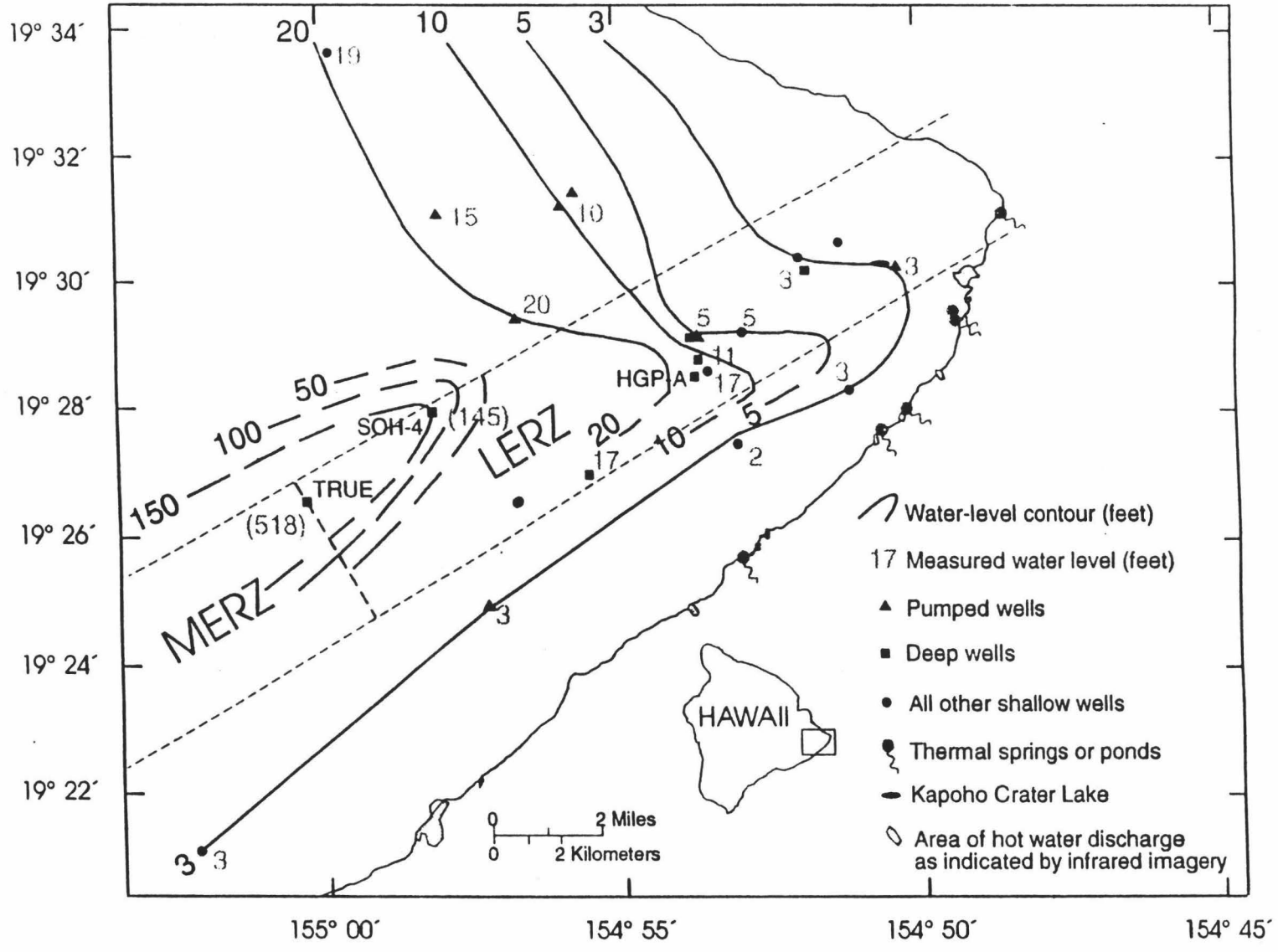

Figure 3. Water table contour map in feet above mean sea level from Sorey and Colvard (1993).

below sea level. Due to the density difference between fresh and salt water the following Ghyben-Herzberg relationship is established under equilibrium conditions:

$$z(x,y) = \frac{\text{density fresh}}{\text{density salt - density fresh}} h(x,y) \quad 1.$$

z(x,y) is the depth to the midpoint of the fresh-salt water transition zone below sea level at location (x,y)
h(x,y) is the elevation of the water table above sea level at point (x,y)
density fresh = 1.000 g/cc at 20^0 C
density salt = 1.025 g/cc at 20^0 C

This relationship predicts 1 m of fresh water head above sea level will depress the mid-point of the fresh-salt water transition zone 40 m below sea level.

Groundwater flux within Kilauea is controlled by the amount of rainfall received, hydraulic gradient, permeability of the country rock, and subsurface geological structures. Horizontal and vertical groundwater flow takes place in Hawaiian lavas through interconnected vesicles, cooling joints, interflow breccias, aa clinker layers, fissures, faults, and lava tubes. On the flanks of the volcano, outside the rift zones, horizontal flow is dominant due to the more or less horizontal emplacement of lava tubes and interflow breccias, however within the rift zones, fissures and faults increase the efficiency of vertical flow. Transmissivities on the order of 25,338 m^2 /day have been estimated for shallow Puna wells (Kroopnik, et al., 1978).

The north flank adjoining the ERZ receives a large groundwater flux traveling down gradient from the upper slopes of Kilauea. Farther from the ERZ and closer to the contact with Mauna Loa, the north flank receives an even larger flux from both Kilauea and Mauna Loa (Thomas, ms). Basal ground water underlies the north and south flanks

of Kilauea, but within the study area, the Ghyben-Herzberg lens is only well established on the north flank. Wells drilled at elevations of less than 300 m on the north flank have encountered a more than 100 m thick lens which thins as the coast is approached (Davis and Yamanaga, 1973; Swain, 1973; Takasaki, 1978).

Hydraulic gradients on the north flank of Kilauea range between 0.4 m and 0.8 m per km, with heads of 3.7 m to 5.5 m at 8.0 km to 9.7 km from the coast (Druecker and Fan, 1976) (Figure 3). The influence of colder water from the higher slopes of Mauna Loa and Kilauea can be seen in some well water temperatures on the north flank of Kilauea, which average 19^0 C to 20^0 C near Keaau. The thermal influence of the ERZ can be seen in well water temperatures near Pahoa, which average 22^0 C to 23^0 C.

The low permeability of the dike complex within the ERZ impedes the flow of groundwater from Kilauea's north flank into and through the rift (Druecker and Fan, 1976). Groundwater within the ERZ is derived predominantly from infiltration of precipitation which falls on the rift zone where large fissures efficiently channel meteoric recharge to depth. Groundwater temperatures in wells in the LERZ are well above ambient recharge temperature (Table 1), ranging from 36^0 C in Kapoho Airstrip well 5 km from Cape Kumukahi to 93^0 C in GTW-3 well just east of Puu Honuaula (Figure 4). GTW-3 shows a strong temperature reversal with depth which indicates it may be near, but down gradient from, a zone of upwelling geothermal fluid (Epp and Halunen, 1978) .

The Kilauea south flank derives its groundwater from direct infiltration and from overflow or throughflow from dike compartments in the ERZ (Druecker and Fan, 1976). Hydrothermal circulation along the southern edge of the LERZ has substantially degraded

TABLE 1. WELLS AND SPRINGS DISCUSSED IN THE TEXT

Well	Abbrev.	ID #	Lat	Lon	Depth to water m	Total Depth m	Elevation m	Temp C
Allison	Al	8-2881-01	19 28'19"	154 51'10"	37.8	42.7	40.3	37.5
GTW-3	G3	8-2982-01	19 29'13"	154 52'35"	169.9	210.4	171.7	84.8
Kapoho Airstrip	KA	8-3081-01	19 30'24"	154 51'59"	86.9	102.8	87.5	36
Kapoho Shaft	KS	8-3080-02	19 30'16"	154 50'21"	43.4	46	38	
KS-3	K3	8-2883-09	19 28'	154 53'	186.4*	2257	188.5	32.2 #
KS-4	K4		19 28'	154 53'	183.3*	2068	188.5	37.8 #
KS-7	K7		19 28'	154 53'		plugged	190.3	32.2 #
KS-8	K8	8-2883-11	19 28'	154 53'	189.0*	plugged	191.8	34.4 #
KS-9	K9	8-2883-13	19 28'	154 53'	185.7*	1271	186.9	32.2 #
KS-10	K10	8-2883-14	19 28'45"	154 53'37"		1550	186.9	32.2 #
Malama Ki	MK	8-2783-01	19 27'28"	154 53'01"	83.3	97.3	83.6	53
MW-1	M1	8-2983-01	19 29'08"	154 53'39"	183.6	219.6	186	34.7
MW-2	M2	8-2883-07	19 28'36"	154 53'30"	174.5	197	179.9	63
MW-3	M3	8-2983-02	19 29'10"	154 53'40"	181.2	219.6	186	41
Paradise Park	PP	8-3588-01	19 35'47"	154 58'34"	41.8	51.2	44.2	19.5
*measured during drilling								
# at water table during drilling								
Spring								
Campbell	Ca	2880-S1	19 27'55"	154 50'21"			1.5	32
Isaac Hale	IH	2780-S1	19 27'40"	154 50'45"			1.5	34
Kapoho Bay	KB	2979-S2	19 29'38"	154 49'30"			3	30.5
Pualaa	Pl	2780-S2	19 28'00"	154 50'17"			1	34.3

Geographical data from Janik, et al (1994).

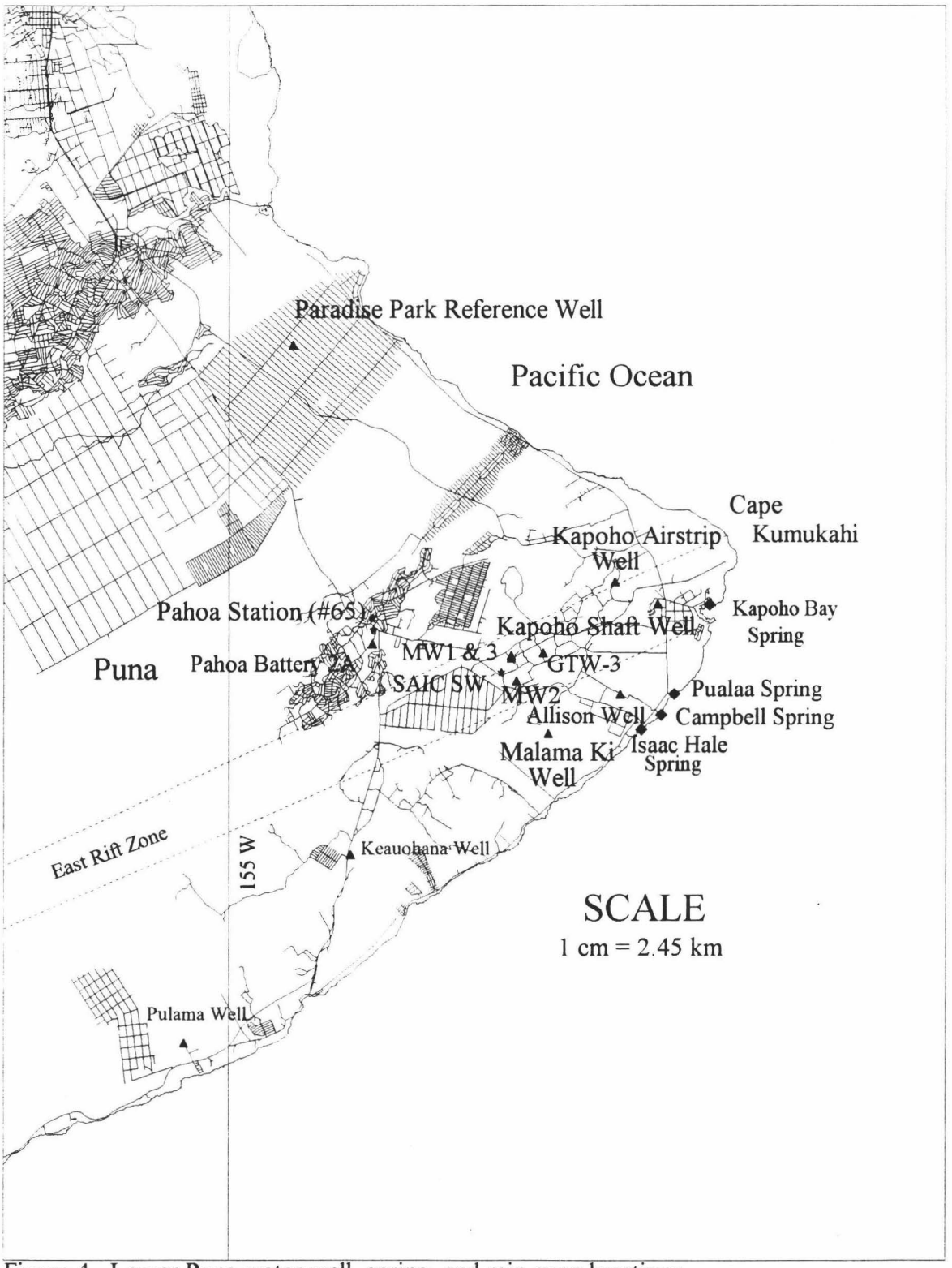

Figure 4. Lower Puna water well, spring, and rain gage locations.

the Ghyben-Herzberg lens in the lower south flank. Here, saline water heated within the LERZ, rises convectively to the surface of the basal lens and forms a broad plume of warm water which floats on fresher, cooler basal water below, which is eventually discharged at the coast line as numerous warm springs and seeps. Lower south flank wells show elevated temperatures, e. g. water in Malama Ki well, 1.9 km from the LERZ is 55^0 C and shows a temperature reversal with depth (Epp and Halunen, 1978), whereas Allison well, 2.2 km from the LERZ, is 37^0 C (Table 1) (Figure 4).

Heads in lower south flank wells are lower than those at the same altitude on the north flank. The south flank hydraulic gradient is 0.2 m to 0.4 m per km, with heads 0.9 m to 1.2 m at a distance of 2.4 km from the coast (Druecker and Fan 1976) (Figure 3). This lower gradient is a result of the dike complex of the ERZ isolating the south flank from north flank flux, the smaller area, and substantially lower rainfall of the south flank (1900 mm per year versus 3175 mm per year).

Keauohana and Pulama wells located further west on the middle south flank (MSF) (Figure 4) show less influence from the ERZ thermal discharge. Nevertheless, temperatures of 24^0 C and 28^0 C respectively (Epp and Halunen, 1979) show that they do receive thermal water.

Hydrogeochemistry

Just as the study area may be divided into geological and hydrological provinces of north flank, lower east rift zone, and south flank, so groundwater in the area may be

geochemically divided into north flank waters, lower east rift zone waters, and south flank waters. Dissolved solid concentrations are typically quite low in north flank waters, having an average of 100 mg/kg or less in the interior portion of the basal lens, but increasing to >200 mg/kg to the east, as the coast is approached. Total dissolved solids concentrations also increase toward the south, as wells encounter water influenced by the LERZ (Thomas, ms). The dominant anion/cation pairs in north flank waters are sodium/calcium bicarbonate, but grade to sodium chloride near the coast (Swain, 1973). Dissolved silica concentrations are low on the north flank, approximately 30 mg/kg, but increase by 50% to 75% as the LERZ is approached (Thomas, ms).

The geochemistry of LERZ waters is much more complicated, where chemical compositions and total dissolved solids span a broad range. Sodium chloride is by far the dominant cation/anion pair present, but does not appear to uniformly increase with proximity to the coast. Chloride concentrations range from 364 mg/kg in Kapoho Airstrip well (Thomas, 1987), located 5 km from Cape Kumukahi at 67 m elevation, to 5,371 mg/kg in GTW-3 well, located 8.5 km from Cape Kumukahi at 200 m elevation (Delanoy, unpub). There is, however, some evidence that chloride concentrations increase from north to south across the LERZ (Figure 5). Wells MW-1 and MW-3, drilled on the north side of Puu Honuaula, have chloride concentrations of 23 mg/kg and 27 mg/kg respectively, while MW-2, drilled on the south side of Puu Honuaula, has a chloride concentration of 884 mg/kg (Delanoy, unpub). Silica concentrations vary considerably in LERZ waters, although all but MW-2 are above the 49 mg/kg average for non-thermal Hawaii island waters estimated by McMurtry, et al., (1977).

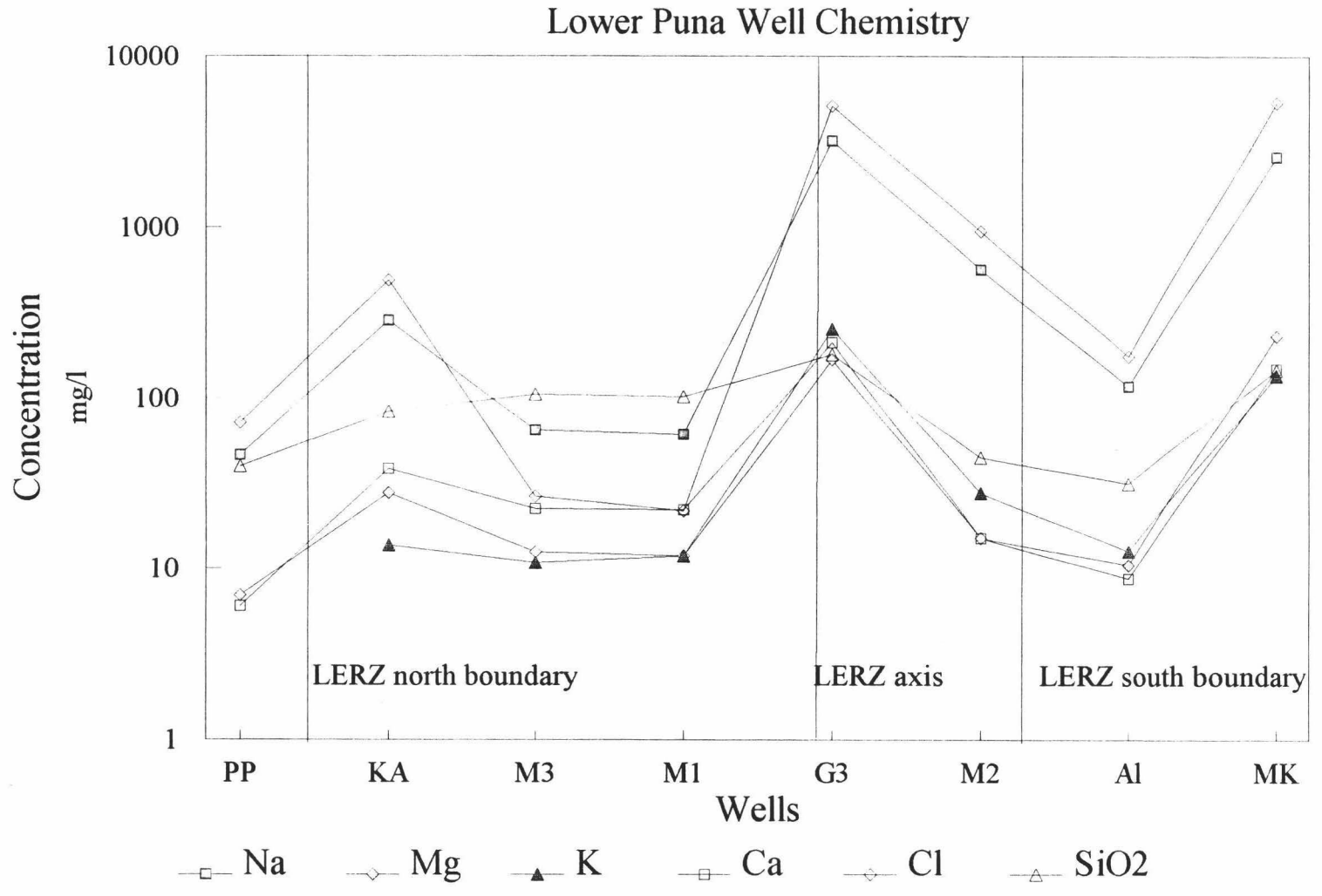

Figure 5. Chemistry of lower Puna wells arranged as a N - S transect across the LERZ.

Kilauea's south flank waters may be further chemically subdivided into middle and lower south flank. The geochemistry of waters in the LSF of Kilauea is strongly influenced by overflow from the LERZ dike complex. As in the LERZ, sodium chloride is the dominant cation-anion pair. Chloride concentrations are higher closer to the LERZ than to the coast: Malama Ki well, located 3 km from the coast, has chloride concentrations of 5,380 mg/kg, while Allison well, located 2 km from the coast, has concentrations of 2,042 mg/kg (Thomas, 1987). Silica concentration also decreases with distance from the LERZ. Malama Ki well has a silica concentration of 100.7 mg/kg, while Allison well has a concentration of 24.1 mg/kg (Thomas, 1987).

The chemical composition of waters from middle south flank (MSF) wells, which lie down gradient from the MERZ and UERZ, do not show as strong a geothermal geochemical signature as those of the LSF. Chloride concentrations in these wells appear to be a function of their proximity to the coast, being 160 mg/kg at Keauohana well, located 3 km inland, and 345 mg/kg at Pulama well, located 2 km inland (Thomas, 1987; Thomas, et al., 1979) (Figure 3). Silica concentrations are, however, elevated above those of non-thermal waters. They are 44 mg/kg and 72.4 mg/kg respectively (Thomas, 1987; Thomas, et al., 1979), which suggests these wells receive some outflow from an up gradient hydrothermal system.

Previous Models

Specific reference to East Rift Zone (ERZ) hydrology was first made by Davis and Yamanaga (1968). They introduced the basic concept that high precipitation on Kilauea

and Mauna Loa evapotranspired or moved down gradient as groundwater in the very porous basalts of the Puna District. Groundwater flow was partitioned by dikes in the ERZ which formed a barrier to southward movement of groundwater from the area of high rainfall north of the rift and west of Hilo. This effect, together with the lower rainfall and smaller area of the south flank, caused a flatter groundwater gradient and higher salinity in groundwater south of the rift. Volcanic activity along the ERZ raised the temperature of groundwater in some adjacent areas and was the cause of warm water discharge from shoreline springs. Davis and Yamanaga were also the first workers to note the effect of ocean tides on inland well water levels in the Puna district.

MacDonald and Abbot (1970) were the first to suggest the existence of a geothermal reservoir within the LERZ. At this time a few shallow exploratory geothermal wells had been drilled in the LERZ. They theorized that a heat source beneath the ERZ heated the plentiful groundwater to the boiling point, but, because of high permeability within the ERZ, super heated water or steam did not exist.

Druecker and Fan (1976) presented a much more detailed model of groundwater in the Puna district. They elaborated on the effect of the ERZ as a barrier to groundwater movement by noting the differences in basal water table levels in wells north and south of the rift. They attributed higher temperatures and salinities in groundwater south of the ERZ to intrusive bodies within the ERZ heating seawater beneath the basal lens along the southern margin of the rift zone, which rose to contaminate the basal aquifer in the Kilauea south flank. Druecker and Fan were the first workers to apply a chemical geothermometer to LERZ waters. Using Fournier and Trusdell's quartz geothermometer

and mixing model (1974) on GTW-3 well waters, they concluded that a large reservoir of super heated water might exist at depth within the LERZ.

Thomas (1987) developed a geochemical model of the Kilauea East Rift Zone from deep exploratory drilling data and long term discharge data from HGP-A, the first producing geothermal well in the LERZ. Building and elaborating on the basic geological and hydrological concepts previously presented, he suggested four sources of recharge to the basal groundwater of the LERZ; cold meteoric water, cold sea water, hydrothermally altered meteoric water, and hydrothermally altered sea water. Because of the large differences in the chemistry of LERZ waters, he also theorized that their hot portions originated from several chemically distinct reservoirs. Using the temperature differential between ambient groundwater outside the ERZ and groundwater in the LERZ, Thomas also estimated the rate of thermal discharge from the LERZ to the shallow groundwater system.

Renewed geothermal well drilling in the ERZ and the advent of commercial electrical production have stimulated a second generation of models. A recent conceptual model of LERZ groundwater hydrology was presented by Geothermex, Inc. (1992). Once again, this model drew on previous models and refined them through the use of more deep well test data. In this model recharge to the ERZ geothermal system was derived from the slopes of Mauna Loa to the west and/or higher elevations of the ERZ to the west, and flowed down gradient parallel to the dikes of the rift. It also identified a low permeability zone at 580 m to 700 m depth in the vicinity of HGP-A as the boundary between the shallow unconfined groundwater aquifer and the underlying geothermal aquifer.

Articles on the hydrology of Kilauea volcano by Moore and Kauahikaua and Ingebritsen and Scholl appeared in Geothermics volume 22 in 1993. These articles were reviews, and though they recapitulated previous models, did not add any new concepts to them.

History of Geothermal Exploration and Production in Kilauea's East Rift Zone

Geothermal exploration began on the ERZ in 1961 and 1962. Hawaii Thermal Power Company drilled four wells in the LERZ, GTW-1, GTW-2, GTW-3, and GTW-4 (Figure 6). These wells ranged in depth from only 54 m to 210 m, and none penetrated more than a few meters below sea level. Water temperatures in these wells ranged from 40^0 C to 93^0 C (Thomas, 1986), therefore they were not considered viable for electricity production and were capped.

A second phase of exploration began in 1975 with the drilling of HGP-A well (Figure 6) (Appendix A). This well was drilled for the state of Hawaii under the Hawaii Geothermal Project. Its site was chosen after completion of a set of geophysical and geochemical surveys which suggested that subsurface thermal anomalies were present in this area of the LERZ. The well was drilled to a depth of 1,968 m with a maximum temperature of 358^0 C at bottom. It produced a mixed phase fluid of 43% steam and 57% liquid with moderate salinity at a wellhead pressure of 1,200 kPa abs. (Thomas, 1986).

In June 1981, a 3 MW experimental electrical generating unit was installed on HGP-A and began continuous operation in December of that year. The well remained in production until December 1989 when the experiment came to an end and the well was

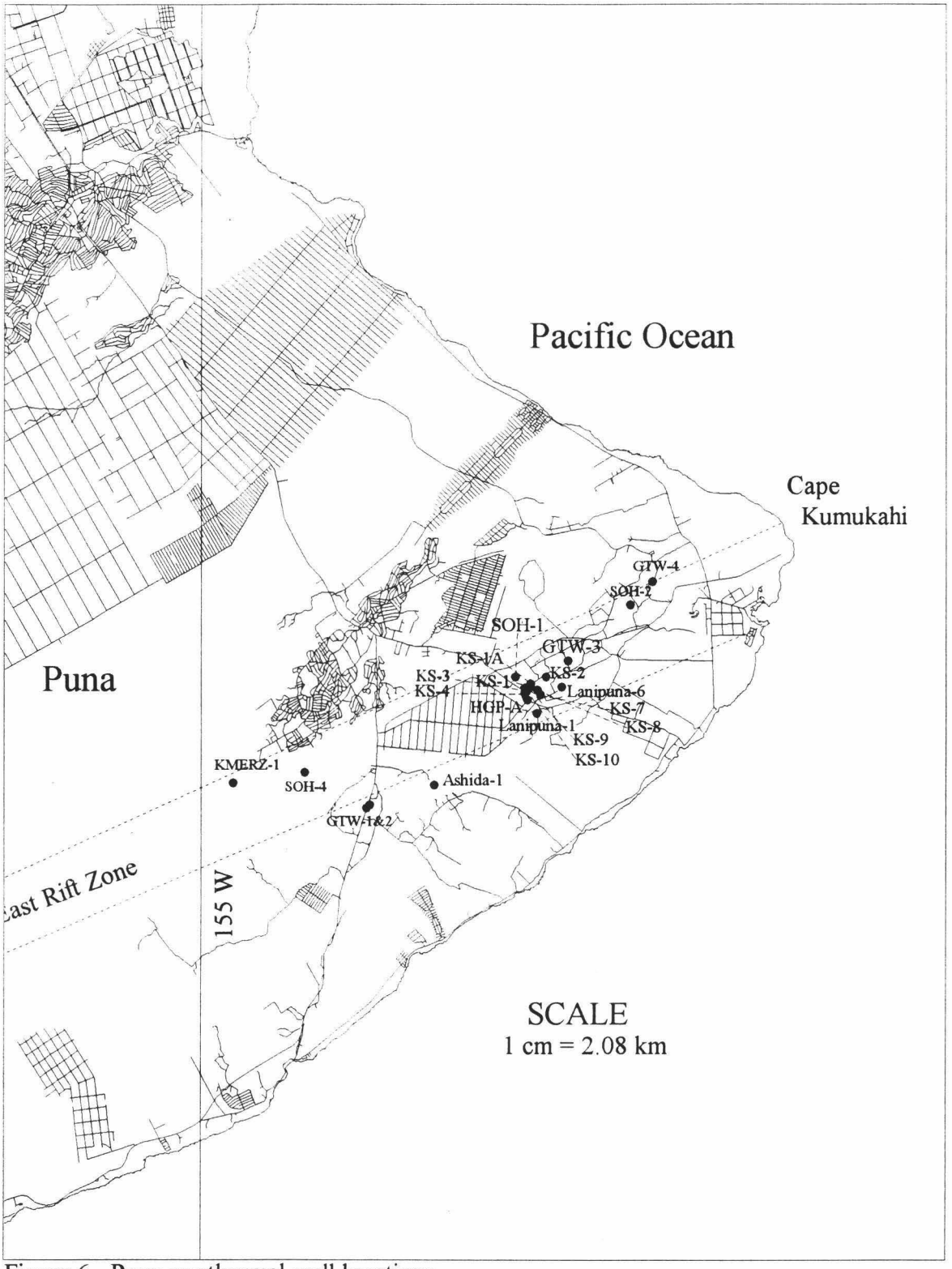

Figure 6. Puna geothermal well locations.

shut in. The HGP-A well was the first to confirm the presence of a commercially exploitable high temperature geothermal resource in Kilauea's LERZ.

With the success of HGP-A, exploration for and development of a commercial geothermal resource began in 1981. Barnwell Industries-Water Resources International drilled three wells, Ashida-1, Lanipuna-1, Lanipuna-6, and a side track, Lanipuna-1-ST, to the south and west of HGP-A between 1981 and 1984 (Geothermex, 1992) (Figure 6). These wells provided subsurface temperature data which delineated important thermal characteristics of this portion of the LERZ. The Lanipuna-1 well showed temperatures even higher than those of HGP-A, but also showed a conductive temperature gradient with minimal permeability. Lanipuna-1-ST, drilled to the northeast from Lanipuna-1 well, and Lanipuna-6 well showed distinct temperature reversals at 1,600 m and 1,300 m respectively. This suggests that both wells may have passed through a reservoir outflow zone and penetrated colder aquifers below. This interpretation in turn suggests that dikes on the southern margin of the LERZ dip to the north; if they dipped to the south, deeper drilling should have penetrated hotter aquifers (Thomas, 1986). The temperature reversals and high chloride concentrations encountered in these wells may serve to define the southern boundary of the geothermal reservoir penetrated by HGP-A. Because none of these wells encountered sufficient temperature or productivity to sustain power generation further efforts to develop a commercial resource south of HGP-A were subsequently abandoned. (Appendix A).

Thermal Power Company, in a joint venture known as Puna Geothermal Venture (PGV), drilled three wells between HGP-A and Puu Honuaula from 1981 to 1985. These

wells, the Kapoho State series, KS-1, KS-2, and KS-1A (Figure 6), were production tested and found to have a production capacity of 2 MW to 3 MW but, because of damage to their casings, were never used for commercial power generation (Appendix A). Their high bottom hole temperatures did, however, serve to further define deep subsurface conditions in the area between HGP-A and Puu Honuaula, which will subsequently be referred to as the Pohoiki geothermal field.

In 1990, the state of Hawaii began the Scientific Observation Hole project, which was a series of three deep continuously cored holes, SOH#4 in Kilauea's MERZ, SOH#1 just north of Puu Honuaula, and SOH#2, 6 km from Cape Kumukahi (Figure 6). Cores from these holes provided the first detailed look at the structure, lithology, and mineralogy of the deep interior of the MERZ and LERZ. Although these holes could not be production tested because of permitting restraints, all encountered high temperatures at depth (Deymonaz, 1991) (Appendix A), demonstrating that, at a depth of 2 km, the LERZ is hot along it's entire length.

True/Mid Pacific Geothermal drilled the first exploration well on the MERZ in 1990, KMERZ 1-A (Figure 6) . This is the deepest hole in the east rift zone, with a total vertical depth of 8,741 ft., and the first geothermal exploration well outside the LERZ. It was reportedly production tested at 5 to 8 MW (Stuhl, verbal communication) (Appendix A).

Puna Geothermal Venture continued the Kapoho State series in 1990-1992, drilling KS-3 and KS-4 in the Pohoiki field between HGP-A and Puu Honuaula (Figure 6). These wells were flow tested at approximately 3 MW each (Appendix A).

As a result of the KS series of wells drilled up to this time, the Pohoiki geothermal field was considered to be a low permeability, high temperature field with moderate to highly saline brines and a production reservoir located below 2,000 m depth capable of producing approximately 50,000 to 80,000 lbs. of steam per hour. In 1991, Puna Geothermal Venture completed its 25 MWe power plant in the Pohoiki field and started drilling the KS-7 (Figure 6) injection well. The KS-7 well encountered high pressure steam and gas at a depth of 506 m and had to be plugged and abandoned (PGV unpub. report, 1992) (Appendix A). In an effort to re-enter what was assumed to be the steeply dipping fracture struck in KS-7 well, the KS-8 well was slant drilled into a high pressure steam and gas zone at 1,050 m depth (PGV unpub. report, 1992) resulting in a 30 hour blowout and suspension of the company's drilling permits (Appendix A) (Figure 6).

When PGV regained its permits in 1992, the company completed and flow tested KS-8 well. The well produced 10 MWe and was brought on line in October 1992 (PGV unpub. report, 1992), however, production was short lived. A lightening strike to transmission lines from the power plant forced an emergency shut in of the well which damaged it's already fragile casing, and forced PGV to plug and abandon KS-8.

PGV had already started slant drilling KS-9 and KS-10 wells (Figure 6) toward the high permeability zone encountered in KS-7 and KS-8 wells when KS-8 well was abandoned. The KS-9 well was brought on line without incident in April 1993 and produced 25 MWe until KS-10 well was brought on line in June 1993. Flow testing showed KS-10 well also capable of producing 20+ MWe; together under restricted flow,

these two wells produce 30 MWe at a wellhead pressure of 11,032 kPa (1600 psig) (Davidson, oral communication) (Appendix A).

The geochemistry and production characteristics of the KS-8, KS-9, and KS-10 wells were distinctly different from those previously drilled in the Pohoiki geothermal field; the older wells had moderately to highly saline brines with high silica concentrations. Although geochemical data from the proprietary wells is extremely sparse, HGP-A well is well documented and its geochemistry and production characteristics are roughly typical of these older wells. After eight years of production, HGP-A had chloride concentrations of 9,514 mg/kg and silica concentrations of 913 mg/kg in the brine phase and produced 43% steam and 57% liquid at a wellhead pressure of 1,100 kPa (Thomas, 1987).

The KS-9 and KS-10 wells initially showed very low concentrations of dissolved solids. Chloride concentrations averaged 6 mg/kg and 1.9 mg/kg and silica concentrations averaged 206 mg/kg and 196 mg/kg respectively in the brine phase (Delanoy, unpub.) from the start of production in April and June 1993 respectively until November 1993. At this time a sudden large increase in dissolved solids and corresponding decrease in steam to brine ratio occurred in KS-10 well. One hundred thirty two days after the start of production, chloride concentrations in KS-10 brine were ~1 mg/l, on day 140 a concentration of more than 7,000 mg/l was measured (Delanoy, unpub.) and the steam fraction of well fluids decreased from 87% to 25% (Davidson, oral comm.). Chloride concentrations stabilized at 13,000 mg/l after another 45 days and the steam fraction currently ranges between 40% and 20%. Dissolved solids concentration and steam to

brine ratio have remained essentially unchanged in KS-9 well from the start of production to the present (6/94).

KS-8, KS-9, and KS-10 wells also showed higher temperatures and pressures at corresponding depths than the previously drilled wells (Appendix A). HGP-A well produced at an average wellhead pressure of 1,100 kPa (Thomas, 1987), while KS-9 and KS-10 wells produce at a pressure an order of magnitude larger. In 1992 a down-hole pressure monitor was installed in HGP-A to assess any changes in reservoir pressure from natural causes or from production elsewhere in the Pohoiki geothermal field. No changes in pressure have been observed during flow tests and subsequent production of KS-8, KS-9, and KS-10 wells (Olson, verbal communication).

Geochemical and geophysical data indicate that KS-8, KS-9, and KS-10 wells intersect a discrete, high pressure, high capacity fracture zone with distinctly higher production rates than those found in the low permeability regional system penetrated in previously drilled wells. Down hole directional surveys have plotted this fracture zone dipping 85^0 north and striking generally parallel to the east rift zone (Teplow, oral communication). It initially contained a saturated steam-water mixture at a pressure of 14,480 kPa, temperature of 335^0 C, and enthalpy of 2,531 kJ/kg (PGV, unpub. report). Production from this fracture appears to have lowered steam pressure in it, and consequently, to have allowed reservoir fluids to rise to a level somewhere above the depth at which KS-10 intersects the fracture; thus causing the increase in chlorides and decrease in steam to brine ratio discussed in the production history of this well.

Reinjection

The subsurface reinjection of spent geothermal fluids has several immediate advantages and possible disadvantages. First, stringent U.S. environmental laws governing the quality of surface and ground waters have made the alternatives to reinjection, e. g. isolating the fluids from the environment or releasing the fluids into surface water bodies, economically unattractive. Isolating large volumes of fluid and/or treating them is difficult and costly. Second, there are reservoir engineering advantages to be gained by reinjection. Replacing reservoir fluids may prevent the decrease in reservoir pressure associated with long term production. Fluid replacement may also prevent localized land subsidence associated with long term production (Kestin, 1980). Third, reinjected fluids may provide the medium for extracting heat from hot rock which remains after the production of the original geothermal fluids (Kestin, 1980). Thus, reinjected fluids may be recycled to production one or more times, greatly extending the life of the field. Fourth, reinjection may impose a warm barrier which delays the ingress of cold water from beyond the geothermal field (Armstead, 1978).

There are several possible disadvantages to reinjection; (1) poor placement of reinjection wells may cool the geothermal reservoir, (2) reinjectate may find its way into the shallow groundwater aquifer, (3) chemical composition of the reinjectate may cause scaling and/or corrosion in the well bore, (4) too much energy may be expended forcing reinjectate into a highly pressured formation for reinjection to be economically feasible, and (5) reinjection in faulted terrain may cause earthquakes (Kestin, 1980). The first two problems can be overcome by very careful well placement and attention to the depth

interval in which the reinjectate is introduced. However, because small scale reservoir structure is seldom known, it is often impossible to know whether these problems will occur until the well is drilled and reinjection has taken place for some time. The third and fourth problems are often linked. Silica rich fluids may cause scaling in the well bore and plugging in the formation (Kestin, 1980). Hydrogen sulfide dissolved in reinjectate may also cause scaling and corrosion in the well bore and plugging, as precipitated sulfides, in the formation (Kestin, 1980). Lastly, when reinjection causes the pore fluid pressure to exceed the hydrostatic pressure in the area, seismic activity may be induced (Kestin, 1980). However, no earthquake activity has ever been linked to reinjection in a geothermal field (Kestin, 1980).

As part of its 25 MWe power production scheme, Puna Geothermal Venture recombines spent steam from its power plant, geothermal brine, and non-condensable gasses, then reinjects this fluid through a depth interval from 1,234 m to 1,979 m in KS-1A, 1,184 m to 2,058 m in KS-3, and 1,194 m to 2,068 m in KS-4 (PGV unpub. report, 1991). When reinjection began in April 1993, the company was reinjecting ~3,000 m^3/d through KS-1A, ~1,100 m^3/d through KS-3, and ~3,500 m^3/d through KS-4. The fluid was reinjected at a temperature of 60^0 C and a pressure of 276 kPa (Davidson, oral communication). At this pressure, non-condensable gasses appear to dissolve in the liquid phase and no gas cap has been reported in these wells. Scaling in the well bore also did not appear to be a problem. Injection capacity increased in each well during the early reinjection period (Davidson, oral communication), perhaps because of fracturing in the formation from thermal shock due to the introduction of the relatively cool injectate.

Although reinjection appears to be going well, high concentrations of hydrogen sulfide and moderate concentrations of silica may eventually cause corrosion in the well bores and plugging in the formations into which the reinjectate is introduced.

Since reinjection is taking place in the highly faulted terrain of the LERZ, it is possible that reinjected fluids may find their way into the shallow groundwater. From the beginning of production in April 1993 until November 1993, fluids being reinjected were lower in dissolved solids than any downgradient groundwater. However, the increase in dissolved solids in KS-10 well after November 1993 has caused a corresponding increase in the salinity of the reinjectate. An analysis done in June 1994 showed a reinjectate chloride concentration of 3,033 mg/l (Delanoy, unpub.), which is still lower than chloride concentrations in some lower Puna wells. The increase in the liquid fraction in KS-10 well has not increased the volume of the reinjectate because production from it has been reduced; PGV's reinjected fluids totaled 4.08×10^8 lb. for October 1993 and 4.01×10^8 lb. for February 1994 (PGV, unpub.). At present (6/94) no significant changes in water level, temperature, or conductivity have occurred in any of the down gradient monitoring wells, however, injection has taken place for only one year.

CHAPTER III.

HYDROGEOCHEMISTRY

Introduction

Previous models of lower Puna groundwater flow have drawn heavily on existing hydrogeochemical data. The unique chemistry of north flank, LERZ, and south flank wells allows their waters to be partitioned into individual provinces, and permits inferences to be made about groundwater flow processes within each. This study will draw on previously published water chemistry data and on unpublished data from recently drilled water and geothermal wells. These data sets will be used to answer the following questions:

1. What processes control the chemistry of lower Puna waters?
2. What component waters are present in each well, and how have they been altered by contact with a thermal source?
3. Are lower Puna waters at geochemical water-rock equilibrium?
4. What was the temperature of the thermal source this water encountered?
5. What percentage of water in each lower Puna well has a thermal origin?
6. Was the parent water of this thermal water meteoric groundwater or seawater?

The answers to these questions will then be used to refine the lower Puna groundwater flow model.

Data Sources

Geochemical data used in this study came from three sources. First, data from Thomas, et al. (1979) was used to obtain a profile of an average groundwater.

Temperatures and silica concentrations from 31 wells on the windward slopes of Kilauea and Mauna Loa were used to obtain an average temperature and silica concentration for this groundwater (Table 2). Major ion concentrations from 22 of these wells which did not show seawater contamination (< 100 mg/l Cl^-) were used to obtain average major ion concentrations (Table 2). This set of wells was chosen to represent an average non-thermal Puna groundwater because these wells penetrate young tholeiitic basalts and are located in areas of moderate to high rainfall. These conditions are analogous to the geology and climate of Puna. This water will be referred to as average Hawaii groundwater in this study.

The second data set consists of groundwater sample analyses which were obtained by bailing during drilling when wells KS-3, KS-4, KS-7, KS-8, KS-9, and KS-10 intersected the unconfined groundwater table. These KS series wells were drilled with air and foam above the water table, so samples should not have been heavily contaminated by drilling fluids. Analyses of these samples were done by Brewer Environmental Industries, Environmental Laboratories Division. Unfortunately analyses were often incomplete and show poor ion balances (Table 3).

TABLE 2. AVERAGE HAWAII GROUNDWATER

Hawaii island water wells located on windward Kilauea or Mauna Loa which do not show thermal influence

Data from Thomas, et al (1979)

Well	Well #	Temp. C	pH	Na mg/l	K mg/l	Ca mg/l	Mg mg/l	Cl mg/l	SO4 mg/l	HCO3 mg/l	SiO2 mg/l
Hawn Shores 1	8-3185-01	21.5	7.7	13	3.2	3.9	3.8	14	5.1		51.9
Hawn Shores 2	8-3185-02		7.6	19	3.5	3.9	4.5	28	7	56	49
Honuapo 1	8-0533-02	19	7.1	320	14	20	44	580	86	42	43
Honuapo 2	8-0632-01	19	7.3	245	11	17	33	440	66	44	41
Honuapo 3	8-0533-03	19	7	272	12	18	38	500	75	41	43
Honuapo Mill	8-0533-01	19	7	680	24	33	86	1240	169	46	43
Kanoelehua 2	8-4203-06	21	6.2	12	2.1	11	3.5	18	5	39	37
Keaau 1	8-3802-01	24.5	7.4	6	2	5.6	1.8	3.4	6.2	36	37.7
Keaau 2	8-3802-02	24.5	7.4	5	2	4.9	2.8	5.4	5.6	86	34.6
Keaau Mill 1	8-3802-03	18.5	7.8	6.5	2	6.9	3.1	3.5	6.2	36	36
Keaau Mill 2	8-3802-04	22	7.4	5.2	2.1	5.5	3.3	4	5.5	38	36
Keaau Mill 3	8-3802-05	22	7.4	5.2	2.1	5.5	3.3	4	5.5	38	36
Keaau Orch 1	8-3900-01	18.5	7.1	38	3.8	7.8	7.7	64	14	44	39
Keaau Orch 2	8-3900-02	19.5	6.8	90	5.6	8.9	13.6	156	25	44	33
Naalehu 1	8-0335-01	19	7.8	11	1.5	6.4	4.6	10	13	42	43
Ninole A	8-0831-02	18	7.3	100	5.9	13	18	150	29	41	43
Ninole B	8-0831-03	21	6.9	89	5.2	13.2	18	165.9	28		48
Ninole GU	8-0831-01	18	7.3	80	4.4	9.2	12	130	24	43	41
Olaa Shaft	8-3702-01	23	7	5.8	2.4	6	2.7	4	5.5	38	40
Pahala	8-1229-01	17		5.7	1.3	7.5	3.3	3.2	6.6	40	42
Pahala Shaft	8-1128-01	19	7.2	7.2	1	6.6	3.6	3.5	10	43	42
Pahoa 2A	8-2986-01	22.5	7.4	17	3.5	4.8	0.86	12	13	51	39.6
Pahoa 2B	8-2986-02	23	6.4	16	3.2	3.9	2.4	5.8	13	48	55
Palima	8-1128-02	21	7	12	1.2	6.1	4.3	12	7.5	41	54
Panaewa 1	8-4003-01	20	7.5	5.1	1.8	6.8	2.7	4	0	45	34
Panaewa 2	8-4003-02	20		5	1.8	7.2	2.3	4	5		36.6
Piihonua	8-4306-01	17.8	8	7.8	2.2	5	3.3	2	5.9	46	37
Punaluu	8-0830-01	19	7.1	118	5.5	9.6	16	205	37	34	32
Wai Pahoehoe	8-3500-01	22	7.1			5.3	6.7	5.5	10.9		46.5
Waiakea TH-2	8-4203-02	21.1	7	10	1	8	4.4	11	2.5	50	33
Waiakea TH-3	8-4203-03	23.5	7.1	7.4	1.8	6	3.6	7.5	2	44	36
Average		20.43	7.217	73.8	4.437	8.919	11.52	122.4	22.39	44.3	40.74
Std. Dev.		2.029	0.382	139.7	4.836	5.995	17.33	253.5	34.07	9.486	5.998

TABLE 2. CONTINUED

Low chloride (<100 mg/l) wells

Well	Well #	Temp. C	pH	Na mg/l	K mg/l	Ca mg/l	Mg mg/l	Cl mg/l	SO4 mg/l	HCO3 mg/l	SiO2 mg/l
Hawn Shores 1	8-3185-01	21.5	7.7	13	3.2	3.9	3.8	14	5.1		51.9
Hawn Shores 2	8-3185-02		7.6	19	3.5	3.9	4.5	28	7	56	49
Kanoelehua 2	8-4203-06	21	6.2	12	2.1	11	3.5	18	5	39	37
Keaau 1	8-3802-01	24.5	7.4	6	2	5.6	1.8	3.4	6.2	36	37.7
Keaau 2	8-3802-02	24.5	7.4	5	2	4.9	2.8	5.4	5.6	86	34.6
Keaau Mill 1	8-3802-03	18.5	7.8	6.5	2	6.9	3.1	3.5	6.2	36	36
Keaau Mill 2	8-3802-04	22	7.4	5.2	2.1	5.5	3.3	4	5.5	38	36
Keaau Mill 3	8-3802-05	22	7.4	5.2	2.1	5.5	3.3	4	5.5	38	36
Keaau Orch 1	8-3900-01	18.5	7.1	38	3.8	7.8	7.7	64	14	44	39
Naalehu 1	8-0335-01	19	7.8	11	1.5	6.4	4.6	10	13	42	43
Olaa Shaft	8-3702-01	23	7	5.8	2.4	6	2.7	4	5.5	38	40
Pahala	8-1229-01	17		5.7	1.3	7.5	3.3	3.2	6.6	40	42
Pahala Shaft	8-1128-01	19	7.2	7.2	1	6.6	3.6	3.5	10	43	42
Pahoa 2A	8-2986-01	22.5	7.4	17	3.5	4.8	0.86	12	13	51	39.6
Pahoa 2B	8-2986-02	23	6.4	16	3.2	3.9	2.4	5.8	13	48	55
Palima	8-1128-02	21	7	12	1.2	6.1	4.3	12	7.5	41	54
Panaewa 1	8-4003-01	20	7.5	5.1	1.8	6.8	2.7	4	0	45	34
Panaewa 2	8-4003-02	20		5	1.8	7.2	2.3	4	5		36.6
Piihonua	8-4306-01	17.8	8	7.8	2.2	5	3.3	2	5.9	46	37
Wai Pahoehoe	8-3500-01	22	7.1			5.3	6.7	5.5	10.9		46.5
Waiakea TH-2	8-4203-02	21.1	7	10	1	8	4.4	11	2.5	50	33
Waiakea TH-3	8-4203-03	23.5	7.1	7.4	1.8	6	3.6	7.5	2	44	36
Average		21.02	7.275	10.47	2.167	6.118	3.571	10.4	7.045	45.32	40.72
Std. Dev.		2.104	0.432	7.455	0.81	1.59	1.448	13.16	3.684	10.94	6.416
Cl/ion				1.008	4.869	1.724	2.954		1.497	0.233	0.259

TABLE 3. KS WELL SERIES WATER SAMPLE ANALYSES

Data from Brewer Environmental Industries, Inc.

Well	Sample Date	Na mg/l	K mg/l	Mg mg/l	Ca mg/l	Cl mg/l	SO4 mg/l	HCO3 mg/l	SiO2 mg/l	pH	ion bal. %
KS-3		33.4	3.3	3.6	10.8	7			41.8		40.2
KS-4	9/17/92	49.2	8.6	15.9	60.8	16.5	115		83.5	6.9	20.5
KS-7	2/13/91	313	30	13.2	41.4	180	312		70		24.1
KS-8	5/9/91	302	26.8	84.8	317	570	303		5.4	7.5	-4.6
KS-9	12/10/92	231	20.3	24.7	65.9	470	200		61	7.3	14.2
KS-10	2/21/93	70.6	7.9	16.3	35.1	61	147		80.8	6.9	-13.2

The third data set consists of analyses of periodic groundwater samples and temperature measurements from wells GTW-3, Kapoho Airstrip, Malama Ki, Allison, MW-1, MW-2, and MW-3. It also includes a single water sample analysis and long term temperature monitoring data from Paradise Park reference well, and single water sample analyses from shoreline warm springs in the Puna district. This data set spans a period from late 1991 to late 1993. Most wells were sampled at two week intervals during this period. The Paradise Park reference well was sampled once in 1992 and the warm springs were sampled once in July or August 1993.

The only existing LERZ well which was not included in this study is Kapoho Shaft, which was excluded because it is not thought to be in contact with the LERZ groundwater system, but instead taps water perched in the tuff of Kapoho Cone (Druecker and Fan, 1976).

Methods

Samples for the third data set were collected with an open stainless steel bailer or by dedicated stainless steel pumps containing a Teflon bladder which was compressed by high pressure nitrogen pulses to bring the sample to the surface. Sample collection bottles were polypropylene sample bottles which were acid washed prior to sample collection. Three types of samples were collected:

1. Raw untreated (500 ml).
2. Filtered acidified (250 ml).

Samples were filtered through a 0.45 um membrane on site or in the field lab and acidified with 5 ml trace metal grade HNO_3.

3. Filtered untreated (20 ml).

   A 20 ml aliquot of the raw untreated sample was filtered through a 0.20 um membrane in the field lab for analysis of anions.

All samples were refrigerated until analyses were completed.

Concentrations of major ions (Ca^{2+}, Mg^{2+}, Na^{+}, Si^{4+}) were determined using Leeman Labs ICP-AES following Leeman Standard Methods for analysis. Concentrations of K^{+} were determined using Perkin Elmer Model 603 Atomic Absorption Spectrometer following Perkin Elmer methods for AAS-Flame. Chloride concentrations were determined using Method 407.B Mercuric Nitrate Method in Standard Methods for Examination of Water and Wastewater-APHA. Anion concentrations were determined using Dionex Ion Chromatograph System using IonPac AS4A Analytical column and a thermal conductivity detector. Alkalinity concentrations were determined using Method 403 in Standard Methods for the Examination of Water and Wastewater-APHA within 14 days of collection. Trace element concentration was determined using Perkin Elmer Model 5100-LC Zeeman Graphite Furnace Atomic Absorption Spectrometer. All analytical methods met EPA protocols.

Results of the analyses of the well water samples are presented as a time series in Figures 7, 8, 9, 10, 11, 12, and 13. The average concentration of each ion in each well and spring water is presented in Table 4.

TABLE 4. UNIVERSITY OF HAWAII WATER SAMPLE ANALYSES AVERAGES

Constituent concentrations from analyses 1991 - 1993
G. Delanoy (unpub.)

WELL	Temp C	pH	Na mg/l	K mg/l	Mg mg/l	Ca mg/l	Cl mg/l	SO4 mg/l	CaCo3 mg/l	HCO3 mg/l	SiO2 mg/l	pH
Kapoho Airstrip												
Average	35.5	7.6	283	13.66	27.62	38.33	487	168	32.77	32.63	83.22	7.6
Std. Dev.		0.176	48.43	5.705	4.081	4.727	79.1	6.04	2.387	2.36	9.549	0.176
Malama Ki												
Average	53	7.4	2585	136	230	149	5373	600	146	145	147	7.371
Std. Dev.		0.2	763.8	24.3	62.6	31.5	1575	48.8	29.9	29.8	27.7	0.2
GTW-3												
Average	84.8	7	3209	252	168	211	5106	733	27.3	27.3	180	6.974
Std. Dev.		0.238	587.3	41.8	44.7	29.9	1751	386	5.36	5.35	48.2	0.238
MW-1												
Average	34.7	7.5	60.96	11.83	11.8	22.03	21.7	298	27.75	27.7	102	6.208
Std. Dev.		0.289	7.426	7.951	0.77	1.69	4.44	165	5.286	5.24	6.53	2.86
MW-2												
Average	67.9	8.2	565.9	27.7	15.1	41.3	943.8	118.1		52.9	44.5	8.013
Std. Dev.		0.311	89.92	7.53	8.22	9.95	141.8	29	21.2	9.47	24.2	1.408
MW-3												
Average	41	7.31	64.54	10.82	12.46	22.34	26.46	300.8	25.69	25.62	105	7.316
Std. Dev.		0.24	3.933	1.554	0.82	1.303	10.22	86.98	1.601	1.599	5	0.24
Allison												
Average	37	7.8	117.8	12.69	10.48	8.727	175.7	42.55	83.2	82.67	31.53	7.77
Std. Dev.		0.219	52.79	6.777	6.359	4.842	72.5	6.845	13.15	13.14	16.97	0.21

Puna Shoreline Warm Springs

SPRING	Temp C	Na mg/l	K mg/l	Mg mg/l	Ca mg/l	Cl mg/l	SO4 mg/l	CaCO3 mg/l	HCO3 mg/l	SiO2 mg/l	pH
Isaac Hale	34	2403	40.9	276	106	6361	594.3	52.9		79.4	
Campbell	32	3150	86.3	329	131	8181	741	53.6		98.2	
Pualaa	34.3	4513	103.5	377	178	7760	686			118.7	7.5
Kapoho Bay	30.5	1687	3	183	81.1	4181	420	43.3		72.5	

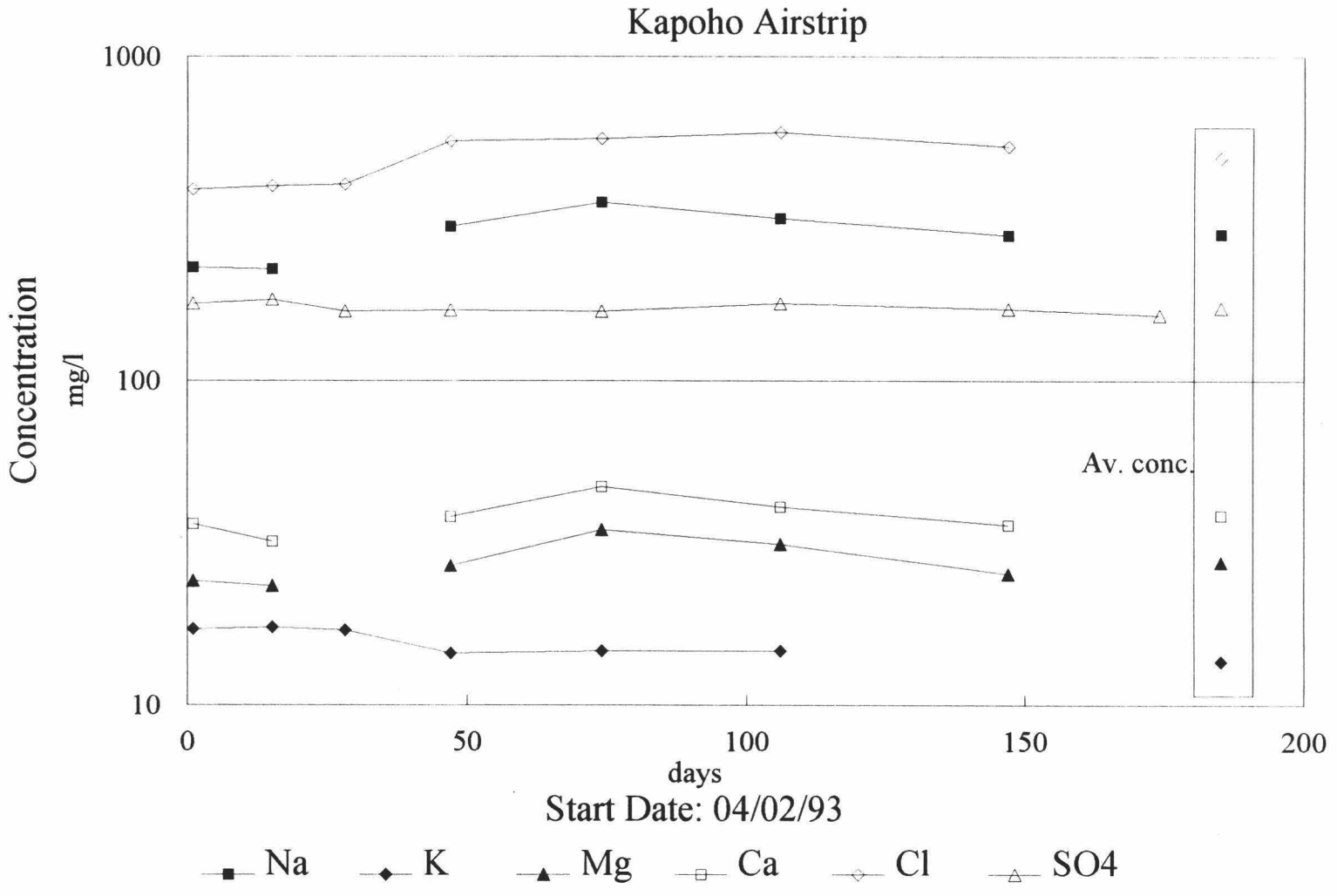

Figure 7. Major ion concentrations in Kapoho Airstrip well during the study period.

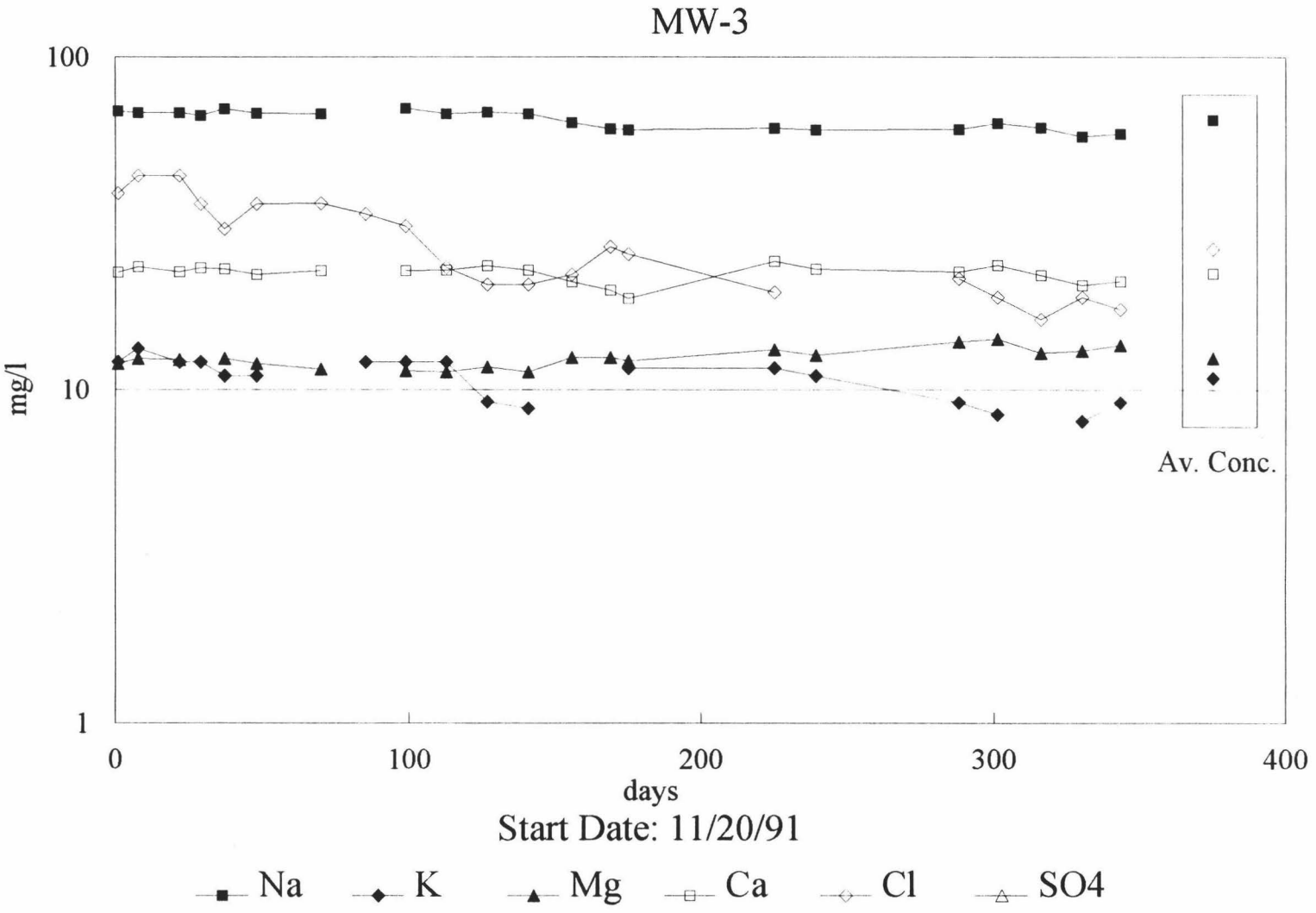

Figure 8. Major ion concentrations in MW-3 during the study period.

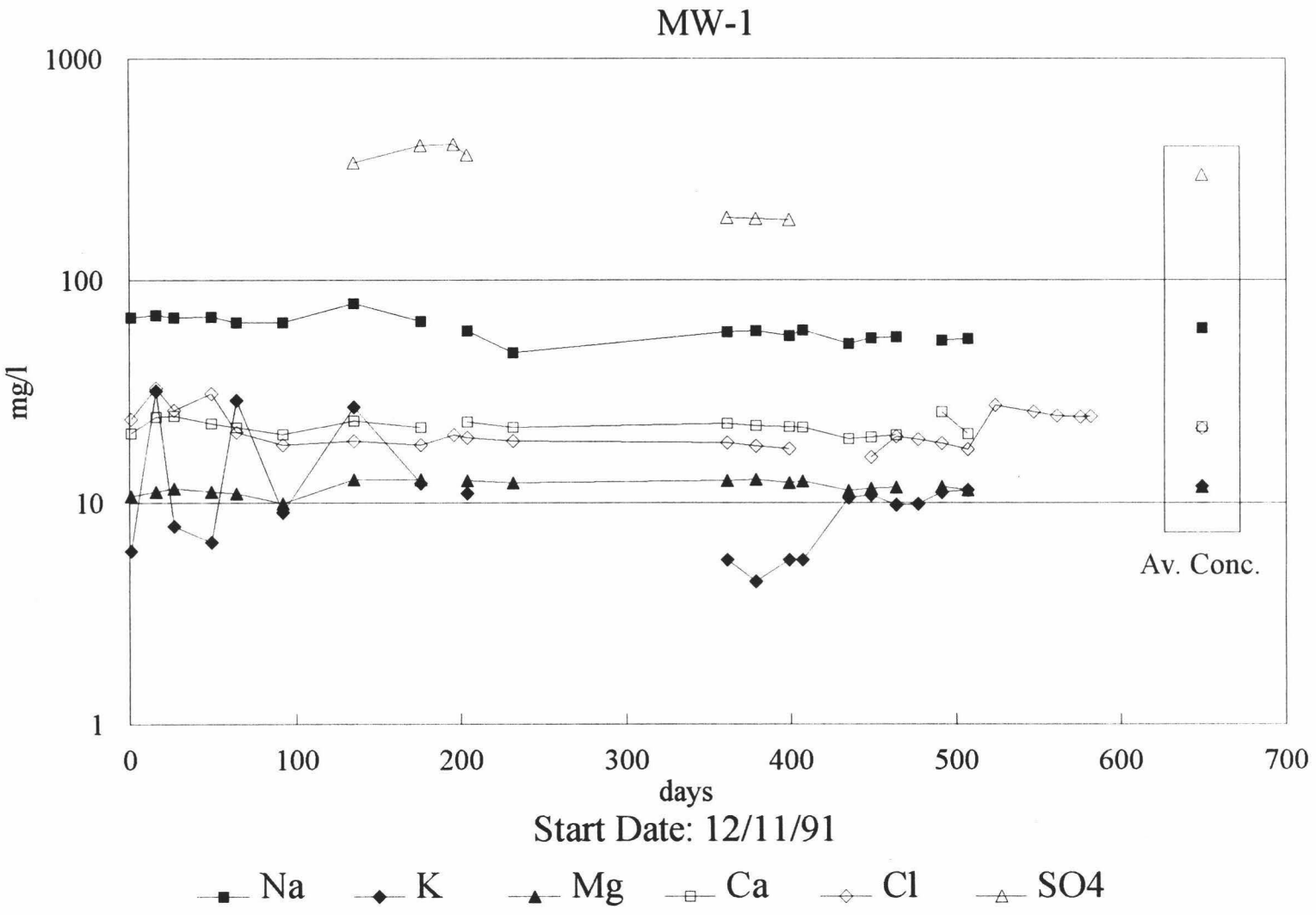

Figure 9. Major ion concentrations in MW-1 during the study period.

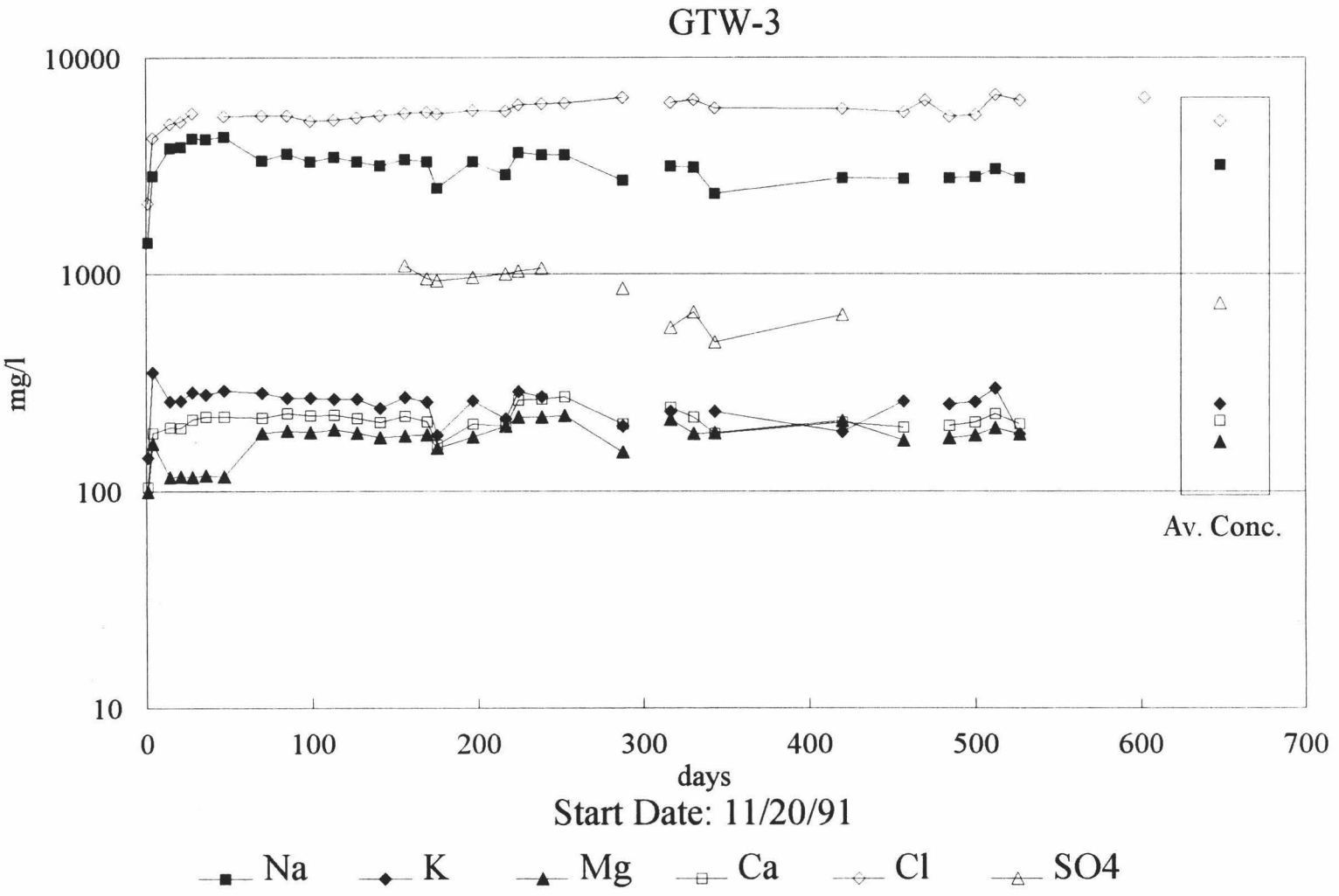

Figure 10. Major ion concentrations in GTW-3 well during the study period.

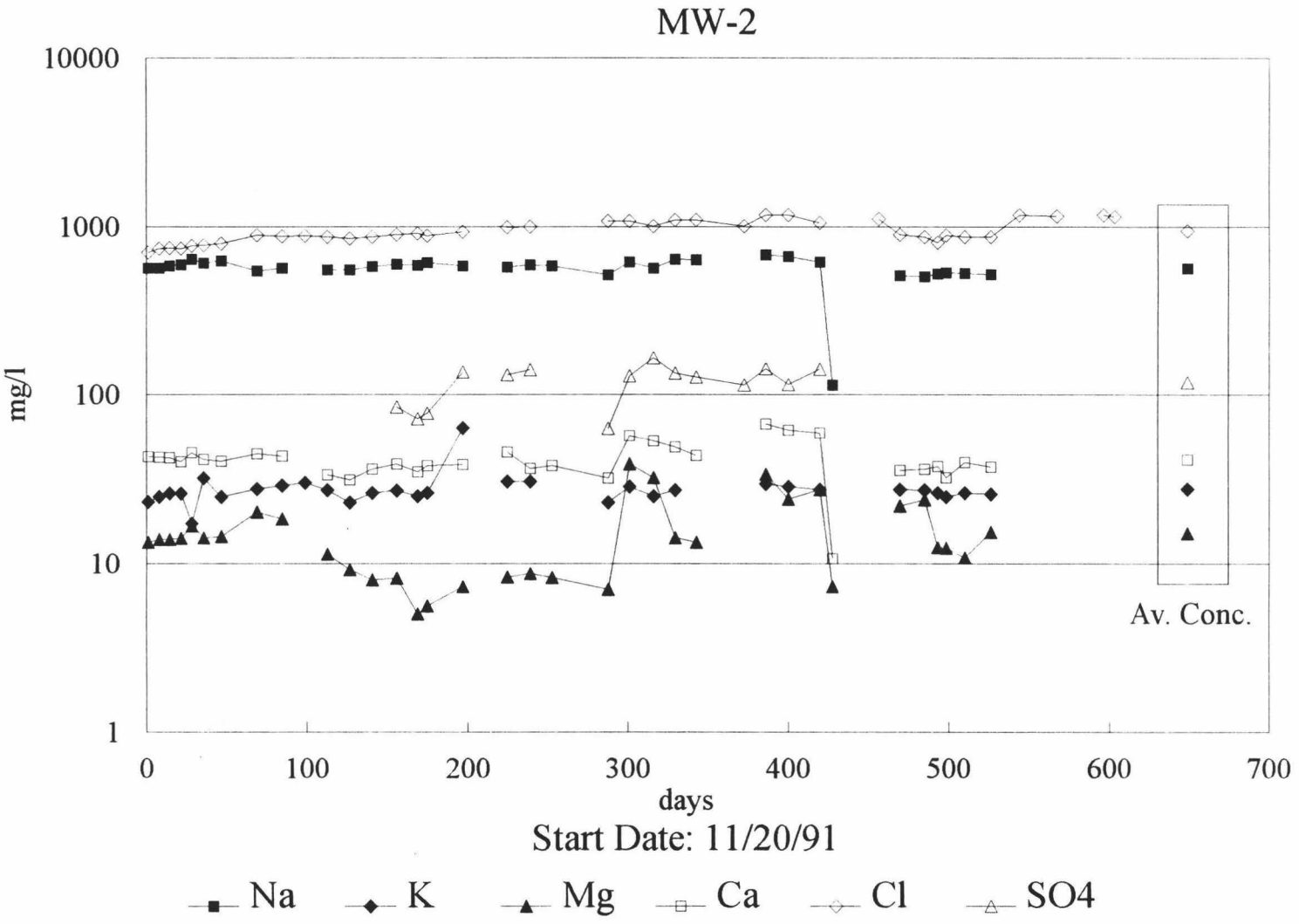

Figure 11. Major ion concentrations in MW-2 during the study period.

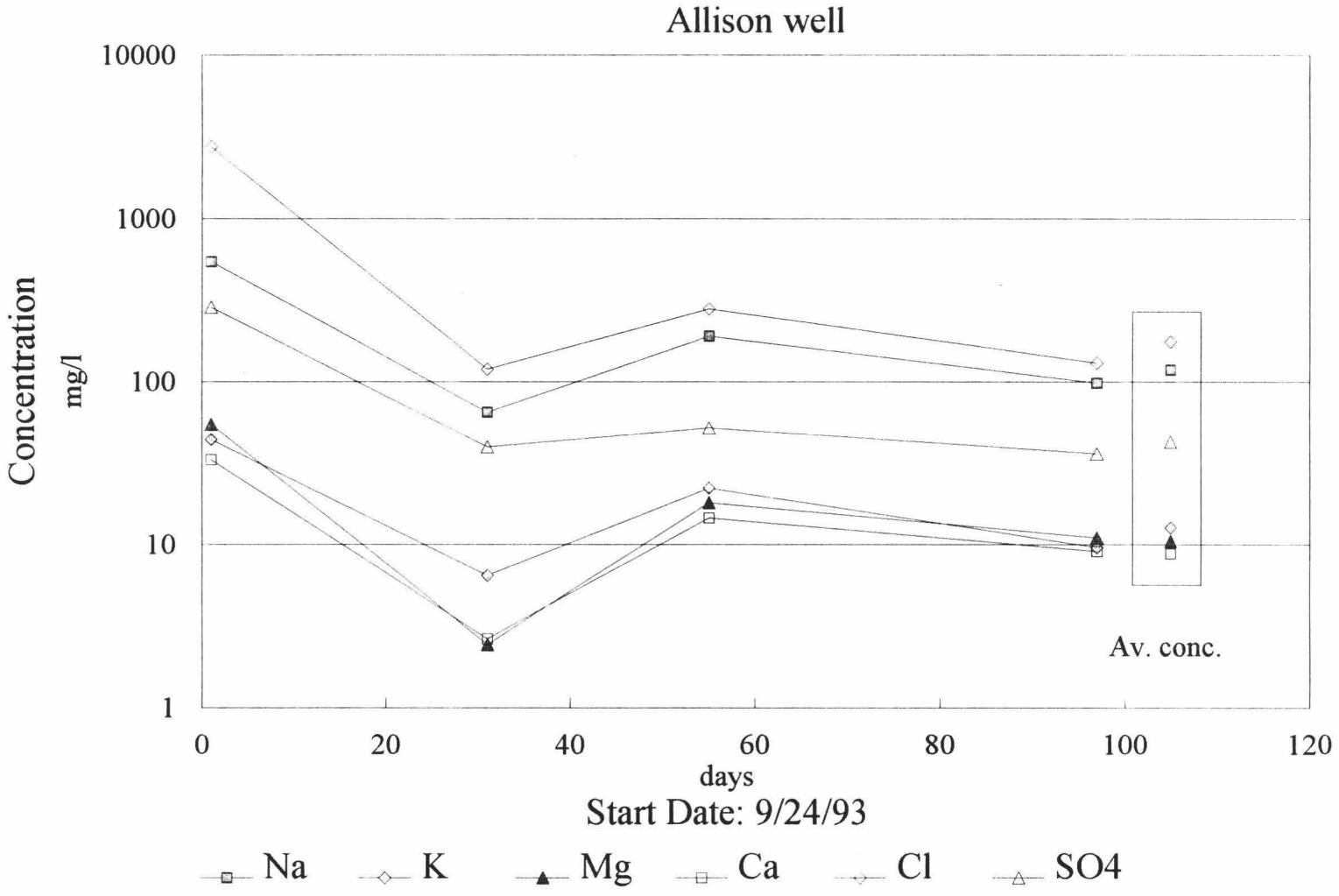

Figure 12. Major ion concentrations in Allison well during the study period.

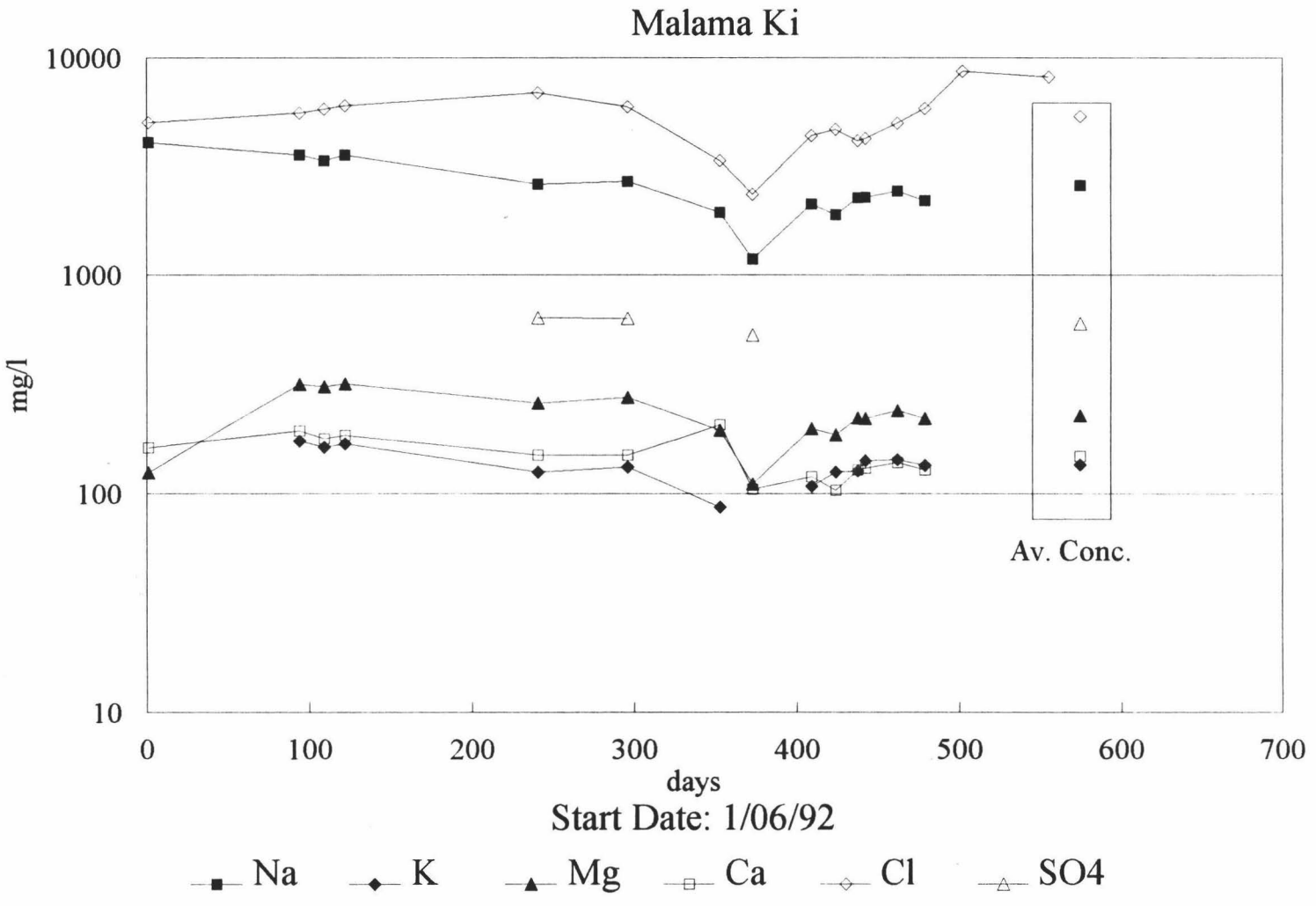

Figure 13. Major ion concentrations in Malama Ki well during the study period.

Ion Geochemistry

Question 1. What processes control the chemistry of lower Puna waters?

For this study, waters from the lower Puna thermal wells were segregated into three groups based on their chloride ion concentrations (Tables 3 & 4). The high chloride thermal wells, GTW-3 and Malama Ki, have chloride concentrations greater than 1,000 mg/l. The medium chloride thermal wells, Allison, Kapoho Airstrip, KS-7, KS-8, KS-9, and MW-2, have chloride concentrations between 999 and 100 mg/l. Major ion ratios in both these groups are similar to those of seawater. The low chloride thermal wells, KS-3, KS-4, KS-10, MW-1, and MW-3, have chloride concentrations less than 100 mg/l and sodium or sulfate as their dominant ion. The Puna shoreline warm springs also have chloride concentrations greater than 1,000 mg/l but will be grouped and discussed separately from the high chloride wells.

Because Hawaii lacks sedimentary basins which may contain saline connate waters, and Hawaiian basalts are very low in chlorine content (Macdonald et al, 1983), the only significant source of saline groundwater contamination is seawater, which has a chloride ion concentration of 19,400 mg/l (Henderson, 1982). Tidal fluctuations cause seawater-fresh water mixing near the coast, but shallow groundwater wells more than 5 km inland generally have chloride concentrations of less than 20 mg/l. These low, but detectable, chloride concentrations are believed to result from sea spray aerosols being blown inland by winds (Druecker and Fan, 1976). An average Hawaii groundwater chloride concentration of 10.4 mg/l was used for this study (Table 2).

In contrast to this general trend, several of the LERZ and LSF thermal wells show substantial chloride concentrations, even though they are well removed from the coast. There is also a positive correlation between chloride concentration and elevated temperature in these wells (Figure 14). The high chloride thermal wells, GTW-3 and Malama Ki, have temperatures of 84.8^0 and 53^0 C respectively, some of the highest temperatures presently encountered in groundwater wells in lower Puna.

Graphs of chloride concentrations in lower Puna high and medium chloride thermal wells and rainfall at Pahoa Station (#65) (Figure 4) over a twenty year period show a delayed inverse correlation between chloride concentration and rainfall (Figures 15 & 16): chloride concentrations increase when rainfall decreases and decrease when rainfall increases. This suggests a steady supply of chloride rich water is mixing with a fluctuating supply of fresh water recharge.

The correlation between elevated chloride concentrations and elevated temperatures in these wells is the heating of seawater, which underlies fresh basal groundwater, by a long lived magmatic heat source within the LERZ. Heating causes seawater density to be reduced. Thermal seawater rises convectively through and mixes with the fresh overlying groundwater, dominating the chemistry of the high and medium chloride thermal wells.

Ion concentrations in the low chloride thermal wells are slightly higher than in average Hawaii groundwater, except for sodium which is moderately enriched in all these wells and sulfate which is extremely enriched in some of them, and will subsequently be discussed in more detail. This enrichment, except for sulfate, is governed by mineral

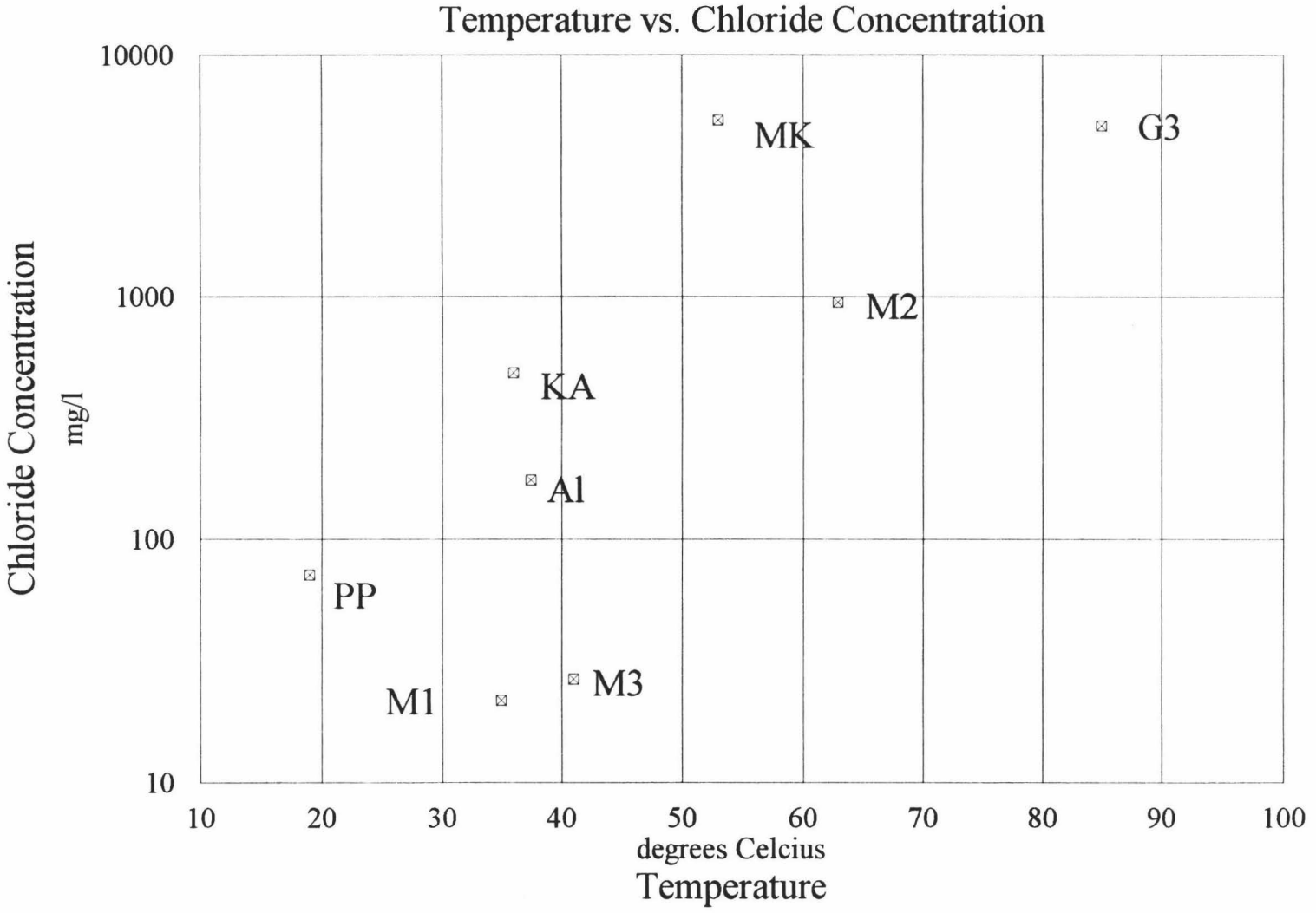

Figure 14. Temperature vs. chloride concentration in lower Puna thermal wells. Well name abbreviations in Table 1.

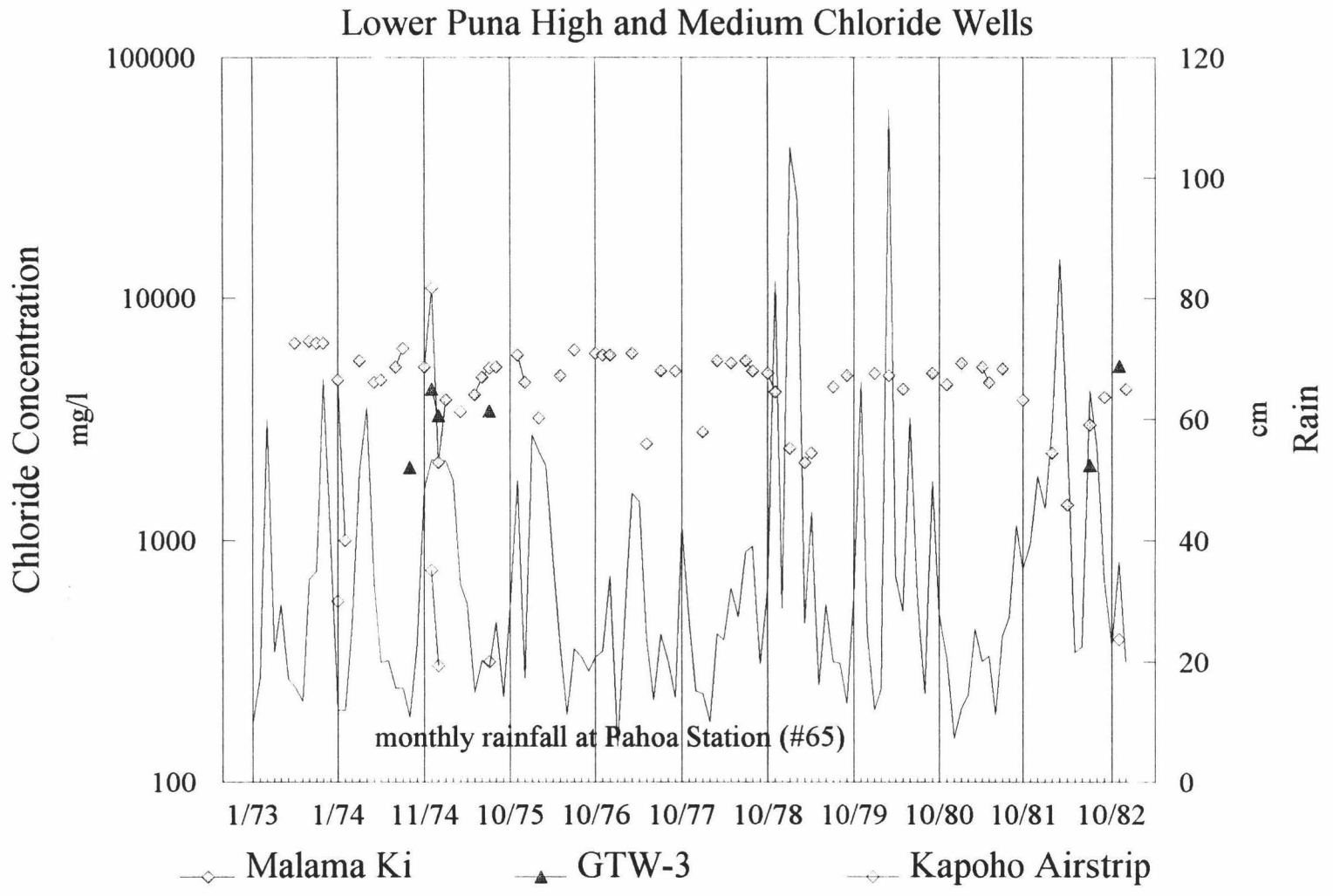

Figure 15. Rainfall versus chloride concentration 1973 - 1982

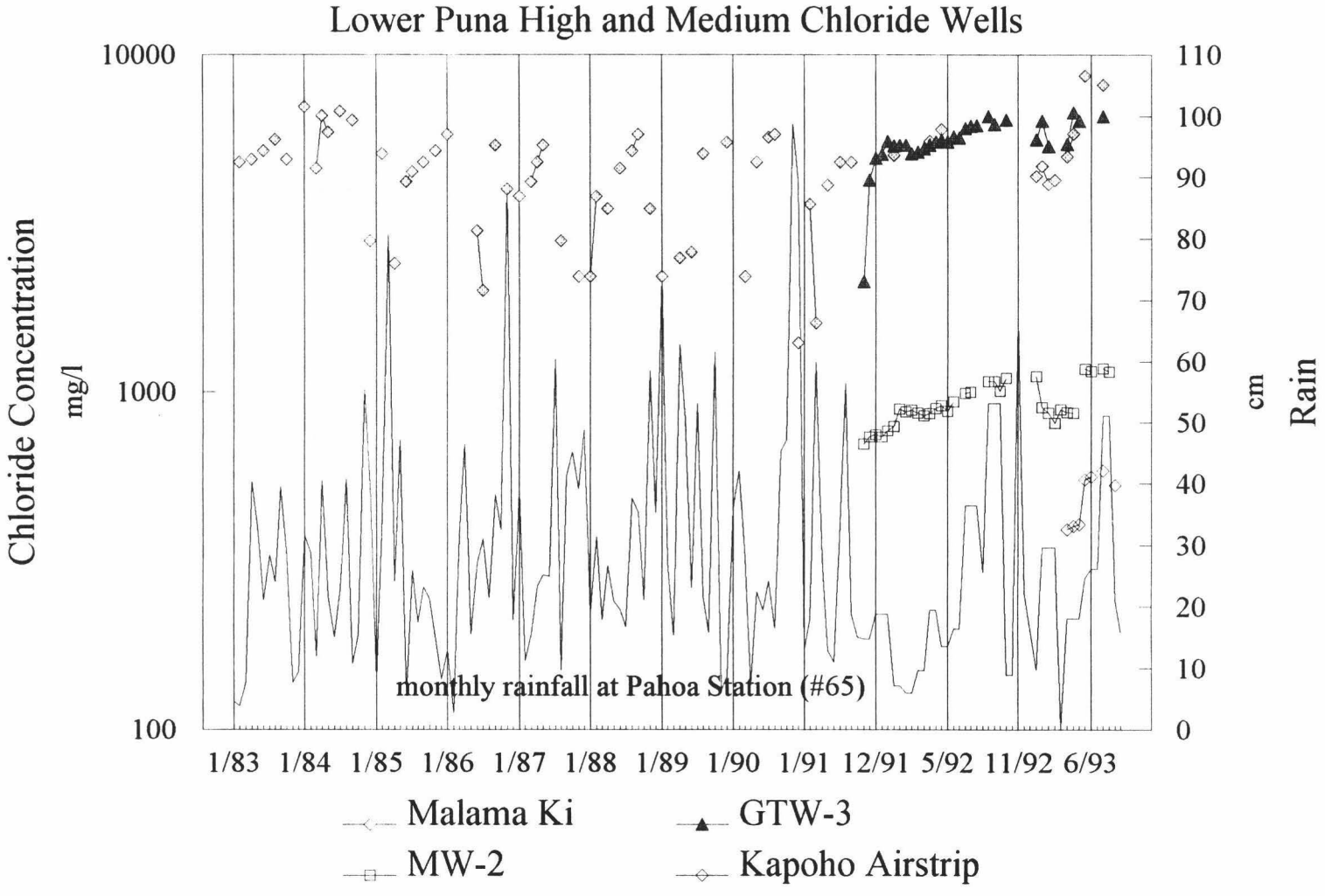

Figure 16. Rainfall versus chloride concentration 1983 -1993

equilibria, pH, and temperature (Ellis, 1970; Mahon, 1975). The tholeiite basalts penetrated by the low chloride thermal wells are no different than the tholeiite basalts penetrated by the non-thermal wells used to construct the ion concentrations for average Hawaii groundwater, and the thermal wells pH's are similar to average Hawaii groundwater pH (Tables 2, 3, & 4). Consequently, the cause of higher than ambient ion concentrations in these thermal well waters must be an effect of their higher than ambient water temperatures which produce greater solution of the major rock forming constituents; silica, sodium, potassium, calcium, magnesium, and iron. There are, therefore, two basic processes which control the chemistry of lower Puna waters; thermal seawater mixing and rock dissolution. Each well contains waters whose chemistry is controlled by a mixture of these two processes; the high chloride thermal wells are dominated by thermal seawater mixing, the medium chloride thermal wells show the effects of both thermal seawater mixing and rock dissolution, and the low chloride thermal wells are dominated by rock dissolution.

Question 2. What component waters are present in each well, and how have they been altered by contact with a thermal source?

The component composition of these mixed LERZ well and spring waters and the degree to which they have been modified by thermal sources may be examined in much more detail by comparing the chloride to ion ratios found in them with chloride to ion ratios for average Hawaii groundwater, Standard Mean Ocean Water (SMOW) (Henderson, 1990), and seawater reacted with basalt at different temperatures and

pressures under laboratory conditions. Ratios are used to remove the effects of variations in ion concentration between the mixed LERZ waters and the experimental samples. Chloride is chosen as the controlling ion for the following reasons:

1. The chloride ion is virtually stable in groundwater in both basaltic and sedimentary rocks, not entering into chemical reaction with other ions or anionic exchange within sediments (Schofield, 1956; Mink, 1961; Swain,1973).
2. Although a minor contribution of chloride from basaltic rocks to groundwater may occur at high temperatures, this effect in Hawaii is negligible, as the chloride content of Hawaiian lavas is 0.01 to 0.12% (Macdonald, et al., 1983).

Several laboratory studies have been undertaken to assess the extent of chemical exchange between basalt and seawater under controlled conditions of temperature and pressure. Those used for this study were conducted by Seyfried and Bischoff (1979), and Mottl and Holland (1978). Seyfried and Bischoff (1979) reacted sea water with a fresh tholeiite basalt glass dredged from the Juan de Fuca Ridge. The rock was powdered and a water to rock ratio of 10:1 was used. Two experiments were conducted, one at 70^0 C for a duration of 3,600 hours at atmospheric pressure, the other at 150^0 C for 3,564 hours at 500 bar pressure (Seyfried and Bischoff, 1979). The change in seawater chemistry at the conclusion of each experiment is presented in Table 5 in both mg/l and as chloride to ion ratios.

TABLE 5. SEYFRIED AND BISHOFF CHLORIDE TO ION RATIOS

Ion	SMOW mg/l	SMOW Cl/ion	70 ° C mg/l	70 ° C Cl/ion	150 ° C mg/l	150 ° C Cl/ion
Na^+	1,0770	1.80	10,270	1.80	10,500	1.76
K^+	380	51.05	371	49.89	388	47.71
Ca^{2+}	412	47.09	636	29.10	1,333	13.88
Mg^{2+}	1,290	15.04	1,083	17.09	1	18,510
Cl^-	19,400		18,510		18,510	
SO_4^{2-}	2,691	7.21	2,620	7.06	300	61.7
SiO_2	2	9,700	45.8	404.15	439	42.16

Ca^{2+} and SiO_2 increased in seawater in the 70° C experiment while K^+, Na^+, and Mg^{2+} decreased. Although the decrease in K^+ and Na^+ was small, the decrease in Mg^{2+} and increase in Ca^{2+} and SiO_2 was appreciable. Ca^{2+} and SiO_2 again increased in the 150° C experiment, Na^+ and K^+ increased slightly in contrast to the 70° C experiment, while Mg^{2+} and SO_4^{2-} decreased significantly.

Mottl and Holland conducted a series of somewhat more complicated experiments using fresh tholeiitic basalt from the Juan de Fuca ridge which was nearly identical in composition to that used by Seyfried and Bischoff (Mottl and Holland, 1978). Their samples were divided into holocrystalline, crystalline, crystalline plus glass, and glassy components which were separated and reacted with seawater at water to rock ratios of 1, 2, and 3. These ratios were chosen as representative of present and past subaerial geothermal systems (Mottl and Holland, 1978). Experiments were run at 200° C, 500 bar; 300° C, 600 bar; 400° C, 700 bar; and 500° C, 1,000 bar. Run times varied between 167 days and 602 days with longer duration runs at lower temperatures and shorter runs at higher temperatures. Averages from the different basalt components at water to rock

ratios of 1 for the 200° C, 300° C, and 400° C runs are presented in Table 6 as mg/l and as chloride to ion ratios. Runs were made with two different seawater samples which had different chloride concentrations (Cl^- = 19,010 mg/l for the 200° C run; Cl^- = 19,980 mg/l for the 300° and 400° C runs).

TABLE 6. MOTTL AND HOLLAND CHLORIDE TO ION RATIOS

Ion	200 ° C mg/l	200 ° C Cl/ion	300 ° C mg/l	300 ° C Cl/ion	400 ° C mg/l	400 ° C Cl/ion
Na^+	11,273	1.69	11,081	1.80	11,516	1.73
K^+	663	28.67	1,176	16.99	1,148	17.40
Ca^{2+}	1,069	17.77	2,112	9.46	1,507	13.26
Mg^{2+}	148	128	11.4	1,757	10	1,978
Cl^-	19,010		19,980		19,980	
SO_4^{2-}	315	60.35	254	78.57	453	44.11
SiO_2	593	32.03	594	33.62	1,626	12.28

Changes in major element concentrations were consistent with those described by Seyfried and Bischoff (1979) and consistent over the entire 200° C to 500° C temperature range. SiO_2 and Ca^{2+} increased significantly, K^+ increased as well, but its increase was supply limited, Na^+ decreased slightly, while Mg^{2+} and SO_4^{2-} dropped to low levels.

The relevance of these laboratory experiments to reservoir conditions in the LERZ geothermal field can be corroborated by comparing alteration mineral assemblages from the experiments with alteration minerals found in drill cores and cited in mud logs from LERZ exploration holes and geothermal wells. Both sets of authors report smectite and anhydrite formed as alteration minerals in their experiments at all temperatures. Mg^{2+} was lost from solution and incorporated into smectite by the following reaction:

$$Mg^{2+} + OH^- + H^+ \rightarrow Mg(OH)_2 + 2H^+ + \text{basalt} \rightarrow Ca^{2+} + \text{clay}.$$

Loss of Mg^{2+} from solution liberated H^+, which caused a radical decline in pH and an increase in the seawater buffering capacity due to the presence of weak acids such as HCO_3^-, HSO_4^-, and HCl, and of $MgOH^+$, a weak base. At temperatures above 200^0 C Mg^{2+} was rapidly and almost completely removed. To conserve charge balance, Mg^{2+} loss from solution was compensated by leaching of Ca^{2+} from the basalt to solution (Mottl and Holland, 1978). Some Na^+ for Ca^{2+} exchange also took place but at a much slower rate. Na^+ was taken from solution and incorporated into analcime which formed in the 300^0 C experiments.

Smectite and anhydrite are the two most abundant alteration minerals found in the Scientific Observation Hole cores (Novak, et al., 1990). They are also cited in the KS-3, KS-4, KS-7, KS-8, KS-9, and KS-10 mud logs (PGV, unpub. rpt.). Almost the entire alteration mineral assemblage reported by both sets of authors is present in both cores and mud logs from the Pohoiki geothermal field. Conversely therefore, the alteration in seawater chemistry produced in the high temperature seawater-basalt experiments discussed above should be a valid standard to judge the degree of alteration of thermal seawater mixed in LERZ well waters.

The seven lower Puna wells whose chloride to ion ratios were constructed from averages of several analyses, MW-1, MW-2, MW-3, GTW-3, Malama Ki, Kapoho Airstrip, and Allison, fall into two distinct groups (Table 7). The low chloride thermal wells, MW-1 and MW-3 (Figure 17), have essentially identical chloride to ion ratios. Their ratios are more similar to average Hawaii groundwater than to SMOW or thermal seawater-basalt solutions, but show a proportional enrichment in Na^+, K^+, Ca^{2+}, and Mg^{2+}

TABLE 7. CHLORIDE TO ION RATIOS OF LOWER PUNA WELLS AND SPRINGS

Well or Spring	Cl/Na	Cl/K	Cl/Ca	Cl/Mg	Cl/SO4	Cl/HCO3
av. Hawaii groundwater	1.07	5.16	1.67	2.8	1.63	0.235
GTW-3	1.592	20.3	24.2	30.6	6.98	187
MW-1	0.335	1.831	0.983	1.85	0.07	0.78
MW-3	0.41	2.445	1.184	2.125	0.088	1.033
Malama Ki well	2.079	39.5	36.1	23.5	8.95	37
MW-2	1.668	32.4	22.9	62.4	8	17.9
Kapoho Airstrip well	1.721	35.67	12.71	17.64	2.91	14.93
Allison well	1.49	13.84	20.13	16.76	4.13	2.12
KS-3 (wtr samp)	0.21	2.12	0.65	1.94		
KS-4 (wtr samp)	0.33	1.92	0.27	1.03	0.14	
KS-7 (wtr samp)	0.575	6	4.35	13.64	0.58	1.19
KS-8 (wtr samp)	1.88	21.3	1.8	6.72	1.88	2.18
KS-9 (wtr samp)	2.03	23.15	7.13	19.03	2.35	
KS-10 (wtr samp)	0.86	7.72	1.74	3.74	0.41	
Isaac Hale spring	2.65	155.52	60.01	23.04	10.7	
Campbell spring	2.6	94.8	62.45	24.87	11.04	
Pualaa spring	1.72	74.97	43.59	20.58	11.31	
Kapoho Bay spring	2.48	1393.7	51.55	22.85	9.95	

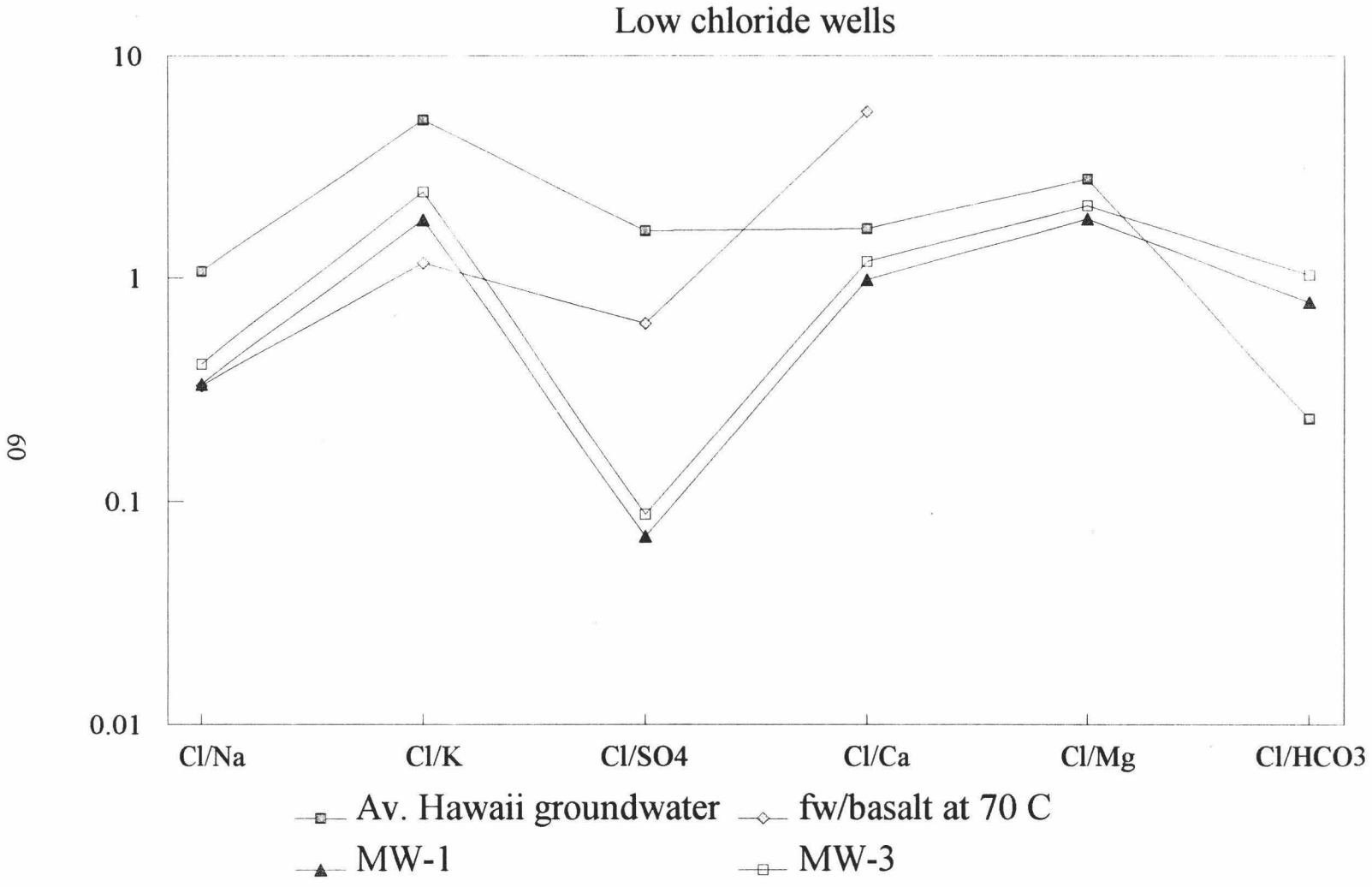

Figure 17. Chloride to ion ratios in low chloride well waters.

compared to average Hawaii groundwater. They also show a disproportional enrichment in SO_4^{2-} and depletion in HCO_3^- when compared to average Hawaii groundwater. The medium and high chloride well chloride to ion ratios, however, show a strong resemblance to those of SMOW or low temperature thermally altered seawater-basalt solutions (Figure 17).

The approximately 2:1 chloride to magnesium ratio, and magnesium concentration of ~12 mg/l found in MW-1 and MW-3 suggest that these waters have not reacted with a high temperature thermal source. Basalt reacted with distilled water at 150^0 C and 200^0 C produced chloride to magnesium ratios of 21:1 and 58:1 respectively (Ellis and Mahon, 1964).

There are two possible sources for the disproportionate enrichment in sulfate in MW-1 and MW-3 waters, solution of anhydrite or steam heating. The solution of anhydrite ($CaSO_4$) would cause a corresponding enrichment in Ca^{2+} which is not present in MW-1 and MW-3 waters. It is, therefore, more probable that the sulfate enrichment in these waters is the result of steam heating. Hydrogen sulfide comprises 67% of the gas fraction in Pohoiki geothermal field steam (Delanoy, unpub.). As geothermal steam leaks up into the LERZ unconfined groundwater aquifer, hydrogen sulfide in it is oxidized to sulfate (Giggenbach, 1988). Consequently, the input from depth to these wells is mostly enthalpic, the gas carries heat but little mass. Therefore, MW-1 and MW-3 are not mixed water wells in the same sense that the medium and high chloride wells are mixed water wells. They are meteoric groundwater wells whose hot component is also steam heated

meteoric groundwater, not thermally altered seawater. This is apparent in their close resemblance to average Hawaii groundwater chloride to cation ratios.

The medium and high chloride wells whose chloride to ion ratios have been constructed from averages of several analyses are Allison, Kapoho Airstrip, Malama Ki, GTW-3, and MW-2 (Table 7) (Figure 18). The chloride to ion ratios of these wells will be discussed in order of their increasingly altered thermal seawater fraction.

Allison well (Figure 19), shows the least altered chloride to magnesium ion ratio, equal to that of SMOW or seawater reacted with basalt at 70 ^{0} C. All other chloride to ion ratios fall between those of SMOW and average Hawaii groundwater. Allison well's moderate chloride concentration, 175 mg/l, and extremely low average silica concentration, 31.5 mg/l, are good evidence that water in this well is a mixture of cold meteoric groundwater and slightly heated brackish water.

Kapoho Airstrip well (Figure 20) also shows an almost unaltered chloride to magnesium ion ratio. It approximately coincides with that of seawater reacted with basalt at 70^{0} C. The chloride to calcium ion ratio, however, is enriched in calcium ion to nearly that of seawater reacted with basalt at 300^{0} C. Kapoho Airstrip also shows an enrichment in sulfate and bicarbonate proportionally greater than that of SMOW. A possible explanation for this anomalous enrichment in Ca^{2+} and sulfate lies in the solution of gypsum and anhydrite. These minerals are common at depth in the Pohoiki geothermal field and are the most abundant secondary minerals in Scientific Observation Hole #1 cores (Novak, et al, 1990). They are precipitated as seawater is heated within the LERZ and, because of their retrograde solubility, may later be taken into solution again as

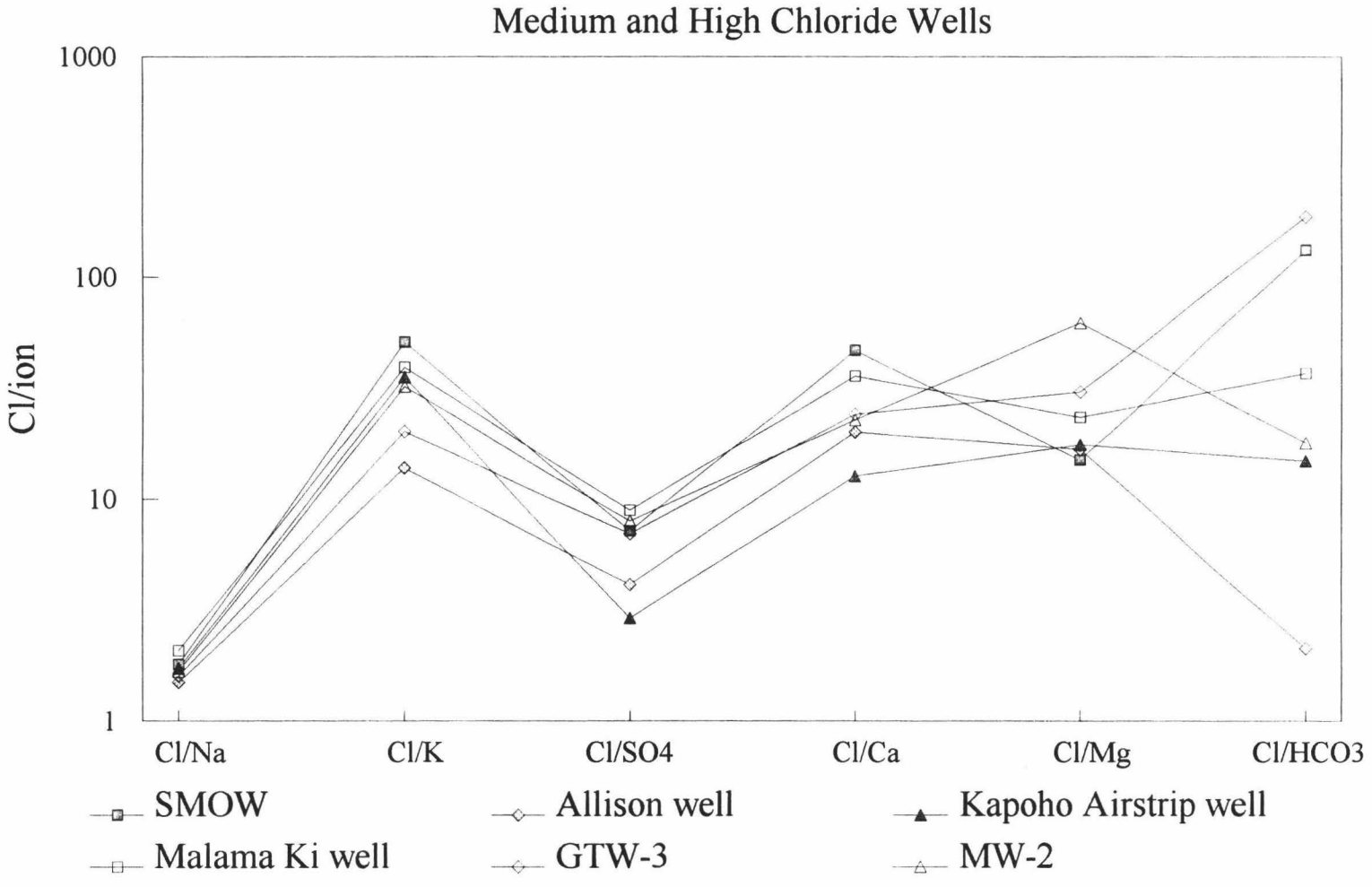

Figure 18. Chloride to ion ratios in medium and high chloride well waters.

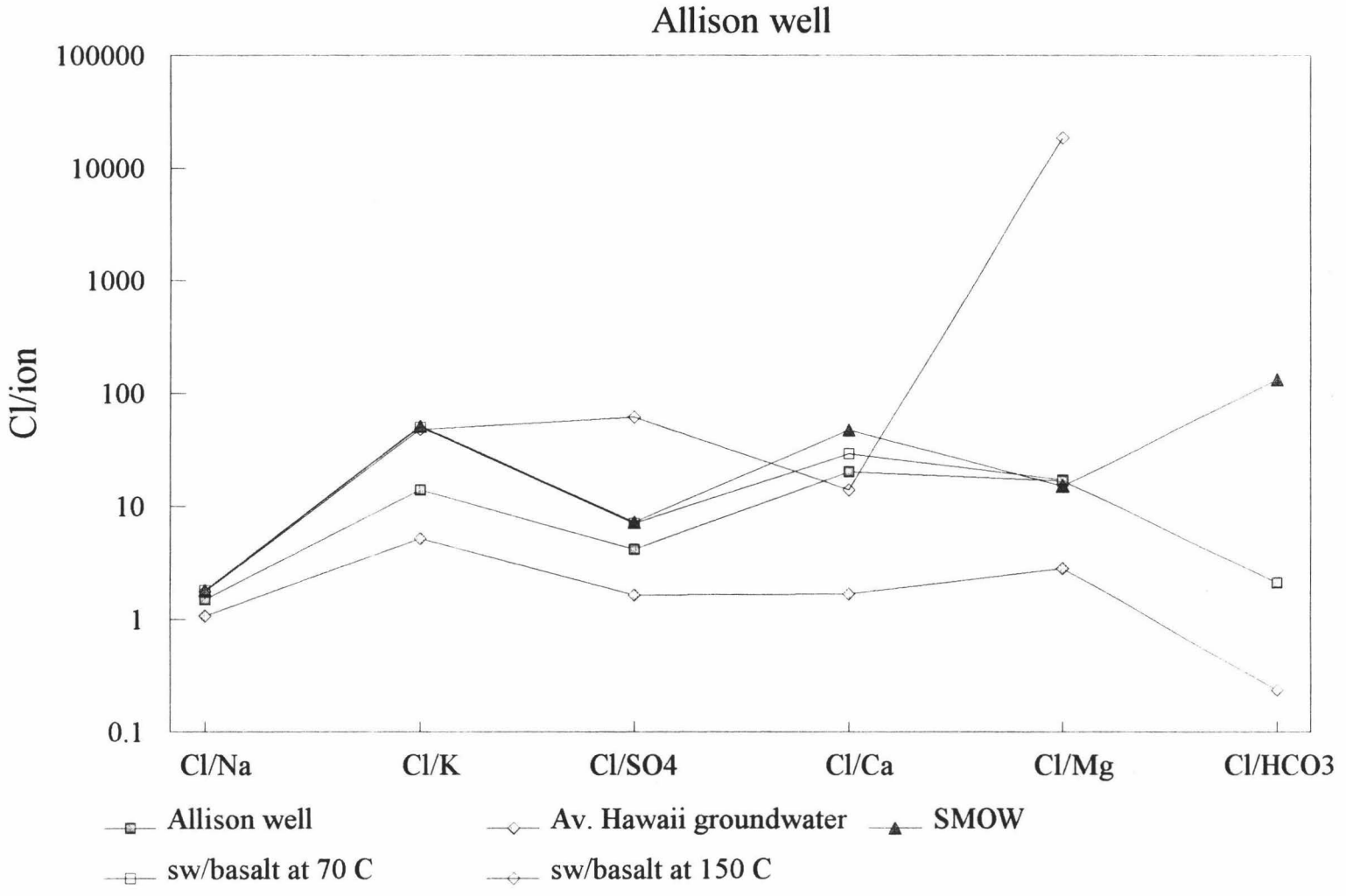

Figure 19. Chloride to ion ratios in Allison well.

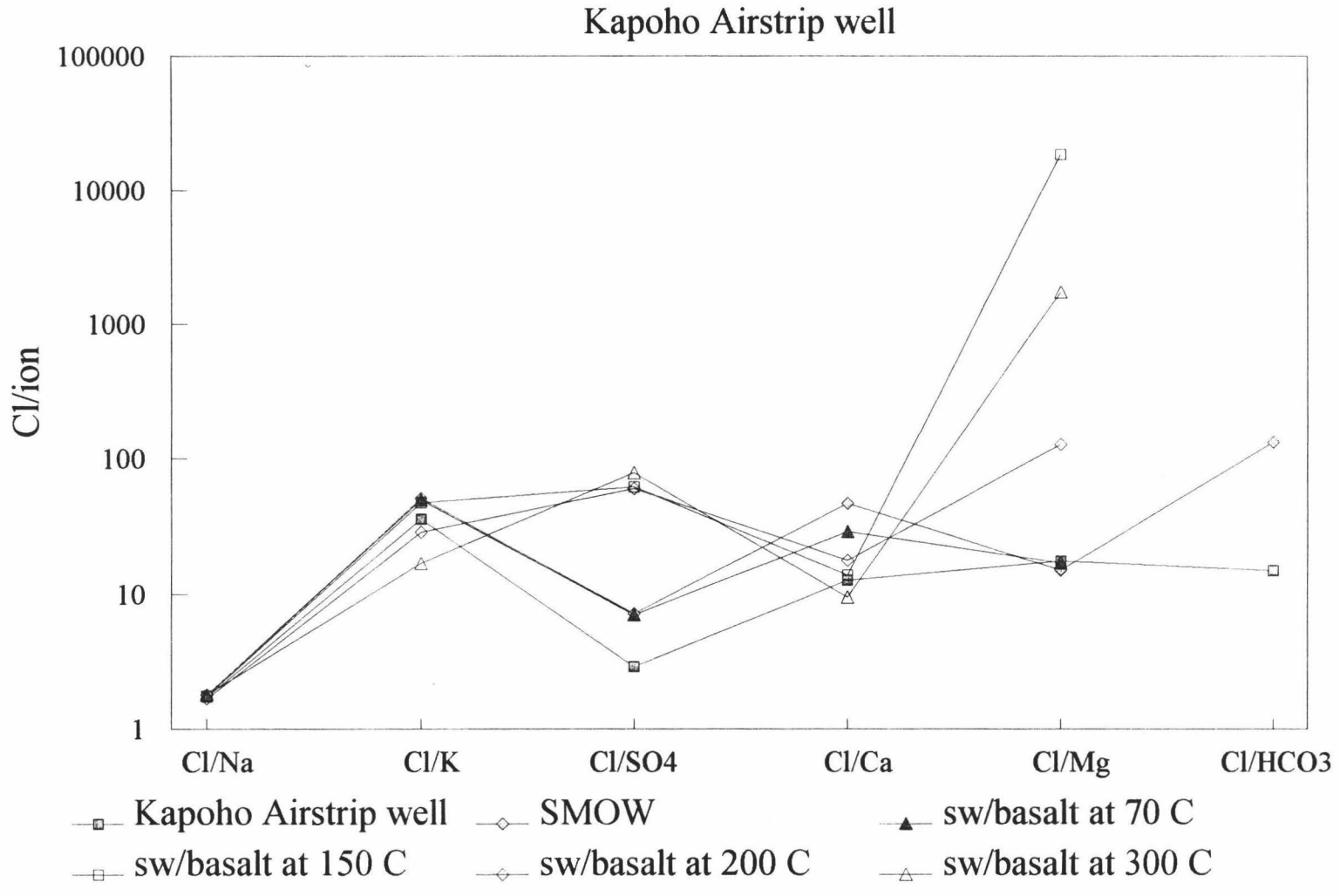

Figure 20. Chloride to ion ratios in Kapoho Airstrip well.

temperatures fall locally within the hydrothermal system. A second possible explanation for Kapoho Airstrip well's sulfate enrichment lies in the close resemblance its chloride to ion ratios bear to those of MW-1 and MW-3 (Figure 17). Because of the increase in chloride and cations compared to MW-1 and MW-3, Kapoho Airstrip well obviously receives an additional fraction of thermal seawater which is absent in these wells, but it may also receive a portion of the waters which pass through MW-1 and MW-3. It is the only well outside the Pohoiki geothermal field to show a significant sulfate enrichment compared to SMOW. From the foregoing discussion it is reasonable to assume that Kapoho Airstrip well water is either a two component mixture of slightly altered thermal brackish water and cold groundwater which has passed through gypsum-anhydrite deposits, or a three component mixture of steam heated groundwater, slightly altered thermal brackish water, and cold groundwater.

Malama Ki (Figure 21) well represents a less complicated system. Its waters appear to be a simple mixture of cold groundwater and slightly altered thermal brackish water. Its chloride to magnesium, sulfate, and potassium ion ratios are between those of seawater reacted with basalt at 70^0 C and 200^0 C, but closer to 70^0 C. Its chloride to calcium ion ratio is between SMOW and seawater reacted with basalt at 70^0C.

GTW-3 well (Figure 22), the hottest of the LERZ water wells, contains a moderately altered thermal brackish water component. Its chloride to magnesium, calcium, and sulfate ion ratios are between those of seawater reacted with basalt at 70^0 C and 200^0 C. Its chloride to potassium ion ratio is between seawater reacted with basalt at 200^0 C and 300^0 C.

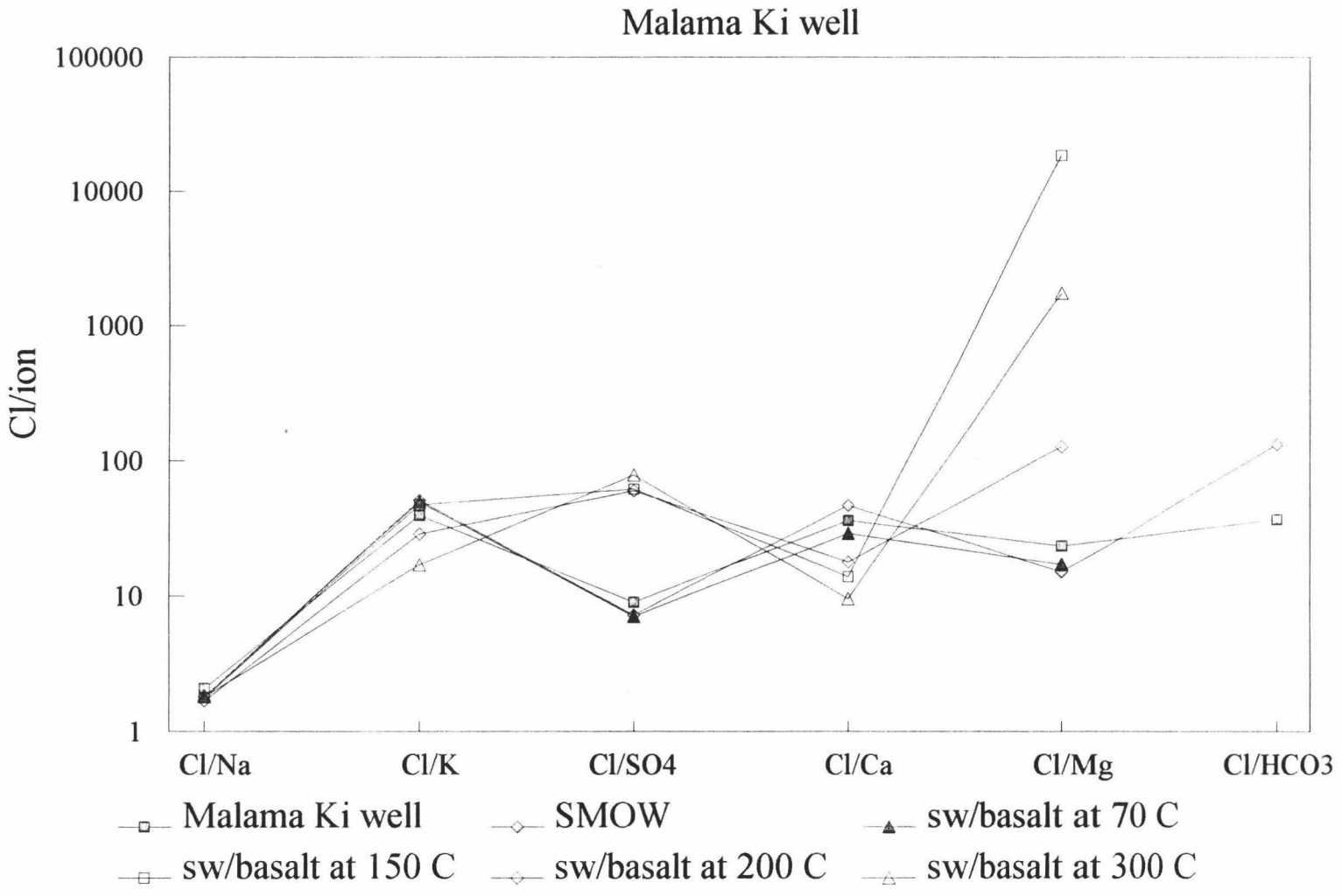

Figure 21. Chloride to ion ratios in Malama Ki well.

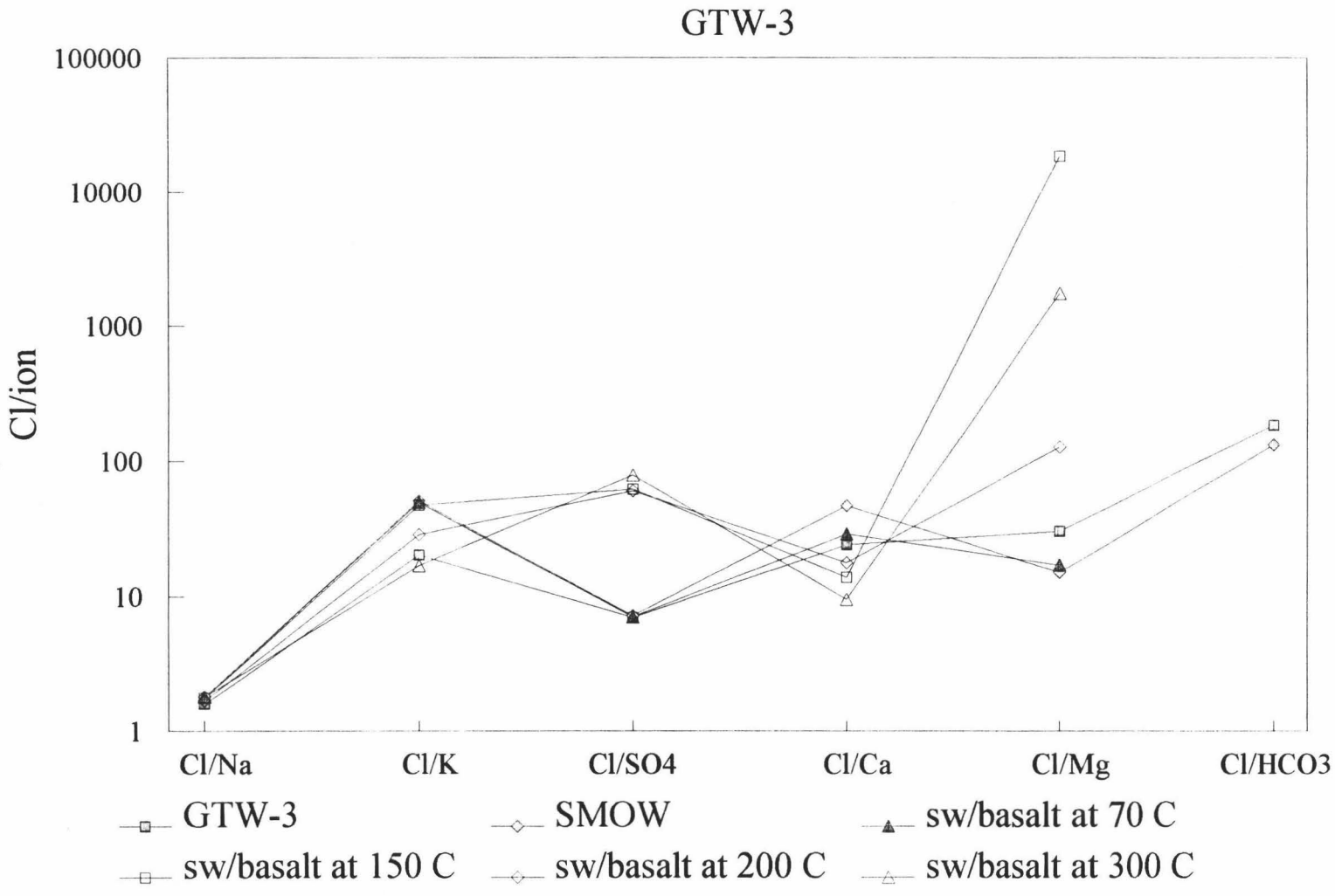

Figure 22. GTW-3 chloride to ion ratios.

MW-2 well (Figure 23), the second hottest LERZ water well, has the most altered thermal brackish water component. Its chloride to magnesium and calcium ion ratios are between those of seawater reacted with basalt at 70^0 C and 200^0 C, but closer to 200^0 C. Its chloride to potassium and sulfate ion ratios are those of SMOW.

Chloride to ion ratios for KS-3, KS-4, KS-7, KS-8, KS-9, and KS-10 (Table 7) were constructed from an analysis of one water sample from each well which was collected by bailing when drilling intersected the water table. They are, therefore, not as accurate a representation of the waters in the various KS series wells as the chloride to ion ratios constructed from numerous samples from the already existing LERZ water wells. Nor are they complete analyses, and often have poor ion balances. Nevertheless, except for the analyses from MW-2, they are the only existing data on groundwater within the Pohoiki geothermal field.

The most striking feature of the KS series wells water sample analyses is their wide range of constituent concentrations over the small area of the Pohoiki geothermal field (Figure 6). Chlorides range from a low of 7 mg/l in KS-3 to a high of 570 mg/l in KS-8. KS-3, KS-4, and KS-10 are low chloride wells and KS-7, KS-8, and KS-9 are medium chloride wells. Only KS-10 shows any resemblance to average Hawaii groundwater (Figure 24). The other low chloride wells, KS-3 and KS-4 are enriched in sodium, potassium, calcium, and magnesium ions compared to average Hawaii groundwater. The medium chloride wells all show calcium and magnesium to chloride ion ratios close to those of SMOW and seawater reacted with basalt at 200^0 C. KS-7 is enriched in sulfate compared to SMOW, whereas KS-8 and KS-9 show chloride to sulfate ratios close to

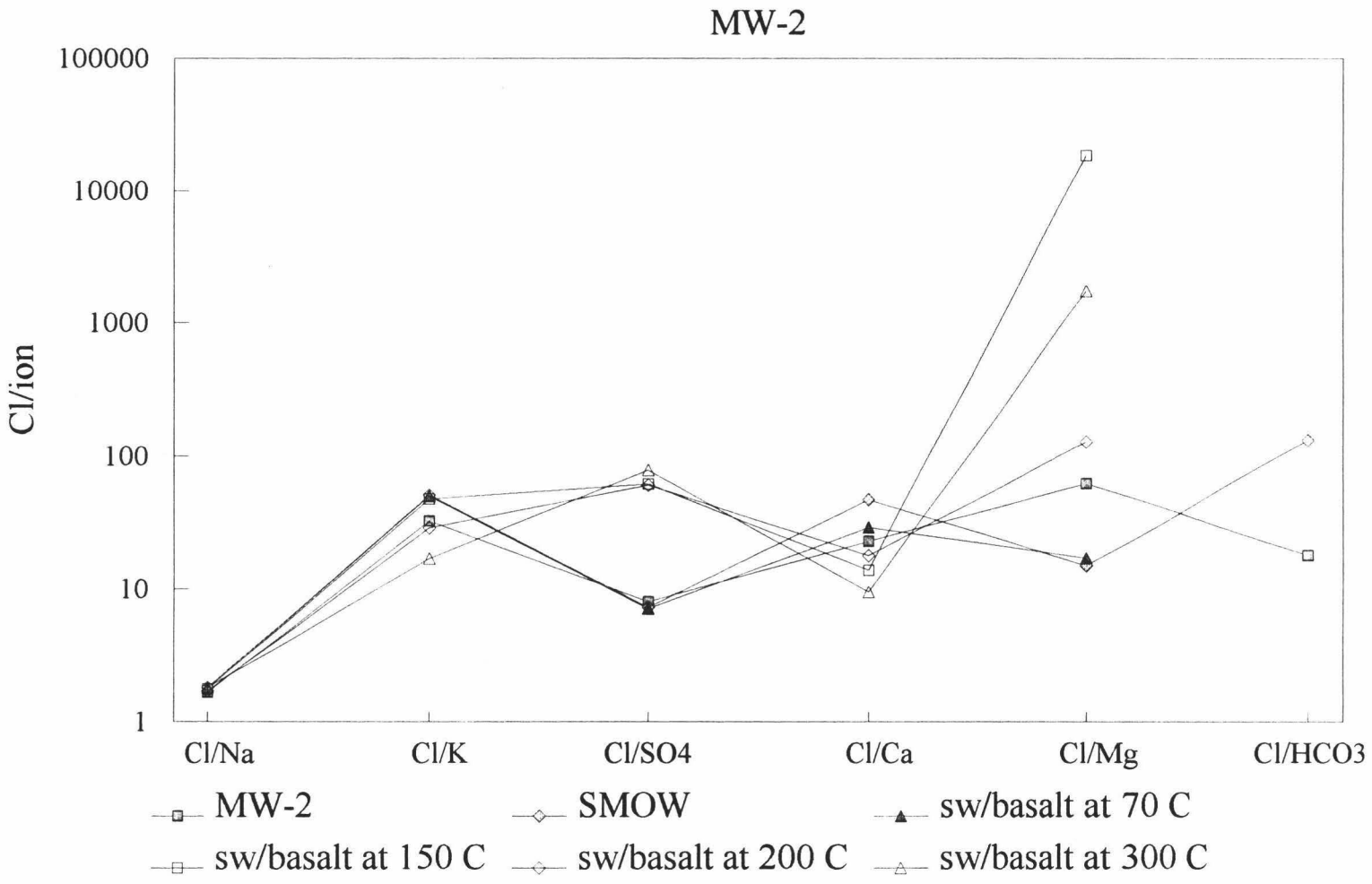

Figure 23. Chloride to ion ratios in MW-2.

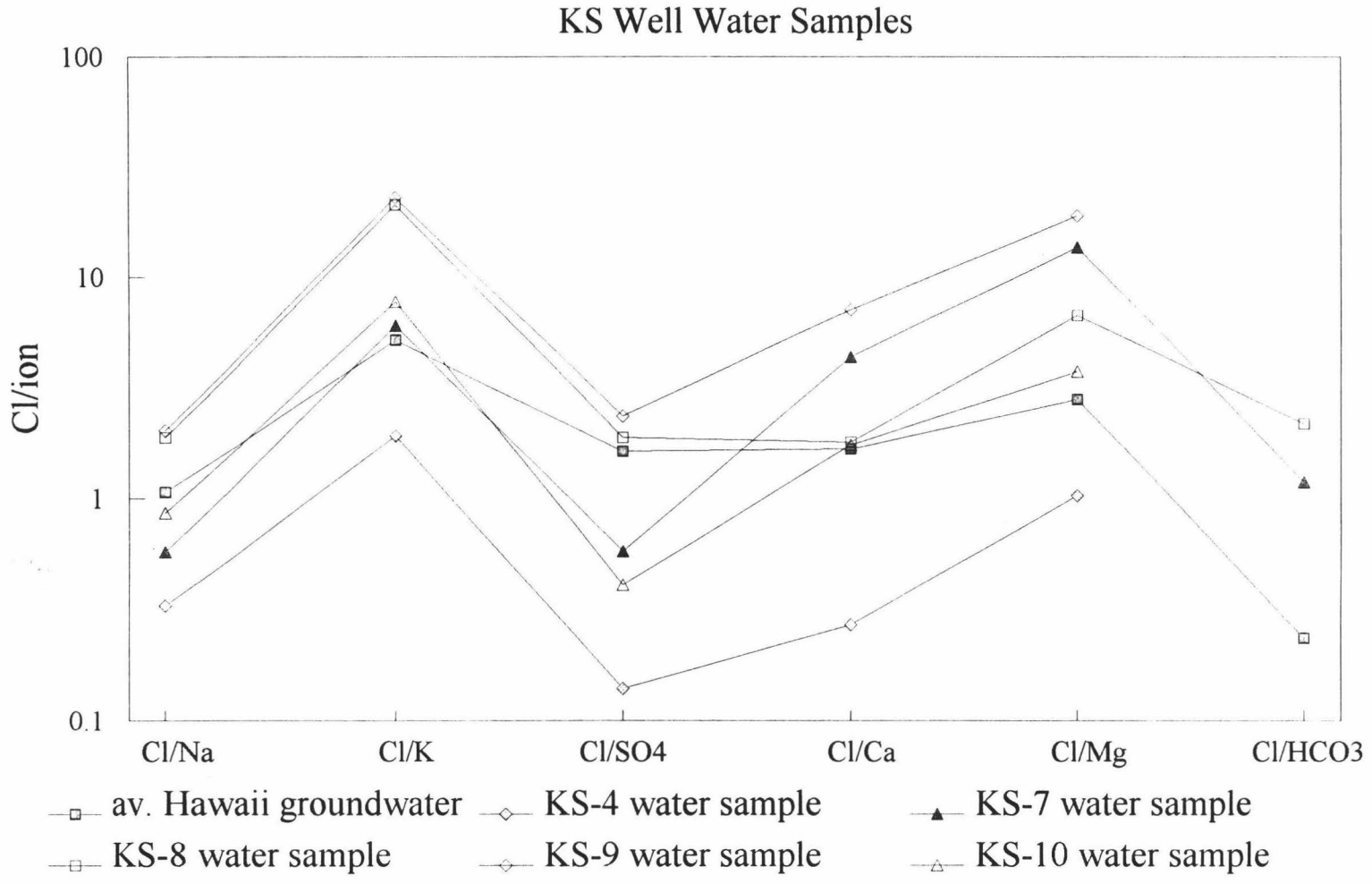

Figure 24. Chloride to ion ratios in KS series wells.

those of SMOW. All the KS series wells are enriched in sulfate compared to SMOW and average Hawaii groundwater which may be evidence of steam heating. The low chloride KS wells are mixed cold meteoric groundwater and steam heated groundwater. The medium chloride KS wells are two or three component wells containing either cold meteoric groundwater and steam heated, thermally altered brackish water, or cold meteoric groundwater, steam heated meteoric groundwater, and thermally altered brackish water.

The Puna shoreline warm springs (Table 7 and Figure 25) form the most coherent chloride to ion ratio group. This, however, is due to the large fraction of cold seawater present in these springs, not to any consistency in the thermal portion of their components. All the springs have chloride to potassium, sulfate, and magnesium ion ratios more depleted than those of seawater reacted with basalt at 70^0 C. Pualaa, the hottest, has a chloride to calcium ion ratio more enriched than that of SMOW. Since sulfate and magnesium depletion and calcium enrichment are the signature of thermally altered seawater, it may be assumed that these springs also contain a fraction of thermally altered seawater. Chloride concentrations in the Puna shoreline warm springs are 25% to 30% those of seawater. These springs, therefore, represent another form of three component mixing. Their waters are composed of cold seawater, thermally altered brackish water, and meteoric groundwater.

In summary, waters of the lower Puna wells and warm springs can be divided into four types of mixed waters, which are presented in Table 8.

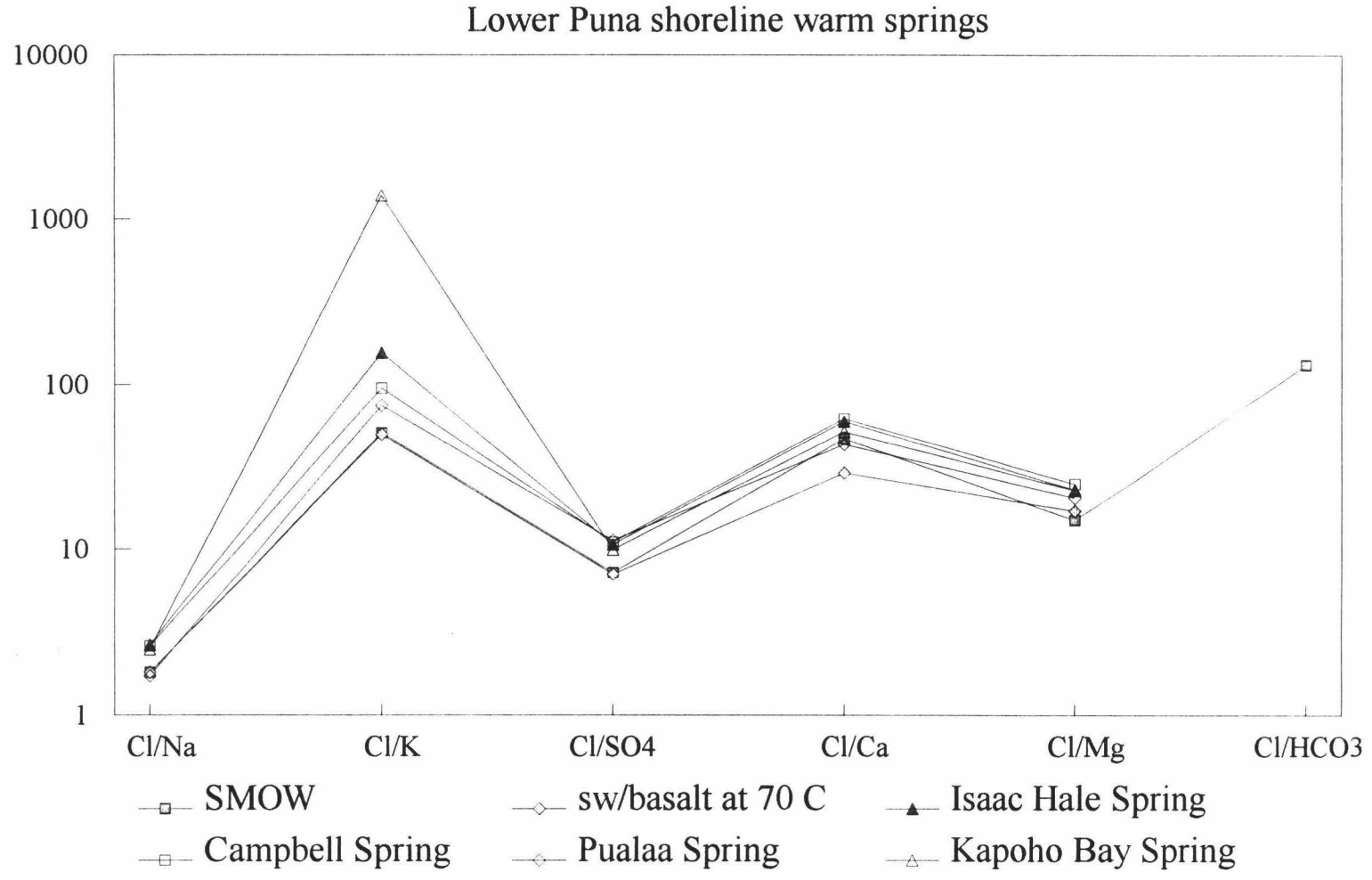

Figure 25. Chloride to ion ratios in lower Puna shoreline warm springs.

TABLE 8. LOWER PUNA MIXED WATER TYPES

MIXED WATER TYPE	MIXTURE	CHEMICAL SIGNATURE	WELL OR SPRING
1	cold meteoric groundwater/ steam heated meteoric groundwater	Cl- <100mg/l enriched SO4	MW-1,-3, KS-4,-10
2	cold meteoric groundwater/ steam heated meteoric groundwater/ thermally altered seawater	100 mg/l<Cl-<1000 mg/l enriched SO4	KS-7,-8,-9 Kapoho Airstrip
3	cold meteoric groundwater/ thermally altered seawater	100 mg/l<Cl-<1000 mg/l Cl->1000 mg/l no SO4 enrichment	MW-2, Allison GTW-3, Malama Ki
4	cold meteoric groundwater/ thermally altered seawater cold seawater	Cl->1000 mg/l no SO4 enrichment	Kapoho Bay Spring Pualaa Spring Campbell Spring Isaac Hale Spring

Question 3. Are lower Puna waters at water-rock equilibrium?

W. F. Giggenbach devised a system which permits assessment of the "maturity" of thermal waters. He postulated two end member processes which govern the composition of thermal waters. The first is isochemical dissolution of rock material in contact with the fluid, and the second is equilibration of the fluid with the thermodynamically stable alteration mineral assemblage resulting from recrystallization of the primary rock at a given temperature and pressure (Giggenbach, 1988). The first process produces an "immature" fluid which implies short aquifer residence time; the second produces a "mature" fluid at full equilibrium which implies long residence in a stagnant aquifer. In dynamic hydrothermal systems fluids usually reach some complex steady state composition between these two end members.

The maturity of a water is graphically assessed in the following manner. A standard trilinear diagram for the system Na^+-K^+-$\sqrt{Mg}^{2+}$ is overlaid by isotherms derived from two geothermometers, K^+-Na^+ and K^+-$\sqrt{Mg}^{2+}$, using the following equations:

$$\log(C_{K}^{+}/C_{Na}^{+}) = 1.75 - (1390/T) \qquad 2.$$

$$\log(C^{2}_{K}{}^{+}/C_{Mg}^{2+}) = 14.0 - (4410/T) \qquad 3.$$

Where C is concentration in mg/kg and T is in degrees Kelvin.

The relative concentrations of K^+ and Na^+ are determined by the equilibrium constant governing the reaction: albite + K^+ = K-feldspar + Na^+. Which becomes, with

$$\gamma Na^+ = \gamma K^+$$

$$K_2 = (a_{Na}{}^{+}/a_{K}{}^{+})(a_{\text{K-feldspar}}/a_{\text{albite}}) \cong 1.7\ C_{Na}{}^{+}/C_{K}{}^{+} \qquad 4.$$

Where γ is the ion activity coefficient, K_2 is the equilibrium constant, and a is the activity.

Similarly, relative concentrations of K^+ and Mg^{2+} were obtained from the reaction:

0.8 muscovite + 0.2 clinochlore + 5.4 silica + $2K^+ \rightarrow$ 2.8 K-feldspar + 1.6 water + Mg^{2+}.

These equilibria are applicable in Hawaii, as Na-feldspar is common in Hawaiian basalts (Macdonald et al, 1983). Muscovite and clinochlore are incorporated into chlorites (Giggenbach, 1988) which are common basalt alteration products and have been found in all Scientific Observation Hole cores (Novak, et al., 1990).

The full equilibration curve for both mineral systems is drawn where the K^+-Na^+ and K^+-Mg^{2+} isotherms intersect (Figure 26). The lower curve defines the border between partially equilibrated waters and immature waters, above which the Na-K-Mg geothermometer can be confidently applied and below which the effects of rock dissolution are dominant and the cation geothermometers are inapplicable (Figure 26). An empirically derived line is present at the bottom right corner of the diagram representing the dissolution of 1,000g, 100g, and 10g of a basalt in 1,000g of water (Figure 26).

Concentrations of Na^+, K^+, and Mg^{2+} in mg/kg are converted to percentages by the following formulae which accommodate differences in concentration and charge;

$$C_{Na}^{+}/1000 + C_{K}^{+}/100 + \sqrt{C_{Mg}} = S \qquad 5.$$

$$\%Na^+ = C_{Na}^{+}/10S \qquad 6.$$

$$\%Mg^{2+} = 100\sqrt{C_{Mg}}/S \qquad 7.$$

and plotted on the trilinear diagram. The results of this method are presented in Figure 26.

The proportion of seawater in the high chloride wells and springs controls their position on the Giggenbach diagram. Seawater plots in the partially equilibrated field at

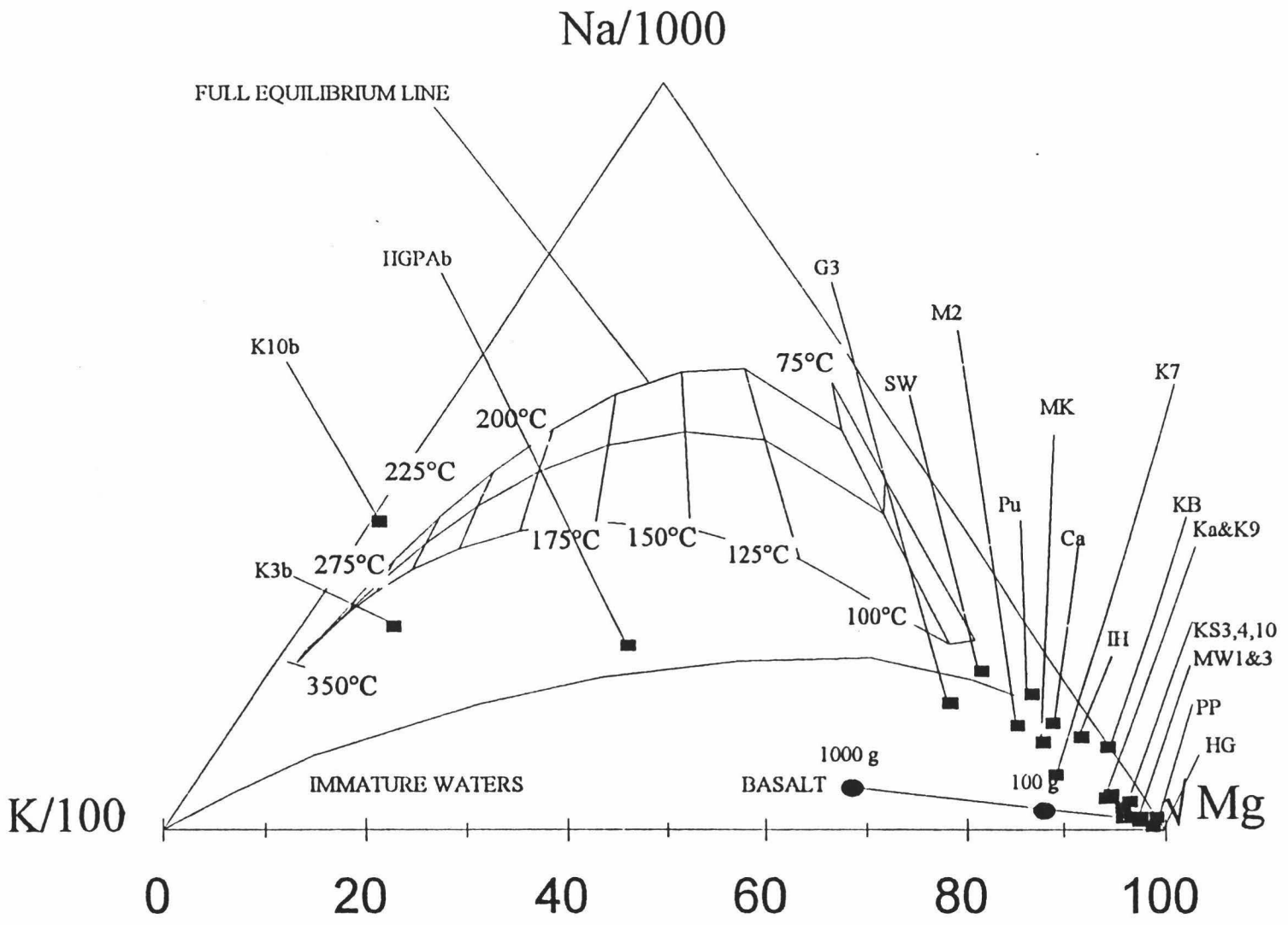

Figure 26. Giggenbach "maturity diagram". Well name abbreviations in Table 1.

160^0 C on the K-Na isotherm and 100^0 C on the K-Mg isotherm, possibly because of its interaction with basaltic material along the mid ocean-ridges. Average Hawaii groundwater plots in the extreme lower right corner of the diagram on the basalt dissolution line and all the low chloride well waters plot in a cloud slightly above the basalt dissolution line. The medium and high chloride well waters plot on an arc which parallels the immature/partially mature boundary arc, and is an indication that their seawater portions have undergone some thermal alteration. The Puna shoreline warm springs, which appear to be the most mature because they contain the most seawater, plot on the boundary arc or on an arc to seawater. From their placement on the Giggenbach diagram, it can be concluded that lower Puna wells and springs contain immature or slightly thermally altered waters whose residence times in the lower Puna groundwater system have been short. None of these wells or springs appear to contain a thermal water portion whose chemistry is typical of deep geothermal reservoir fluids. An early analysis of brine from HGP-A (Thomas, 1985) and an analysis of post 11/93 brine from KS-10 (Delanoy, unpub.) have been included on the diagram to illustrate the difference between these fluids and the lower Puna well and spring waters.

Silica Geochemistry

Question 4. What was the temperature of the thermal source this water encountered?

The last three of the introductory questions are intimately related and can be quantitatively assessed. Several workers, but especially R. O. Fournier and A. H. Truesdell, have developed geothermometers based on the concentration of silica, or the

ratios of the major cations (sodium, calcium, magnesium, and potassium) in thermal waters (Fournier and Truesdell, 1973; Truesdell and Fournier 1975). The cation geothermometers are inapplicable to shallow Hawaii groundwater for two reasons. First, the cation geothermometers assume equilibria between fluid and secondary minerals. As has been shown in the previous section, the chemistry of the lower Puna low chloride thermal wells is controlled by rock dissolution. Their waters are "immature", therefore, not at water - rock equilibrium. Second, the lower Puna high and medium chloride thermal wells are contaminated by seawater, and the seawater cation ratios obscure the cation ratios produced by thermal fresh water - rock interaction.

R. O. Fournier's silica geothermometers utilize a species which is present in seawater at only 2 mg/kg (Henderson, 1982). Although silica is a rock dissolution product, it's concentration is governed strictly by increasing temperature and pressure (Fournier, et al, 1974). Five basic conditions should be met for the application of a silica geothermometer to be accurate. They are:

1. Temperature dependent reactions occur at depth.
2. All constituents involved in a temperature dependent reaction are sufficiently abundant (supply is not a limiting factor).
3. Water-rock equilibration occurs at the reservoir temperature.
4. Little or no re-equilibration or change in composition occurs at lower temperatures as the water flows from the reservoir to the surface.
5. The hot water coming from deep in the system does not mix with the cooler shallow ground water (Fournier, et al, 1974).

The first condition requires the identification of the polymorph of silica which controls solubility at depth. Arnorsson (1975) applied the silica geothermometers to high temperature hydrothermal areas in Iceland, a basaltic environment similar to Hawaii. He found, from comparison of calculated "silica temperatures" with temperatures measured in drill holes, that the solubility of chalcedony controlled the amount of dissolved silica in thermal waters when temperatures were below about 110^0 C, and that solubility of quartz was the control at temperatures above 180^0 C. Neither mineral's solubility appeared to control exclusively the amount of dissolved silica in the interval between 110^0 and 180^0 C (McMurtry, et al, 1977).

The second condition is validated by the presence of the controlling polymorph within the hydrothermal system. Secondary quartz is present in all Scientific Observation Hole cores (Novak, et al., 1990) and is cited in mud logs from KS-3, KS-4, KS-7, KS-8, KS-9, and KS-10 (Puna Geothermal Venture, Drilling Reports, 1990-1992).

Conditions three and four are dependent on the volume and rate of groundwater flow through the hydrothermal system. The average volume of groundwater visibly discharged along the coast by basal springs from Hilo to Kalapana is 215 billion liters per year (Stearns and Macdonald, 1946). This large flow rate coupled with high intrinsic permeabilities, estimated at 4,000 to 5,000 darcies in the lower Puna groundwater aquifer (Druecker and Fan, 1976), suggests that little or no re-equilibration occurs as water rises from the deep reservoir to the surface. Ion geochemistry suggests that water flowing through the hydrothermal system may not have time to establish equilibrium with reservoir conditions, but experimental work has shown that silica dissolution is very rapid above

150^0 C, coming to equilibrium, in a pumice, in less than 24 hours (Ellis and Mahon, 1964).

Condition five is not met in the lower Puna wells, as the high and medium chloride well waters are obviously mixed with thermal seawater. Since silica in the low chloride wells is not at equilibrium for either quartz or chalcedony for their temperatures, they must be considered to represent mixtures of groundwater and thermal water of meteoric origin.

R. O. Fournier and A. H. Truesdell (1974) have developed two models for estimating the temperature and fraction of hot water mixed with cold water in a warm well or spring. Model 1 assumes that steam rises to the surface with the warm mixed water, while model 2 assumes that steam is separated from the hot water at atmospheric pressure before mixing occurs. Model 2 has been chosen for this study for a number of reasons.

1. Although there are few permanent fumaroles on the LERZ, steaming ground is occasionally observed and fumaroles are numerous on the MERZ and UERZ.
2. Steam escapes from all Kilauea fumaroles at atmospheric pressure and, from almost all, at or below atmospheric boiling temperature (Casadevall and Hazlett, 1983).
3. High permeability of Hawaiian lavas favors the escape of steam from unconfined groundwater.

In addition to the first four conditions for applying the silica geothermometers, the application of model 2 requires a knowledge of the temperature and silica content of the cold water. This was obtained from the average Hawaii island groundwater (Table 2) and

is 20.43^0 C and 40.74 mg/kg respectively. The temperature and silica content of the warm spring must also be known (Tables 3 & 4).

Model 2 consists of an enthalpy and a mass balance equation. These two equations can be written to solve for two unknowns, the temperature of the hot water and the proportions of the hot and cold water, because the silica content and temperature of the warm spring are different functions of the original hot water component (Fournier and Truesdell, 1974). The first equation relates the enthalpies, in calories per gram, of the hot water, H_{hot}; the cold water, H_{cold}; and the spring water, H_{spg}; to the fractions of the cold water, X; and the hot water, (1-X) as follows:

$$(H_{cold})(X) + (H_{hot})(1-X) = H_{spg} \qquad 8.$$

(Fournier and Truesdell, 1974)

The second equation (Equation 9) relates the silica content, in mg/kg, of the hot water, Si_{hot}; the cold water, Si_{cold}; to the spring water, Si_{spg}, as follows:

$$(Si_{cold})(X) + (Si_{hot})(1-X) = Si_{spg} \qquad 9.$$

(Fournier and Truesdell, 1974)

Equation 8 is solved by substituting the atmospheric boiling temperature, 100^0 C, of the sea level lower Puna water table, for H_{hot} to obtain X. This value of X is then used in Equation 9 to obtain Si_{hot}, the residual silica content of the hot water. Once the residual silica content has been estimated, it's logarithm can be inserted into the following quartz geothermometer equation to yield the minimum temperature, in degrees Celsius, of the hot water fraction present in the spring or well.

$$1522/(5.75 - \log Si) - 273.15 = t\ ^0C \qquad 10.$$

(Fournier, 1981)

When the temperature of the hot water fraction is known, it can be converted to enthalpy, in cal/g, from steam tables (Keenan et al, 1969). This value is substituted for H_{hot} in equation 8 and the value of X again obtained. This value of X is the fraction of cold water in the spring or well.

The concentration of chloride in the well can be divided by the fraction of hot water in the well to yield the concentration of chloride in the hot water fraction. This method was not used to estimate the concentration of chloride in the hot fraction of the shoreline springs because they are in direct contact with seawater.

The results of these methods are presented in Table 9. The two highest hot water component temperatures obtained by these methods are from Pualaa and Campbell springs, shoreline springs with high silica concentrations and relatively low temperatures. These results are problematic; since these springs are located south of the LERZ, their waters may have cooled by conduction from lateral flow through the unconfined aquifer, they have lost enthalpy but not precipitated silica. However, since their silica contents are higher than all other Puna shoreline warm springs, they may truly be expressions of outflow from a an unusually high temperature reservoir.

The temperature of the hot water component of the next eleven of the sixteen wells and springs sampled falls into an approximately 55 degrees Celsius range from 205.4^0 C to 149.1^0 C, with an average of 181.5 C^0 and a mean of 183.9^0 C. This range, 182^0 to 184^0 C, may be a good estimation of the average temperature of the thermal sources which most LERZ ground waters have encountered.

TABLE 9. QUARTZ GEOTHERMOMETER TEMPERATURES

Maximum steam loss quartz geothermometer temperatures
and % hot water in each well
from Truesdell and Fournier (1977)

Well	T Well C	SiO2 mg/l	T Hot C	% Hot	Cl mg/l	Cl Hot mg/l
Pualaa spring	34.3	118.7	222	6.8		
Campbell spring	32	98.2	215	6		
MW-1	34.7	101	206	7.8	21.6	277
KS-10 (water sample)	32.2	80.8	194	6.8	61	901
Malama Ki	53	147	192	18.9	5372	28480
MW-3	41	105	190	12.2	26.9	220
Kapoho Bay spring	30.5	72.5	190	6.1		
Isaac Hale spring	34	79.4	184	8.4		
Kapoho Airstrip	35.5	83.2	184	9.3	487	5233
KS-7 (water sample)	32.2	70	177	7.5	180	2387
GTW-3	84.8	180	172	42.4	5485	12936
KS-9 (water sample)	32.2	61	162	8.5	470	5527
KS-4 (water sample)	37.8	83.5	149	13.7	16.5	120
KS-3 (water sample)	32.2	41.8	104	14.5	7	48
MW-2	67.9	44.5	100	59.9	943.7	1575
KS-8 (water sample)	34.4	5.4			57	
Allison	37	31.5			175	
av. Hawaii groundwater		40			10.5	
SMOW		2			19400	
Average	40.34		176.1			
Std. Dev.	14.38		34.19			

The remaining three wells have hot water component temperatures near or below 100^0 C and silica contents near or below average Hawaii groundwater. This suggests that their waters have encountered only weak thermal sources or that sampled silica concentrations in them may not be representative of aquifer silica concentrations, a problem which will be addressed in subsequent chapters.

Question 5. What percentage of water in each lower Puna well has a thermal origin?

The calculated percentage of hot water component in each well is presented in Table 9. It is a function of the calculated temperature of the hot water component and the temperature of the well water. Consequently, the hottest wells, or wells with relatively cool hot water components, have the largest calculated percentages of hot water.

Question 6. Was the parent water of this thermal water meteoric groundwater or seawater?

Whether this hot water component had a meteoric groundwater or seawater origin can be ascertained by estimating its chloride concentration (Table 9). In all wells but Malama Ki, hot water component chloride concentrations are less than that of seawater (19,400 mg/l). This suggests that the hot water component in each well is a brackish mix of meteoric groundwater and seawater. The concentration of chloride in the hot water component of Malama Ki is 147% that of seawater, which may be an artifact of the methods used to estimate its concentration. Malama Ki is located on Kilauea's south flank, at least 2 km from the LERZ. Its waters may have lost enthalpy conductively as

they flowed downgradient from the LERZ. Ion concentrations in Malama Ki are similar to those in GTW-3 (Table 4), which is located on the LERZ. If the original temperature of Malama Ki water was similar to that of GTW-3, the concentration of chloride in its hot water component would also be similar to GTW-3's and less than that of seawater. Furthermore, Malama Ki water plots to the right of seawater and to the left of average Hawaii groundwater on Giggenbach's trilinear diagram (Figure 26) which is another indication that it is a mixture of the two.

CHAPTER IV.

HYDROLOGICAL STUDY

Introduction

A continuous monitoring program was initiated in May 1992 by the University of Hawaii in lower Puna to gain a better understanding of the hydrology of the Kilauea lower north flank (LNF), LERZ, and lower south flank (LSF) groundwater systems; it was the first program of its kind in this area. The objectives of the program were twofold; first, to assemble data on the lower Puna groundwater aquifers in their natural state of dynamic equilibrium; and second, to use these data as a baseline with which to assess the impact, if any, of production and reinjection of geothermal fluids on the aquifers. These data were used to examine the effects of ocean tides, barometric pressure changes, and recharge events on the aquifers. Transmissivity and storativity values for the lower north flank, LERZ, and lower south flank shallow groundwater aquifers were also developed from these data.

Methods

The data for this chapter were collected from five unpumped wells which were instrumented with pressure, temperature, and conductivity sensors manufactured by Terra Systems, Inc. (Table 10). Data were collected at one hour intervals and stored in electronic dataloggers also manufactured by Terra Systems, Inc. Four of these wells have been identified in the previous chapter; they are Kapoho Airstrip, MW-2, Allison, and Malama Ki. In addition to these four, a fifth well was chosen (Figure 4) which is located

TABLE 10. SENSOR SPECIFICATIONS

Well	Pressure Sensor Range psi	Pressure Sensor Precision psi	Temperature Sensor Range degrees C	Temperature Sensor Precision Degrees C	Conductivity Sensor Range micromhos	Conductivity Sensor Precision micromhos
Paradise Park	0-15	0.015	0-100	1	0-5000	50
Kapoho Airstrip	0-15	0.015	0-100	1	0-5000	50
MW-2	0-15	0.015	0-100	1	0-7000	70
Allison	0-15	0.015	0-100	1	0-5000	50
Malama Ki	0-15	0.015	0-100	1	0-50000	500

in Kilauea's north flank near the intersection of Kaloli St. and 13th St. in Paradise Park subdivision, 14.5 km northwest of the Pohoiki geothermal field at an elevation of 43 m. This well will be referred to as the Paradise Park reference well (8-3588-01) (Table 1). It was chosen to represent an average Hawaii groundwater well, free of any possible influence from the LERZ geothermal reservoir. A water sample analysis from this well (Table 4) shows close resemblance to the average Hawaii groundwater calculated for this study. The continuous groundwater monitoring study was conducted from May 1992 to May 1994; the periods of time during which each well was monitored are presented in Table 11.

Trend, a running average program which filters harmonics of less than twenty four hour duration, was run on the hourly pressure, temperature, and conductivity records from each well to remove the short term tidal signal. Trend was also run on hourly barometric pressure records from Lyman Field at Hilo to remove the daily high and low in barometric pressure. The smoothed water level records from each well and smoothed barometric pressure records were then statistically correlated with each other to determine the effect of barometric pressure changes on well water levels. Water level, smoothed water level, temperature, conductivity, barometric pressure, and hourly precipitation data collected by Science Applications International Corp. at Puna Geothermal Venture southwest station (SAIC SW) (Figure 4) were graphed to evaluate LNF, LERZ, and LSF responses to recharge events.

TABLE 11. SENSOR CHRONOLOGY

Well	Date in	Date out	Pump	Av. Sensor Depth cm	Av. Temp. degrees C	Av. Conductivity uMhos	Average Daily Water Level Change cm	Average Daily Temp. Change degrees C	Average Daily Conductivity Change uMhos	Average Seasonal Water Level Change cm	Average Seasonal Temp. Change degrees C	Average Seasonal Conductivity Change uMhos
Paradise Park	09/21/92	10/20/92	no	149.63		230	+/- 5.28	+/- 0.05	+/- 1.5	+/- 25.61	+/- 0.025	+/-20
Reference well	10/20/92	11/10/92	no	246.08	19.46	240	+/- 5.28	+/- 0.05	+/- 1.5			
	11/10/92	05/18/93	no	33.65	19.48	150	+/- 5.28	+/- 0.05	+/- 5.0			
	05/18/93	09/17/93	no	111.38		240	+/- 5.28	+/- 0.05	+/- 1.5			
Kapoho Airstrip	03/25/92	03/23/93	no	105.92	34.72	2570	+/- 10.31	+/- 1.0	+/- 62.5	+/- 20.09	+/- 0.75	+/- 300
well	05/25/93	06/01/94	yes	166.12	34.78	2554	+/- 10.31	+/- 1.0	+/- 62.5	+/- 7.60	NA	+/- 400
MW-2	08/01/92	08/27/92	no	sensors failed								
	04/03/93	07/10/93	yes	135.1	68.02	NA	+/- 0.51	+/- 1.75	NA	+/- 17.10	+/- 0.5	NA
	07/10/93	08/19/93	yes	216.63	67.29	NA	+/- 0.51	+/- 1.75	NA			
Allison well	11/01/93	06/01/94	yes	175	36.87	NA	+/- 27.83	+/- 0.01	NA	+/- 6.35	+/- 1.5	NA
Malama Ki well	05/22/92	10/27/92	no	116.84	53.31	34544	+/- 14.21	+/- 1.25	+/- 625	+/- 8.27	+/- 1.25	+/- 4000
	03/23/93	05/21/93		285.01	NA	29967	+/- 14.21	NA	+/- 150	NA	NA	NA

The figures which accompany this chapter have an arbitrary numerical left axis which is referenced to sensor depth as inches of water, temperature as degrees Celsius, conductivity as micromhos, and precipitation as mm of rain per hour. The right axis is referenced to barometric pressure as inches of mercury. Water level is presented in these figures as the depth at which the sensors were installed below the water table. This form of presentation was used for two reasons. First, elevation data were not well constrained on some of the wells, so accurate heads could not be determined; and second, conditions varied with depth in the water column, and therefore, had to be referenced to depth.

Water level records (pressure) were compared with hourly tidal data recorded at Hilo harbor to determine tidal lag and tidal efficiency for each well. Transmissivity and storativity values for the LNF, LERZ, and LSF were calculated from these data.

Paradise Park Reference Well

Pressure, temperature, and conductivity sensors were installed in the Paradise Park reference well on 09/21/92 and had to be withdrawn on 09/17/93 when the well was vandalized (Table 11). Virtually a complete year of hourly data was collected from this well (Figures 27 through 30). During the course of monitoring the sensors were positioned at four different depths to evaluate conditions at a range of depths within the water column.

Water level showed a moderate average daily tidal fluctuation of 10.57 cm. A long term seasonal variation of 51.23 cm was recorded between average high water on 12/30/92 and average low water on 5/14/93. Water temperature averaged 19.52 ^{0} C

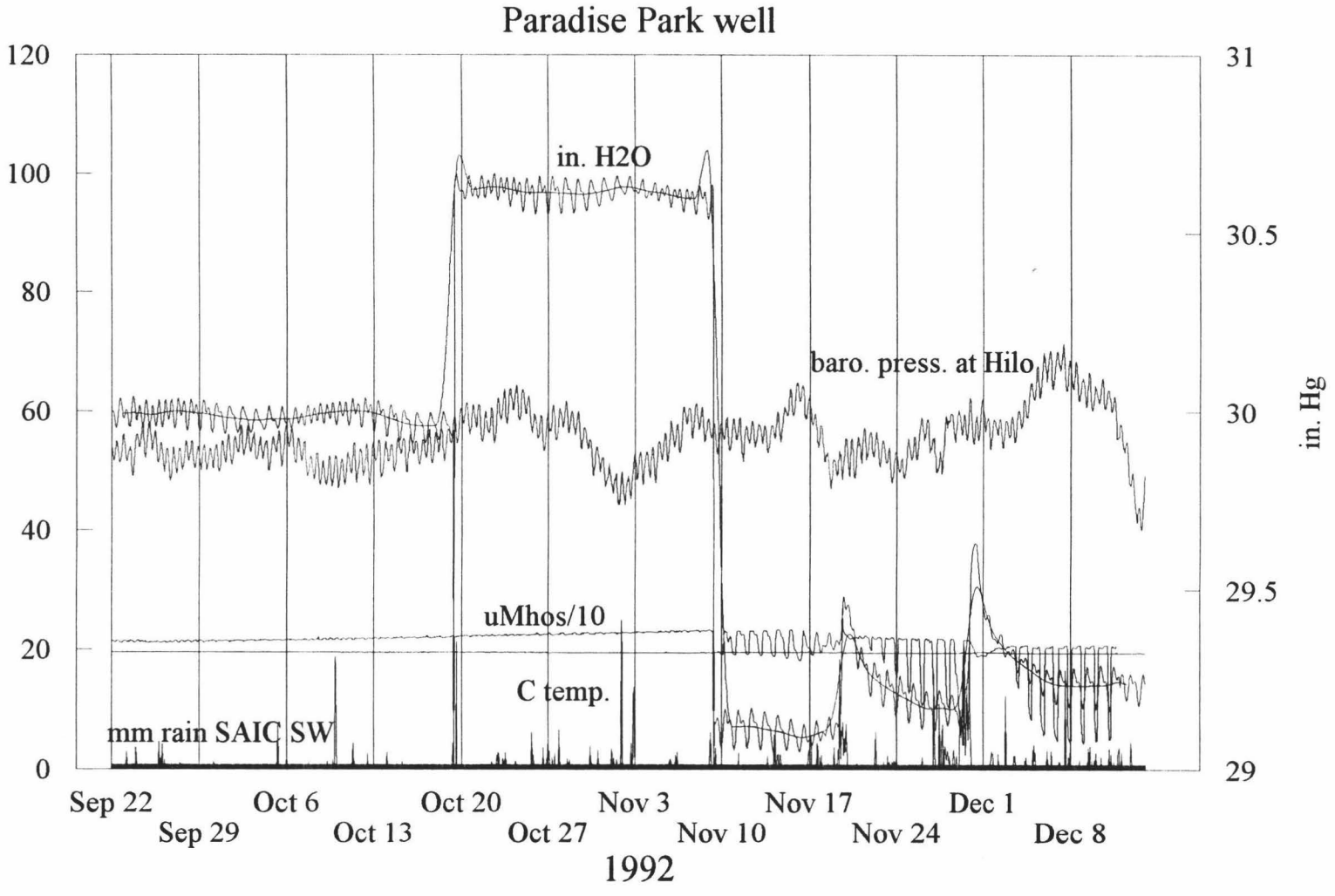

Figure 27. Paradise Park reference well hourly hydrological data 9/92 - 12/92.

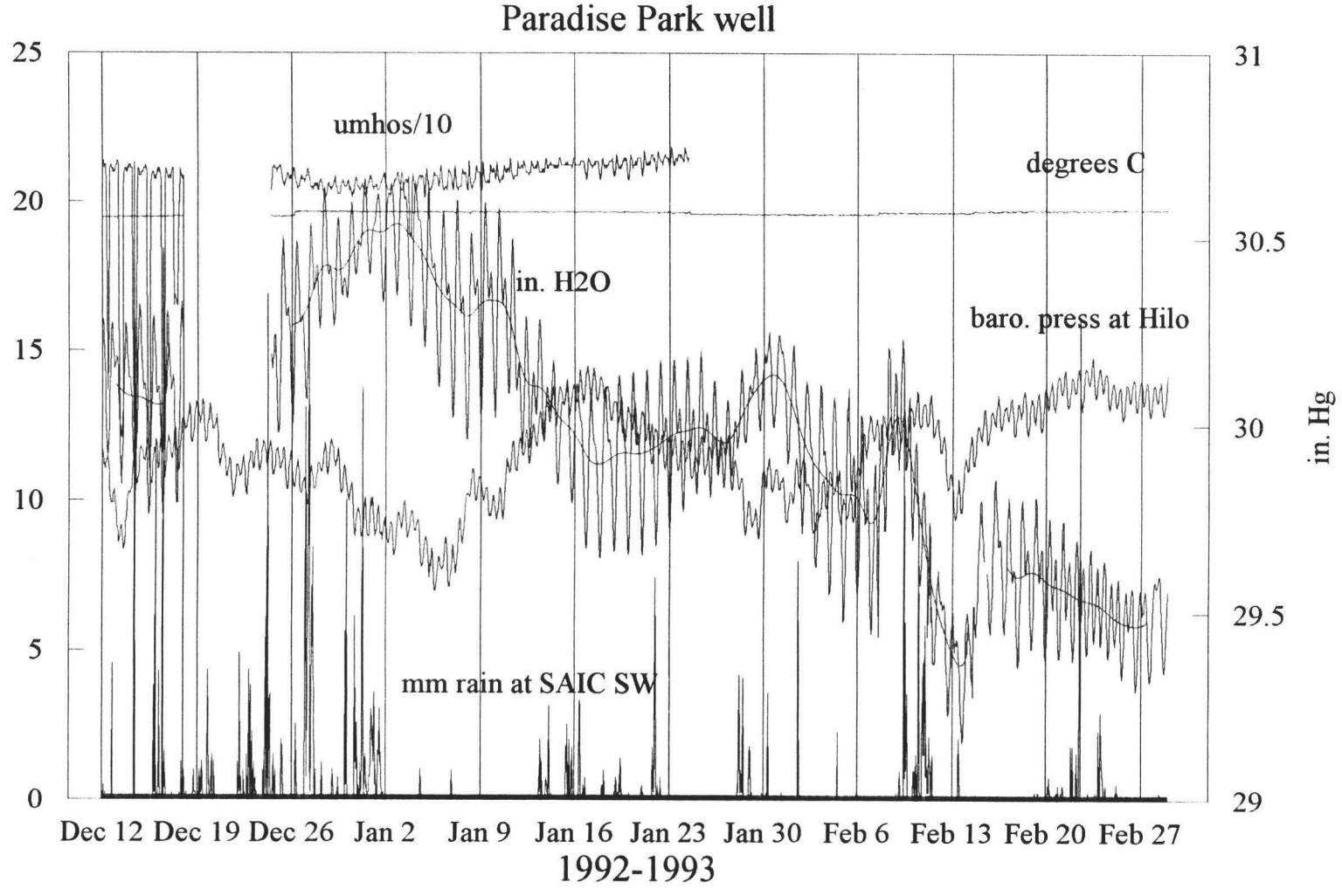

Figure 28. Paradise Park reference well hourly hydrological data 12/92 - 2/93.

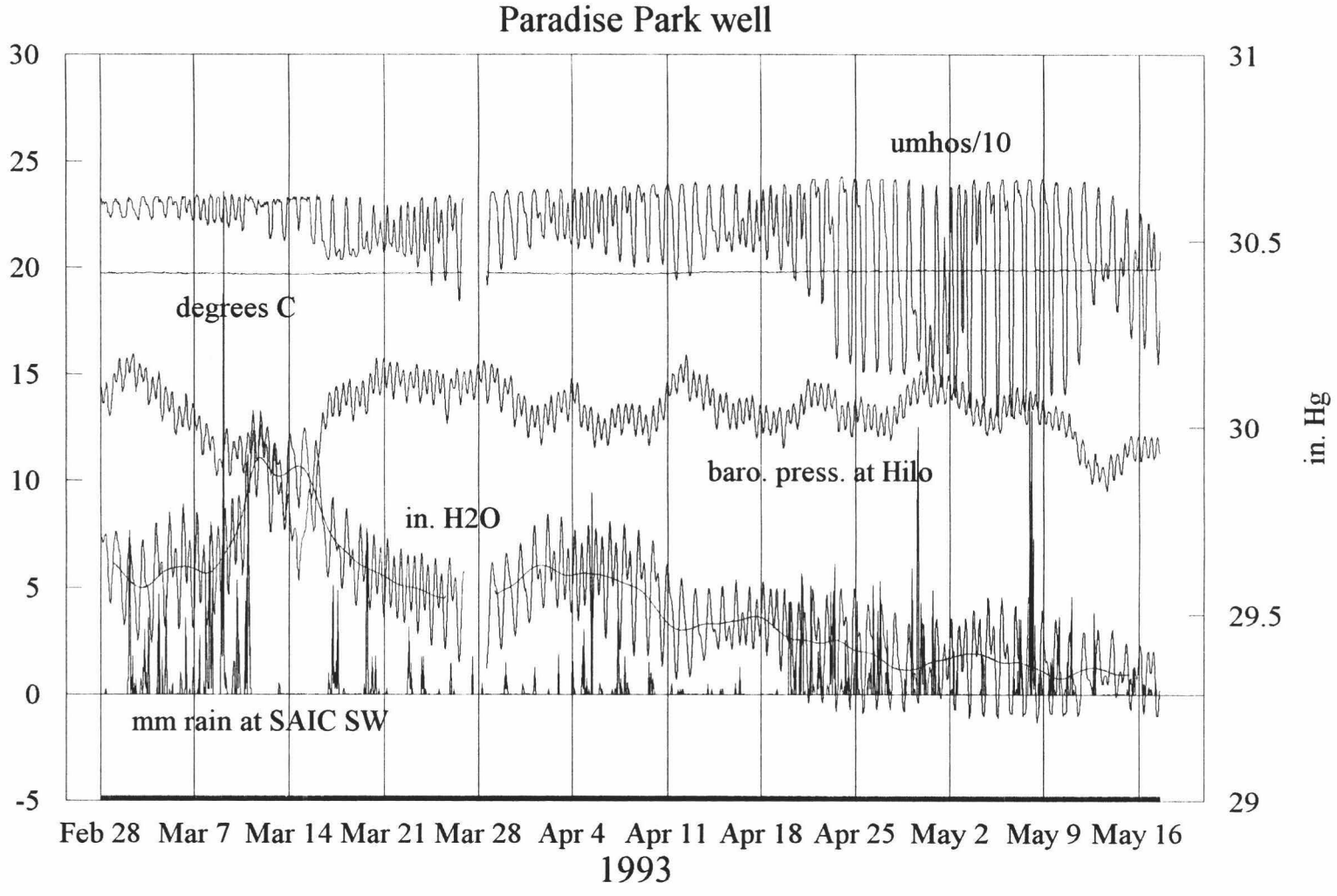

Figure 29. Paradise Park reference well hourly hydrological data 3/93 - 5/93.

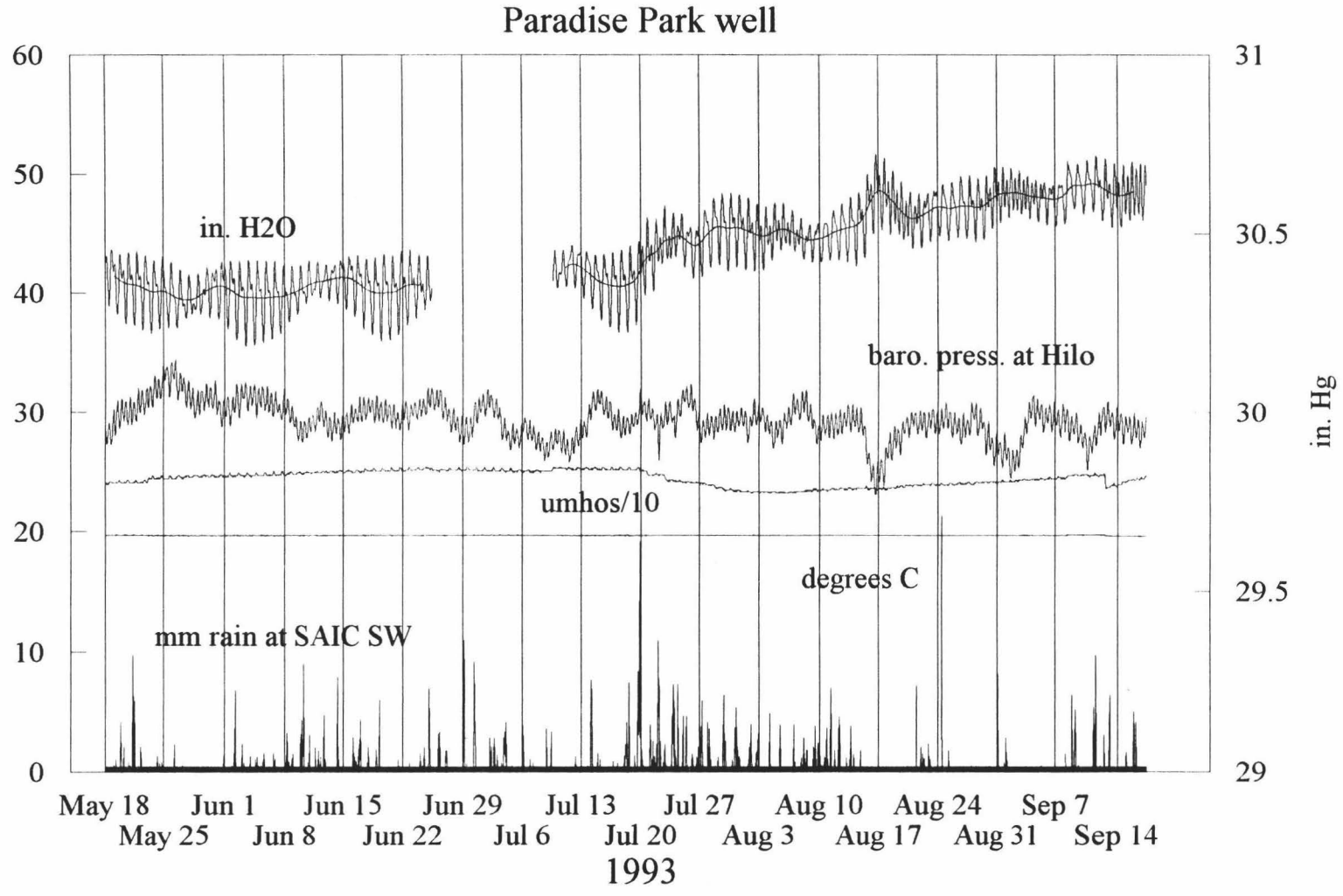

Figure 30. Paradise Park reference well hourly hydrological data.

over the complete monitoring period, and seasonal water temperature variations were only 0.05 ^{0} C. Well water showed minor temperature stratification, averaging 19.48 ^{0} C at 33.65 cm average depth and 19.46 ^{0} C at 246.08 cm average depth in winter. Groundwater conductivity was highly stratified with depth, and stratification was not linear nor did it remain uniform over time. At the three deepest sensor deployment depths, which averaged 111.38 cm, 149.93 cm, and 246.08 cm, daily conductivity changes, which were a function of tidal water level variations, averaged only 3 micromhos. However, at the shallowest sensor deployment depth, which averaged 33.65 cm, daily conductivity changes averaged 10 micromhos. During the time the sensors were deployed at this depth several distinct events occurred that produced daily conductivity changes of 150 microMhos; these events correlate with episodes of intense rainfall (Figures 27 & 28).

Figure 31 shows a more detailed view of two of these events in the Paradise Park reference well. Intense rainfall events occurred on 11/19/92 and 11/29/92. Eight hours and eleven hours, respectively, after the peak rainfall, well water level peaked sharply, and completely overwhelmed the daily tidal signal. Over the course of the next day or two, as the tidal signal reestablished itself, conductivity variations increased dramatically with a maximum value at high water and a minimum at low water. Water temperature showed an inverse correlation with water level and conductivity, with a maximum value at low water and a minimum at high water.

The events described above are episodes of vertical infiltration recharge to the groundwater aquifer. The infiltration front moving downward through the unsaturated

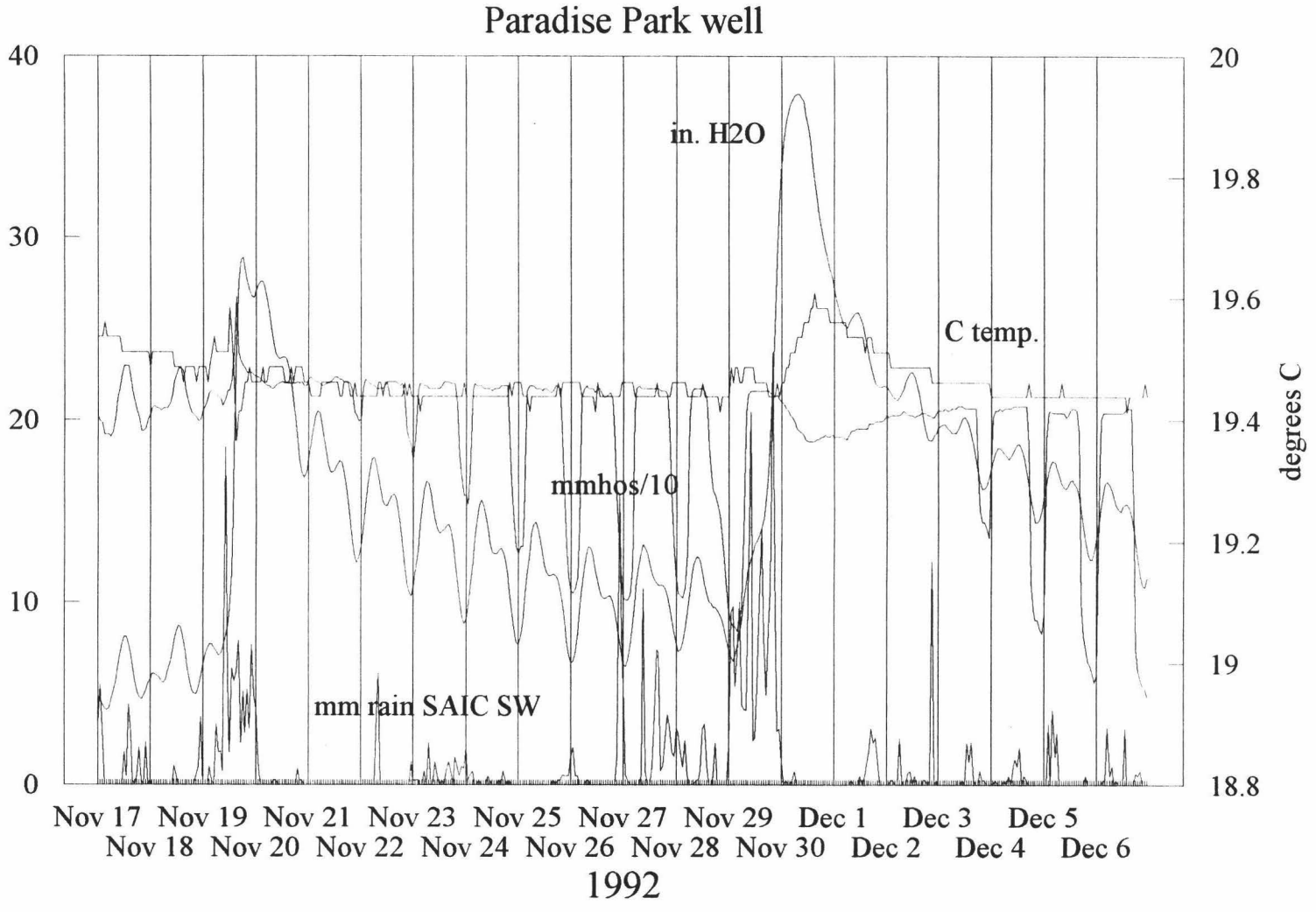

Figure 31. Vertical infiltration in Paradise Park reference well.

traveling much greater distances horizontally through the aquifer from higher elevations. This infiltration front is also slightly warmer than the groundwater it encounters. Since it is both lower in dissolved solids and warmer than groundwater, the infiltration front floats in a thin layer at the top of the water table for a few days, causing the initial rise in water level and subsequent large flux in conductivity seen in Figure 31. Eventually, horizontal throughflow moves this water away from the well, replacing it with higher conductivity groundwater which has flowed farther from higher elevations, thus damping the conductivity flux. This effect was most obvious when the sensors were deployed at their shallowest depth from 11/10/92 to 5/16/93 (Figures 27, 28, & 29).

By dividing the depth to water in the well by the lag time between the hour of most intense rainfall and the peak water level which followed it, an estimate of vertical infiltration rate was made. Three infiltration events were distinct enough to be used for this calculation, they yielded lag times of 8, 9, and 11 hours. Depth to water in the well was 41.24 m and an average vertical infiltration rate of 4.42 m per hour was calculated.

When the conductivity sensor was deployed at an average depth of 111.38 cm longer term changes in conductivity were also apparent (Figure 30). While large short term variations in conductivity resulted from intense rainfall at the well, smaller long term changes in conductivity resulted from prolonged upgradient rainfall; this effect can be seen in Figure 29. Water level rose sharply with late summer rains while conductivity dropped ~20 micromhos. Then as water level began to stabilize, conductivity rose with the arrival at the well of upgradient recharge.

Figures 27 through 30 show several medium term water level changes in Paradise Park reference well which do not correlate with rainfall, but do show an inverse correlation with barometric pressure. When smoothed hourly water level data from the Paradise Park reference well was statistically correlated with smoothed hourly barometric pressure data from General Lyman Field, Hilo, an average correlation coefficient of $r = -0.44026$ for the period 9/21/92 to 9/17/93 resulted. These medium term water level changes are a result of changes in sea level in response to barometric pressure changes. Low barometric pressure raises sea level which raises well water level, high barometric pressure produces an opposite response.

Kapoho Airstrip Well

The longest hourly data set used in this study has been accumulated from Kapoho Airstrip well (Figures 32 through 37). Pressure, temperature, and conductivity sensors were installed in this well on 03/25/92 at an average depth of 105.92 cm and removed, due to a pressure sensor malfunction, on 03/23/93. The repaired sensor package plus a downhole pump was again installed on 05/25/93 at an average depth of 166.12 cm. Although the temperature sensor failed soon after, on 06/23/93, the remaining sensors functioned until removed on 06/01/94.

Water level showed a daily average tidal fluctuation of 20.62 cm. A seasonal difference of 40.18 cm was recorded between average low water on 07/27/92 and average high water on 12/09/92. However, this difference may be partly a function of the pressure sensor malfunction. In 1993, only a 15.21 cm difference between average low water on

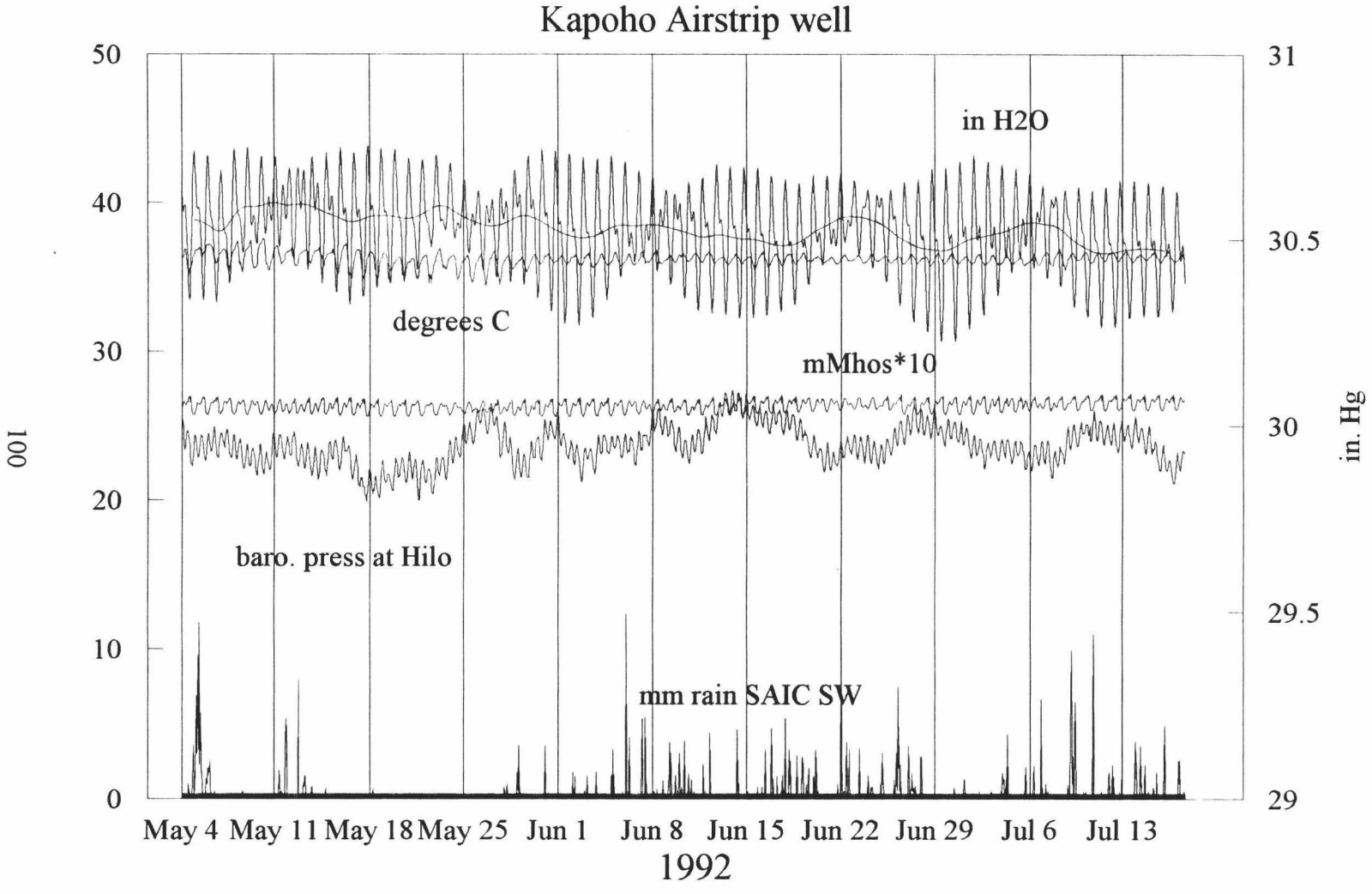

Figure 32. Kapoho Airstrip well hourly hydrological data 5/92 - 7/92.

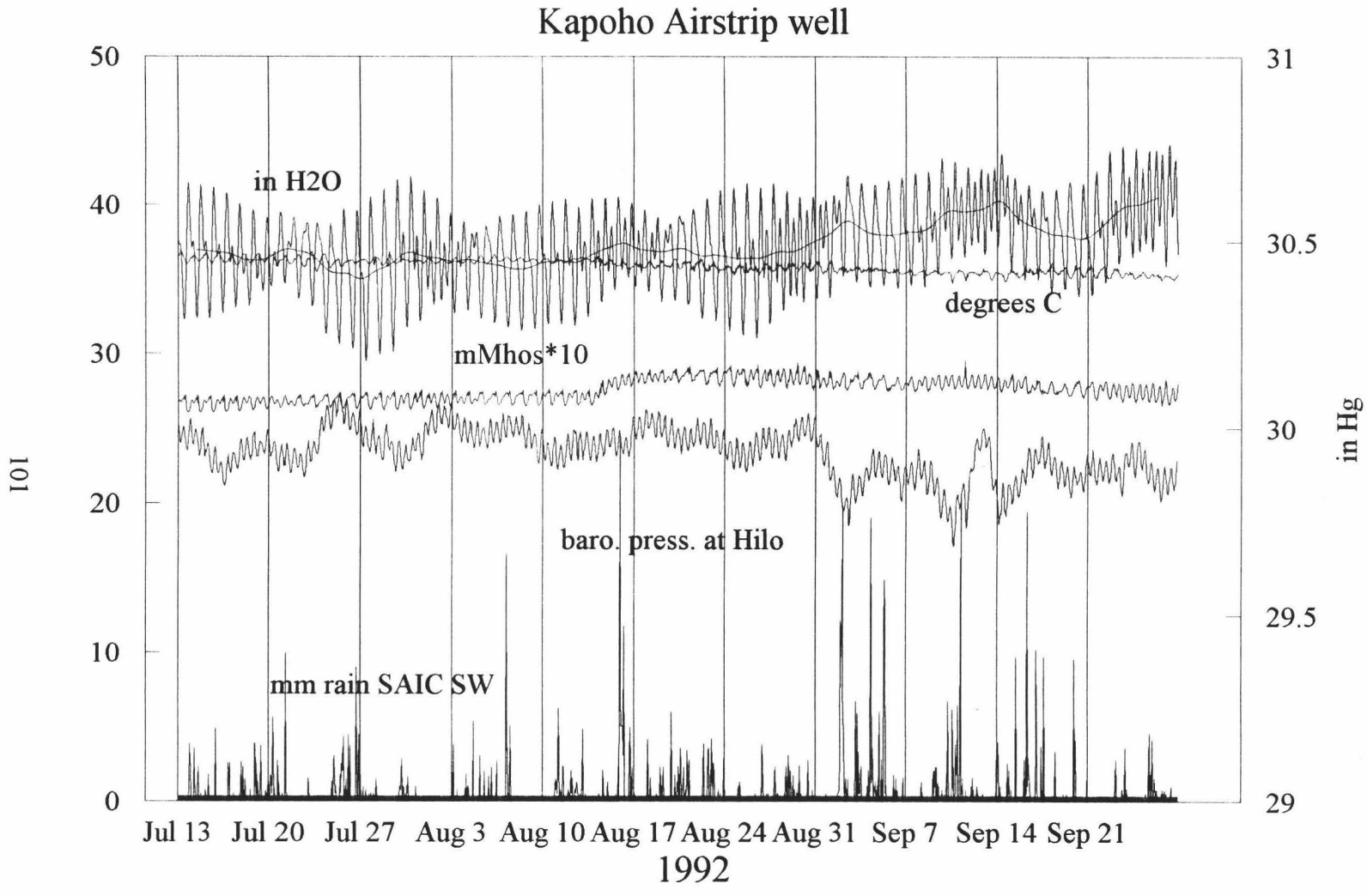

Figure 33. Kapoho Airstrip well hourly hydrological data 7/92 - 9/92.

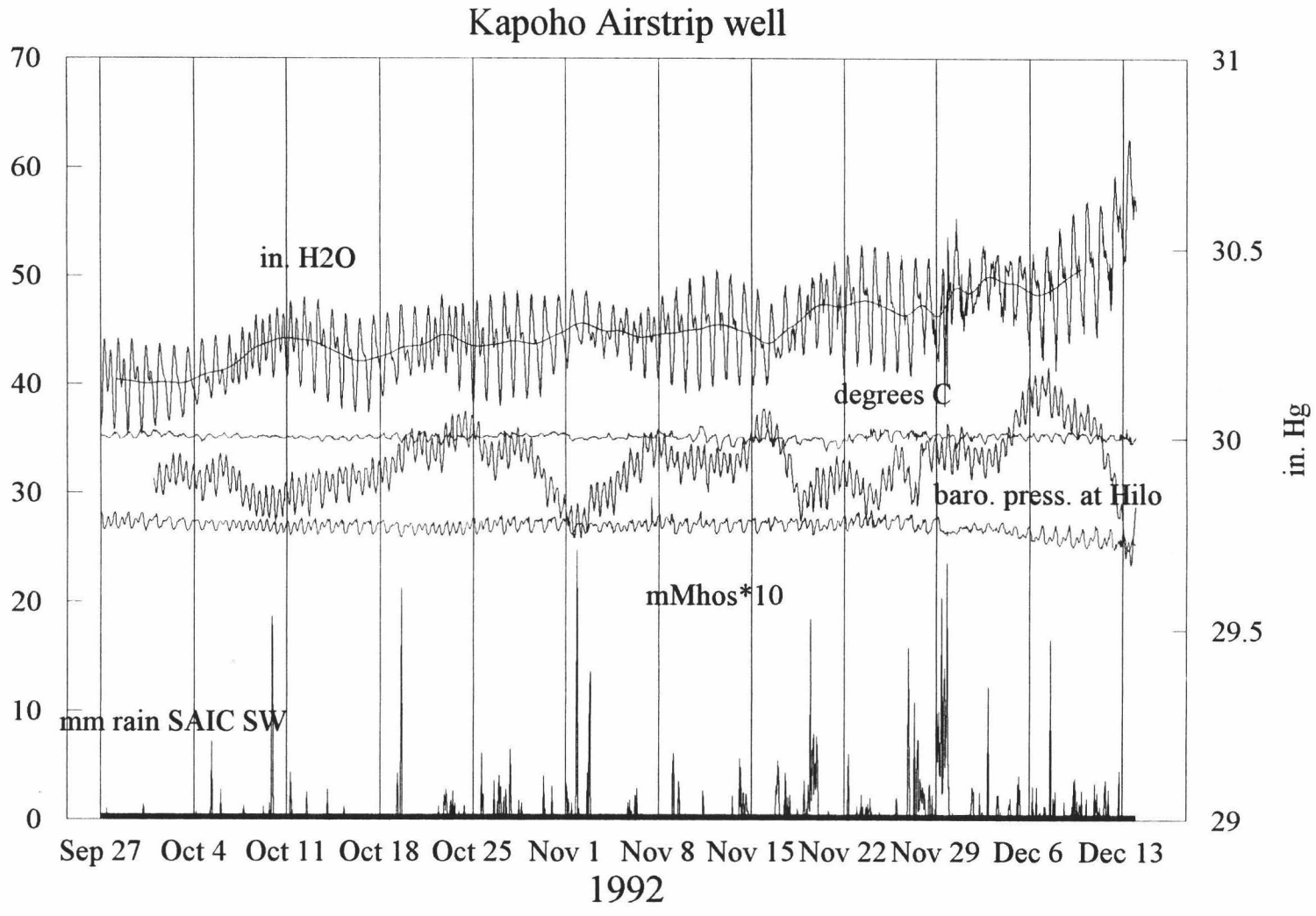

Figure 34. Kapoho Airstrip well hourly hydrological data 9/92 - 12/92.

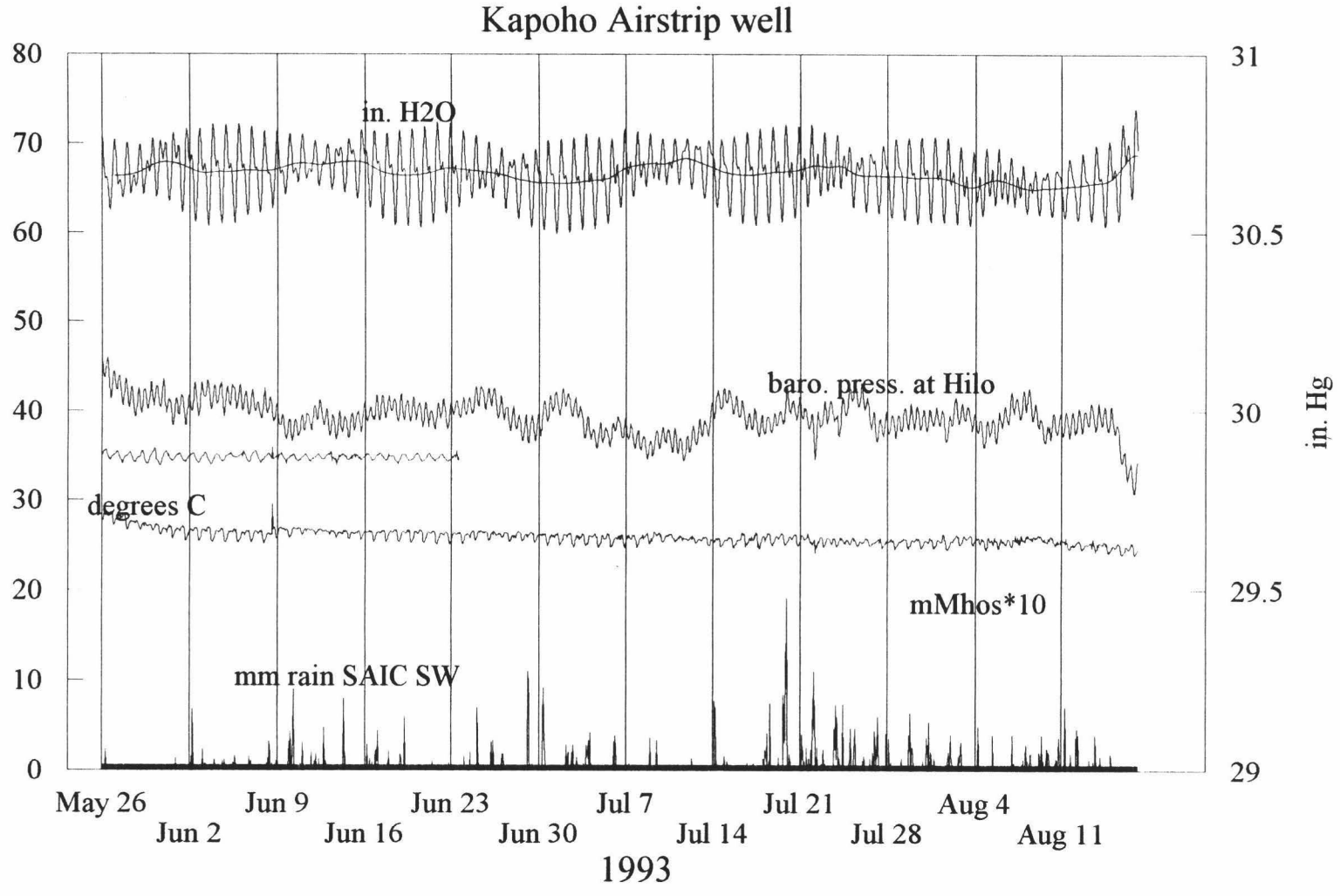

Figure 35. Kapoho Airstrip well hourly hydrological data 5/93 - 8/93.

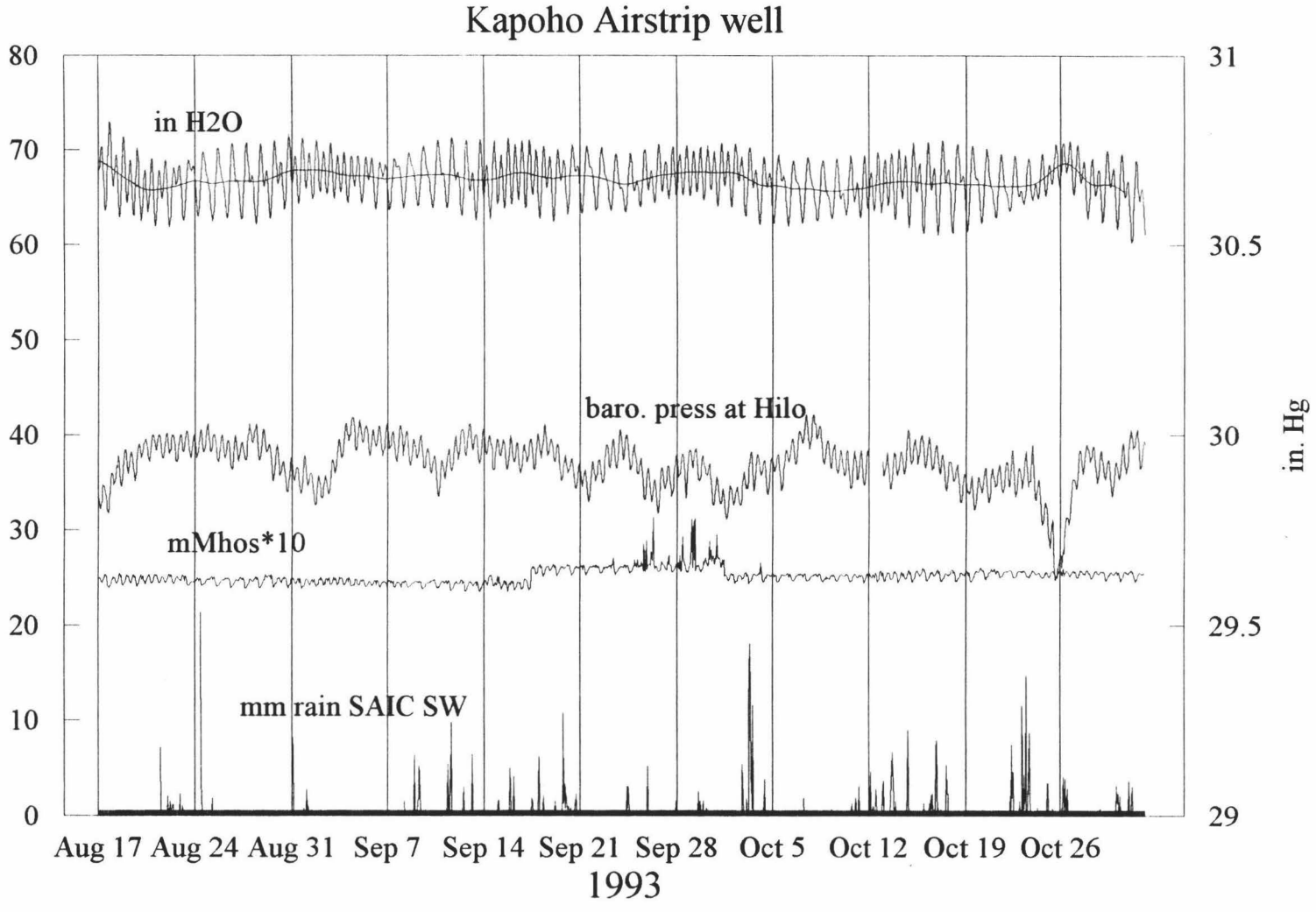

Figure 36. Kapoho Airstrip well hourly hydrological data 8/93 - 10/93.

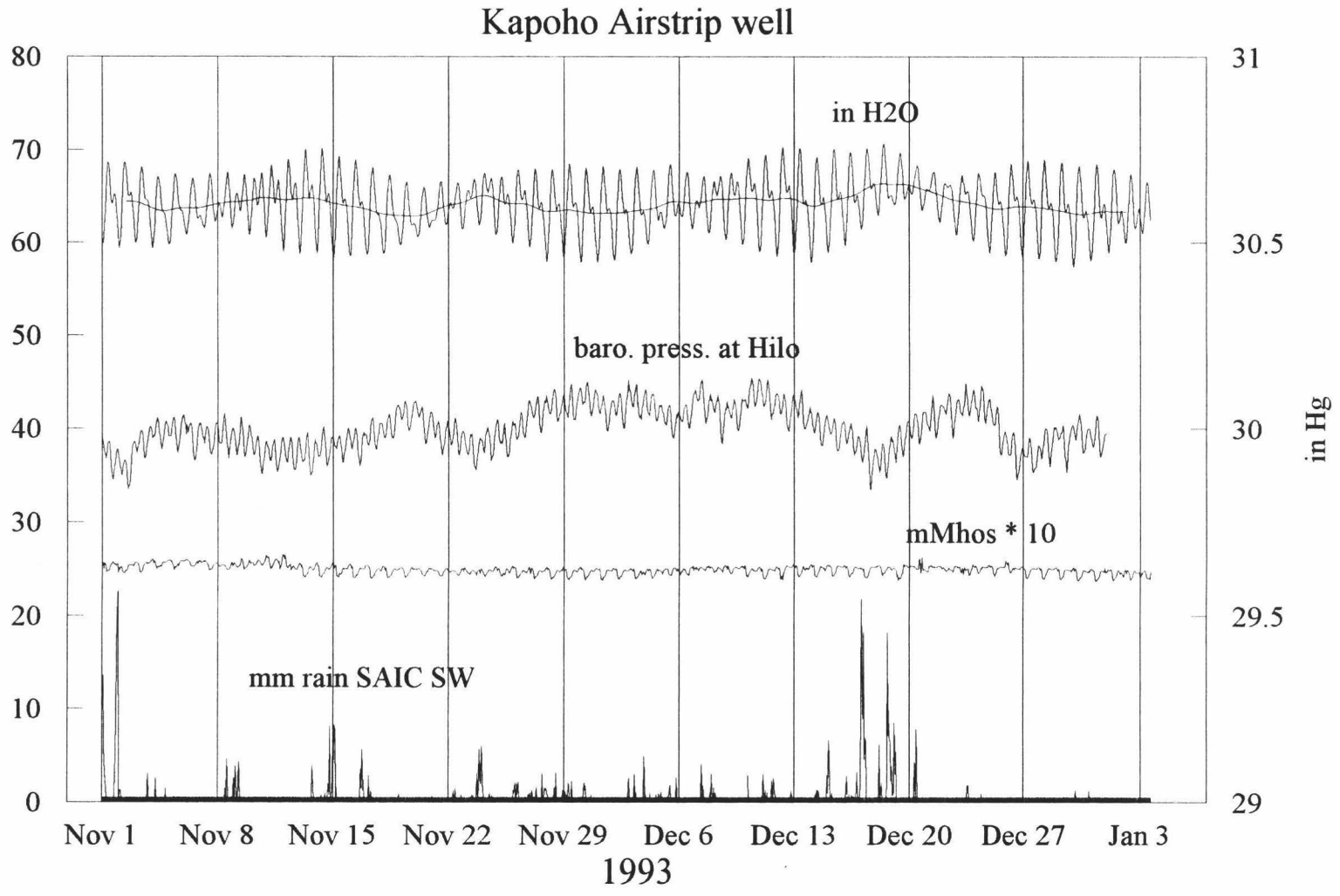

Figure 37. Kapoho Airstrip well hourly hydrological data 11/93 - 12/93.

11/19/93 and average high water on 08/16/93 was recorded, where as rainfall at Pahoa Station #65 (Figure 4) was similar for both years, 286.00 cm for 1992 and 310.03 cm for 1993.

Water temperature showed a daily fluctuation of ~2 ^{0} C, with low temperatures occurring at noon and high temperatures at midnight. This was interpreted as being a spurious signal resulting from the datalogger reference thermistor in the well head heating and cooling slightly with daily rise and fall in air temperature. Seasonal variation in temperature was 1^{0} C. Water temperature was slightly stratified with depth, averaging 36.17 ^{0} C at 97.13 cm average depth in summer 1992 and 34.72 ^{0} C at 169.29 cm average depth in summer 1993.

Conductivity showed an average daily tidal fluctuation of ~125 micromhos at both sensor installation depths. Seasonal changes averaged 57 micromhos at 105.92 cm average depth and 79 micromhos at 166.12 cm average depth. Conductivity was stratified with depth. In summer 1992 average conductivity was 2,636 micromhos at 97.13 cm average depth and, in summer 1993, 2,570 micromhos at 169.29 cm average depth. In winter 1992 average conductivity was 2,693 micromhos at 114.78 cm average depth and, in winter 1993, 2,491 micromhos at 162.92 cm average depth.

Figure 38 shows two weeks of water level, temperature, and conductivity flux. The inverse relationship between water level and conductivity is obvious, when water level is high, conductivity is low, and when water level is low, conductivity is high. This conductivity gradient correlates with water temperature. The high conductivity water is

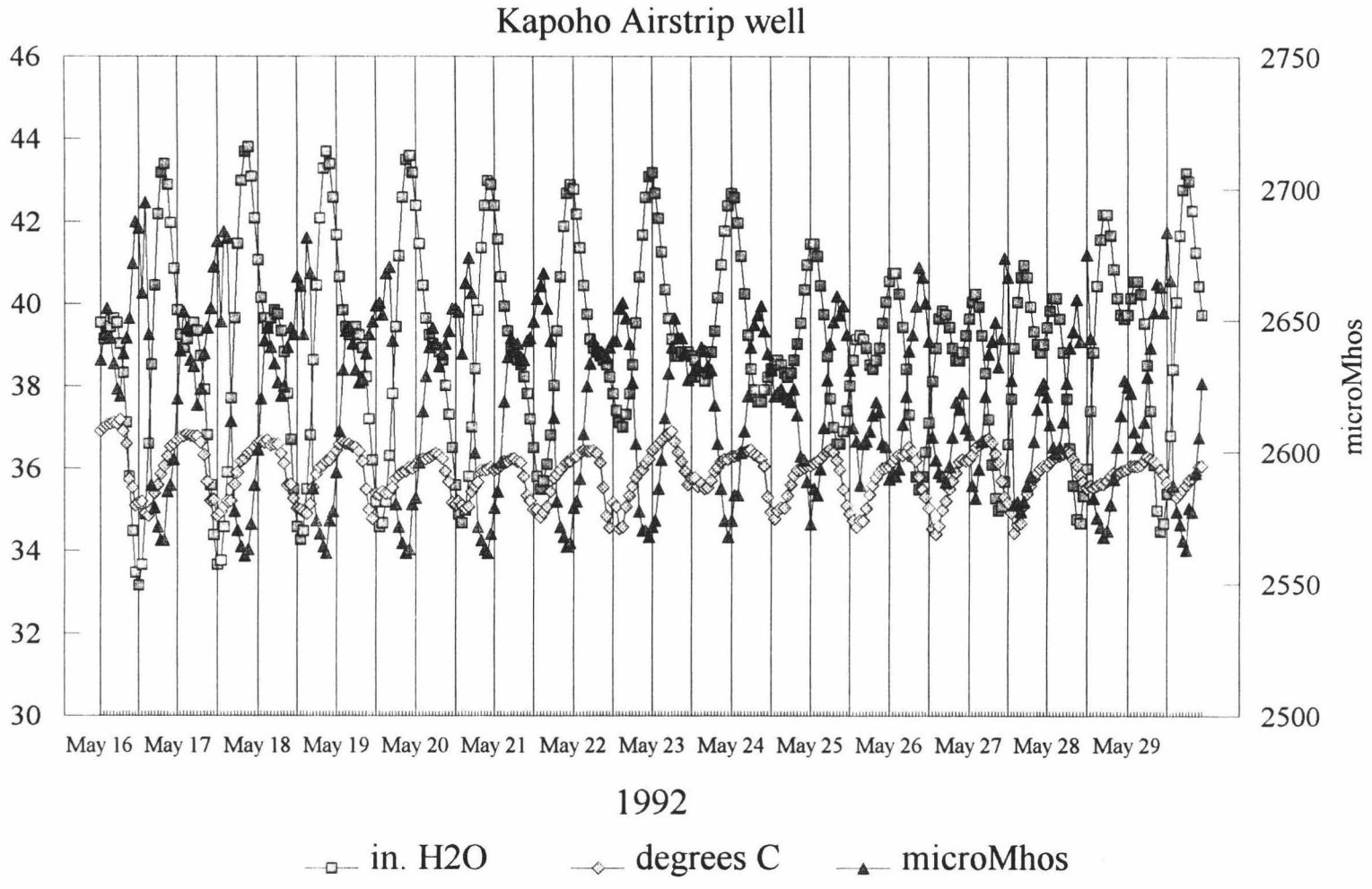

Figure 38. Kapoho Airstrip well hourly hydrological data (two week period).

slightly warmer than lower conductivity water, thus it is able to float at the top of the water table.

Although rises in water level in response to recharge events are discernible in Kapoho Airstrip well in Figures 32 through 37, large conductivity fluxes are not. This may be due to the elevated groundwater temperature. Low conductivity, relatively cool infiltration fronts cannot float at the top of a thermal water table. Because of their lower temperature, they must sink through it until they have thoroughly mixed with it and achieved a density equilibration depth. Although the Kapoho Airstrip well sensors were set too deep to record the large conductivity fluxes seen after an intense rainfall in the Paradise Park reference well, evidence of this phenomenon can be seen in the greater seasonal flux in conductivity at deeper depths in Kapoho Airstrip well, as infiltration from relatively cold winter rains sank through the water column.

Smoothed hourly water level data from Kapoho Airstrip well and smoothed hourly barometric pressure data produced a statistical correlation of $r = -0.36164$ for the period 05/04/92 to 09/28/92 and $r = -0.26769$ for the period 05/25/93 to 12/31/93.

Monitor Well #2 (MW-2)

Pressure, temperature, and conductivity sensors were installed in MW-2 on 08/01/92 and removed after unsatisfactory performance on 08/27/92. The repaired sensors plus a downhole pump were again installed at an average depth of 135.10 cm on 04/03/93 (Figures 39 & 40). On 07/10/93 it became necessary to lower the sensors and pump to an average depth of 216.23 cm because of dropping water level in the well. An

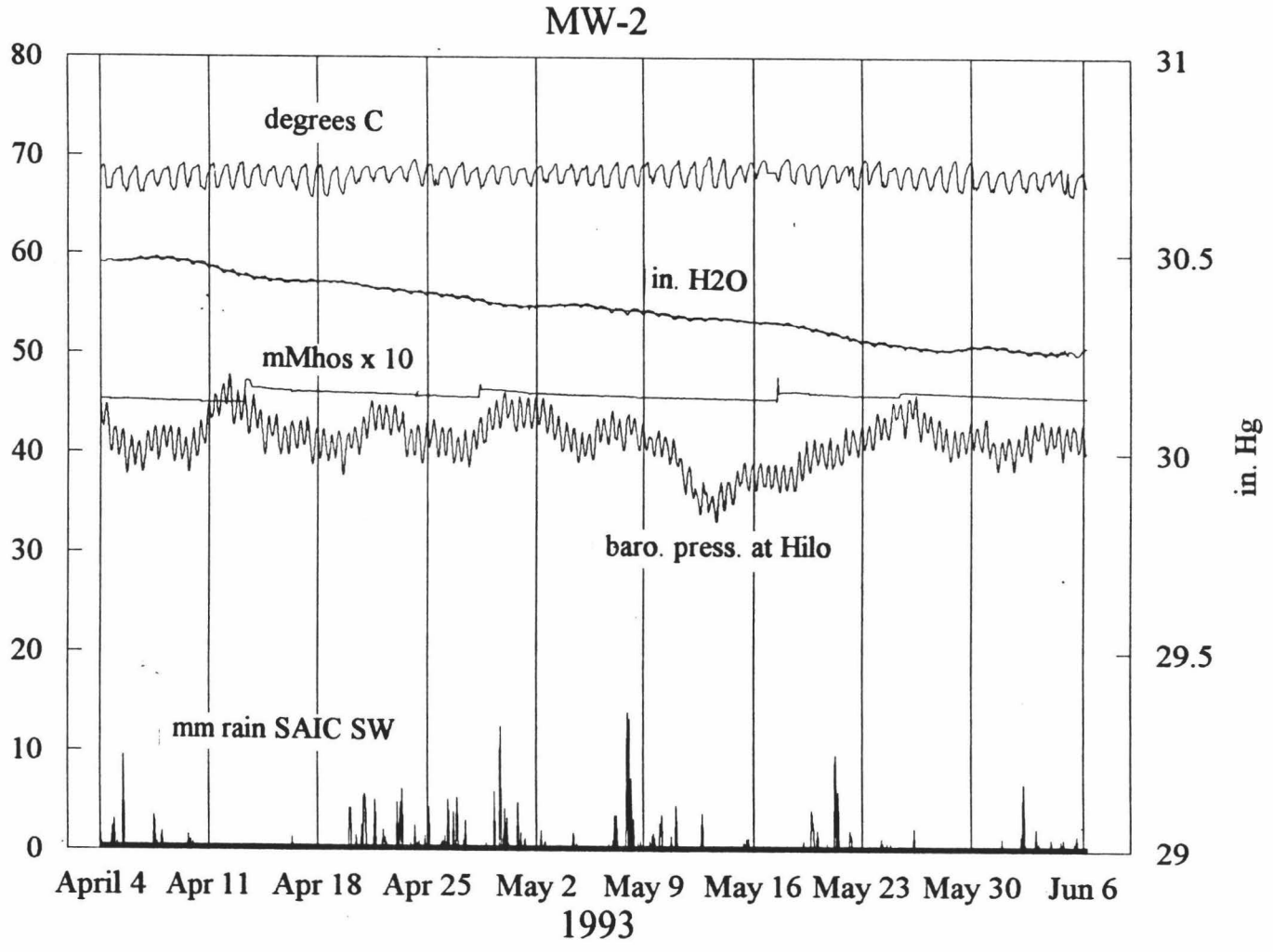

Figure 39. MW-2 hourly hydrological data 4/93 - 6/93.

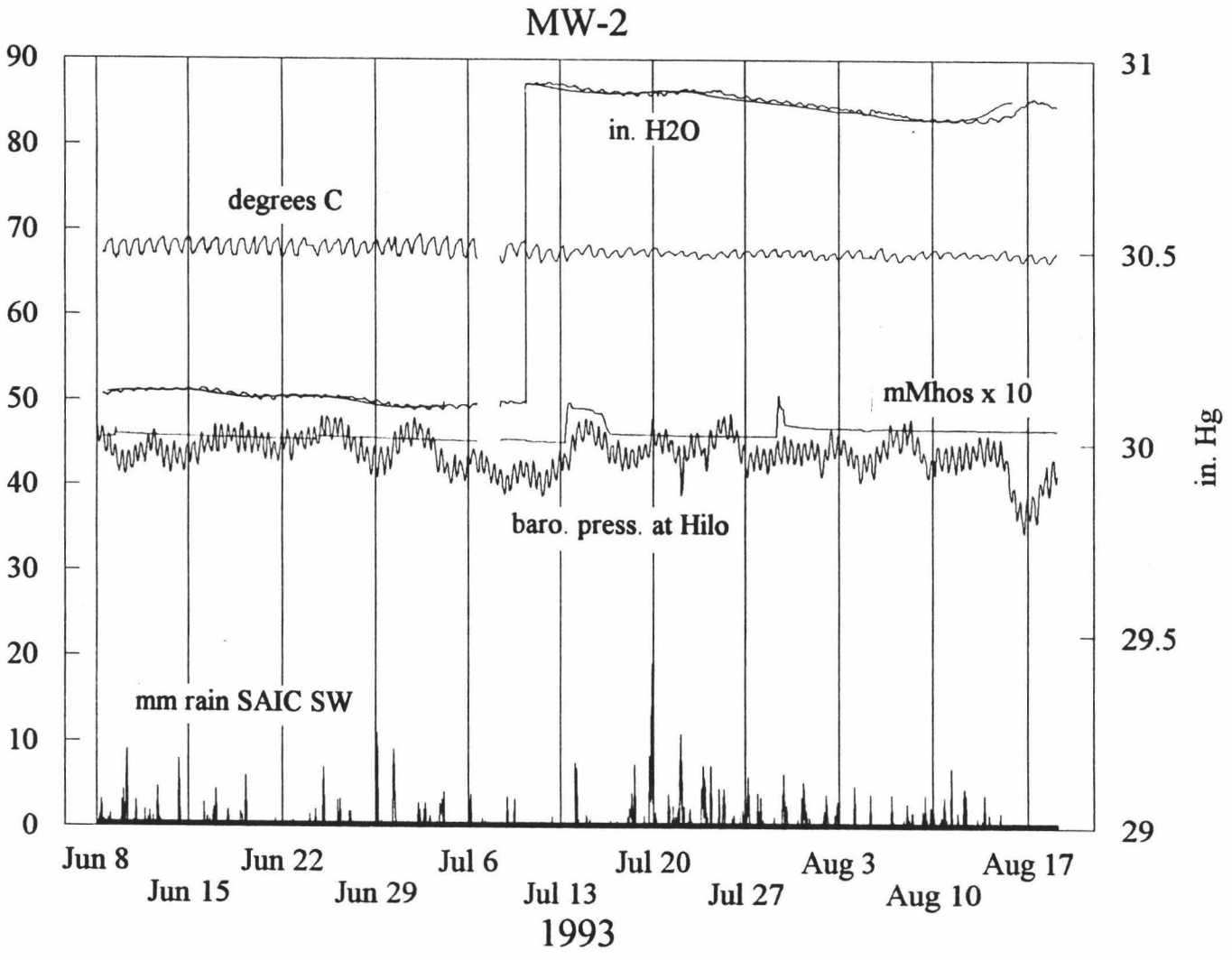

Figure 40. MW-2 hourly hydrological data 6/93 - 8/93.

attempt was made on 08/19/93 to remove the sensors and pump in order to replace the pump, but during this procedure the sensors and pump became fouled in the well and the MW-2 monitoring program was suspended.

MW-2 showed an extremely small daily tidal water level fluctuation of 1.02 cm. Water level change over the duration of the monitoring period was 34.21 cm between high water on 04/07/93 and low water on 08/11/93.

Water temperature showed a daily fluctuation of 3.5^0 C. This was again assumed to be a spurious signal. At 135.10 cm average depth temperature averaged 68.02^0 C and 67.29^0 C at 216.23 cm average depth.

Because of the small daily tidal water level fluctuations, daily conductivity fluctuations were correspondingly small, averaging less than 10 micromhos. During the course of the monitoring program several sharp increases followed by gradual declines in conductivity were observed (Figures 39 & 40). These events occurred immediately after the well was pumped. An "as built" casing schematic of the well (Appendix B) was obtained from the drilling company and it was determined that the slotted liner had been installed 7.32 m below initial water level. Consequently, the sensors and pump were sampling stagnant water trapped in the solid casing. Under these conditions, pressure and temperature data were still valid but conductivity data and water sample analyses did not reflect actual conditions in the aquifer. This may be the reason for unusually low silica concentrations found in MW-2 water sample analyses.

Smoothed hourly water level data from MW-2 and smoothed hourly barometric pressure data produced a statistical correlation of r = -0.35579 for the period 04/03/93 to 08/19/93.

Allison Well

Pressure, temperature, conductivity sensors, and a downhole pump were installed at an average depth of 175 cm in Allison well on 11/1/93 (Figure 41). The sensors and pump functioned until they were removed on 06/01/94.

Allison well showed a large average daily tidal water level fluctuation of 55.66 cm. Water level remained essentially unchanged during the 1993 portion of the monitoring program.

Water temperature averaged 36.87 ^{0} C at 175 cm average depth. Water temperature showed a very small daily fluctuation which was inversely correlated with water level. Two sharp decreases in water temperature in December 1993 were correlated with intense rainfall events (Figure 41).

Conductivity never established an average value, but rose steadily from an initial value of 1,128 micromhos until the sensor overranged at 5,000 micromhos, then fell to 644 micromhos immediately after the 12/19/93 intense rainfall event, and again began to increase steadily (Figure 41).

Smoothed hourly water level data from Allison well and smoothed hourly barometric pressure data produced a statistical correlation of r = .17638 for the period 11/01/93 to 12/31/93.

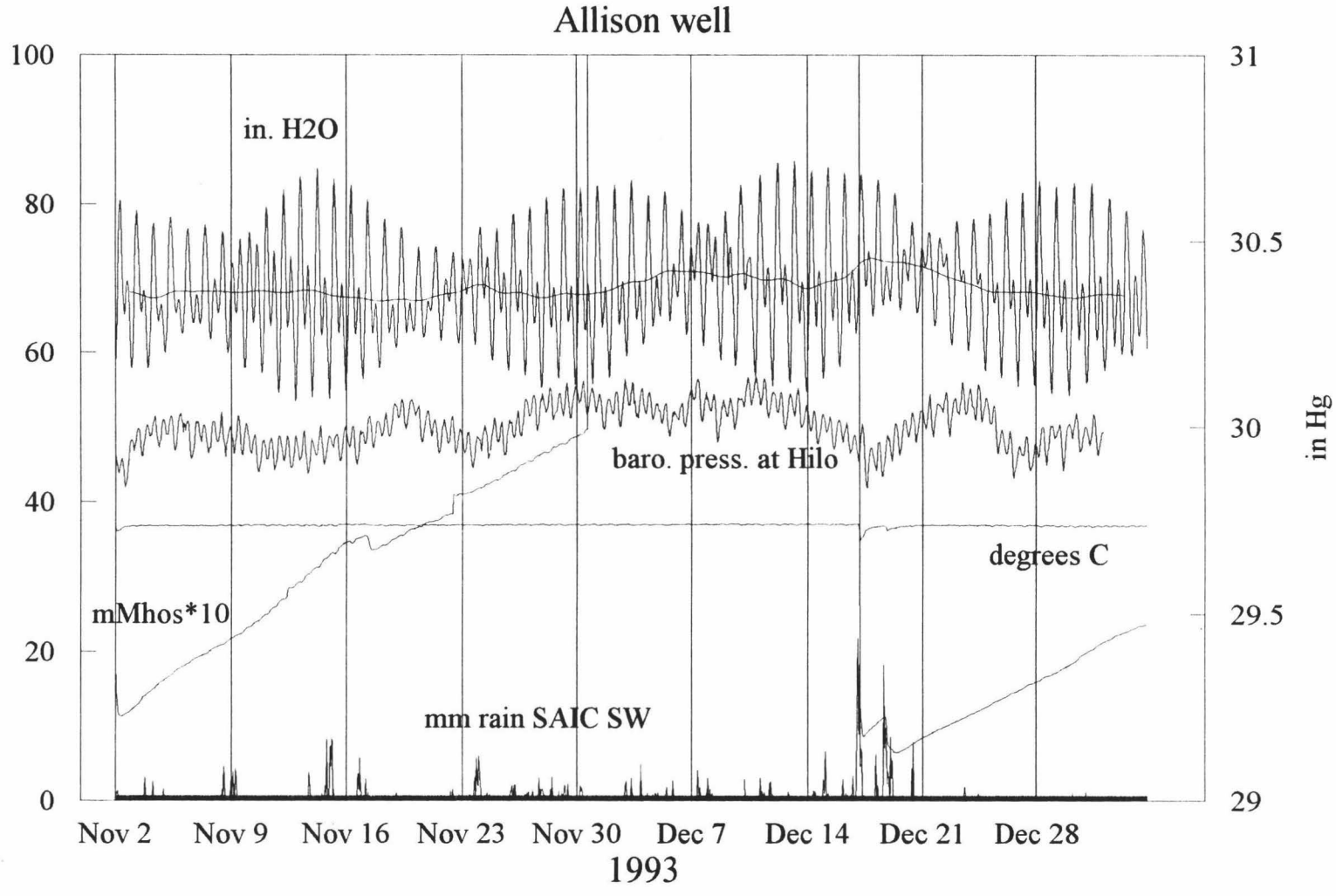

Figure 41. Allison well hourly hydrological data 11/93 - 12/93.

The unusual pattern of conductivity flux and positive correlation coefficient discussed above suggest some non-environmental influence on Allison well. To access this well, a defunct downhole pump had to be removed, and a water based lubricant introduced into the well to ease the pump removal. The presence of this lubricant may have affected water conductivity in the well. Although the strong tidal signal recorded in Allison well suggests the well is in connection with the aquifer, the conductivity response to rainfall discussed above, the positive correlation between well water level and barometric pressure, lack of long term water level change, and unusually low silica concentration (Table 4) suggest some form of stagnation has taken place in the well.

Malama Ki Well

Pressure, temperature, and conductivity sensors were installed in Malama Ki well on 05/22/92 at an average depth of 116.84 cm and removed, after several datalogger failures, on 10/27/92 (Figures 42 & 43). They were again installed along with a downhole pump on 03/23/93 at an average depth of 285.01 cm, and again removed due to failure of the pump, temperature, and pressure sensors on 05/21/93.

Water level showed an average daily tidal fluctuation of 28.42 cm. A seasonal water level change of 16.54 cm was observed between low water on 07/27/92 and high water on 10/10/92. However, because of the brevity of the Malama Ki data set, this probably does not represent the full range of seasonal water level change.

Water temperature showed a rather large daily fluctuation of 2.5^0 C, with a high near midnight and a low near noon. This was again assumed to be a spurious signal

produced by daily heating and cooling of the datalogger thermistor. At an average depth of 116.84 cm, water temperature averaged 53.31^0 C. Malfunction of the temperature sensor prevented acquiring an average temperature for the 285.01 cm average depth. Seasonal water temperature change over the period of the data set was 2.5^0 C.

Conductivity showed an average daily tidal fluctuation of ~1,250 micromhos at 116.84 cm average depth and ~300 micromhos at 285.01 cm average depth. Average conductivity was 34,544 micromhos and 29,967 micromhos respectively at the two average depths. Conductivity showed an inverse correlation with daily tidal fluctuation in water level, low when water level was high, and high when water level was low.

Several medium term events occurred in Malama Ki well in which water temperature and conductivity rose suddenly and showed larger than usual hourly changes (Figure 42). These events do not correlate with intense rainfall events or changes in barometric pressure; they are probably electronic "noise" from the datalogger. The most obvious of these events (07/17/92) occurred immediately after data was downloaded.

Short term rises in water level in response to vertical infiltration are not visible in the Malama Ki well data set, but water temperature and conductivity may show a delayed response to these events (Figure 43, 8/1 - 8/22). Although there is a slight seasonal rise in water level with a slight increase in rainfall, medium term changes in water level do not correlate with rainfall events (Figures 42 & 43). They do, however, show an inverse correlation with barometric pressure variations. Smoothed hourly water level data from Malama Ki and smoothed hourly barometric pressure data produced a statistical correlation of r = -0.47319 for the period 05/22/92 to 08/11/92.

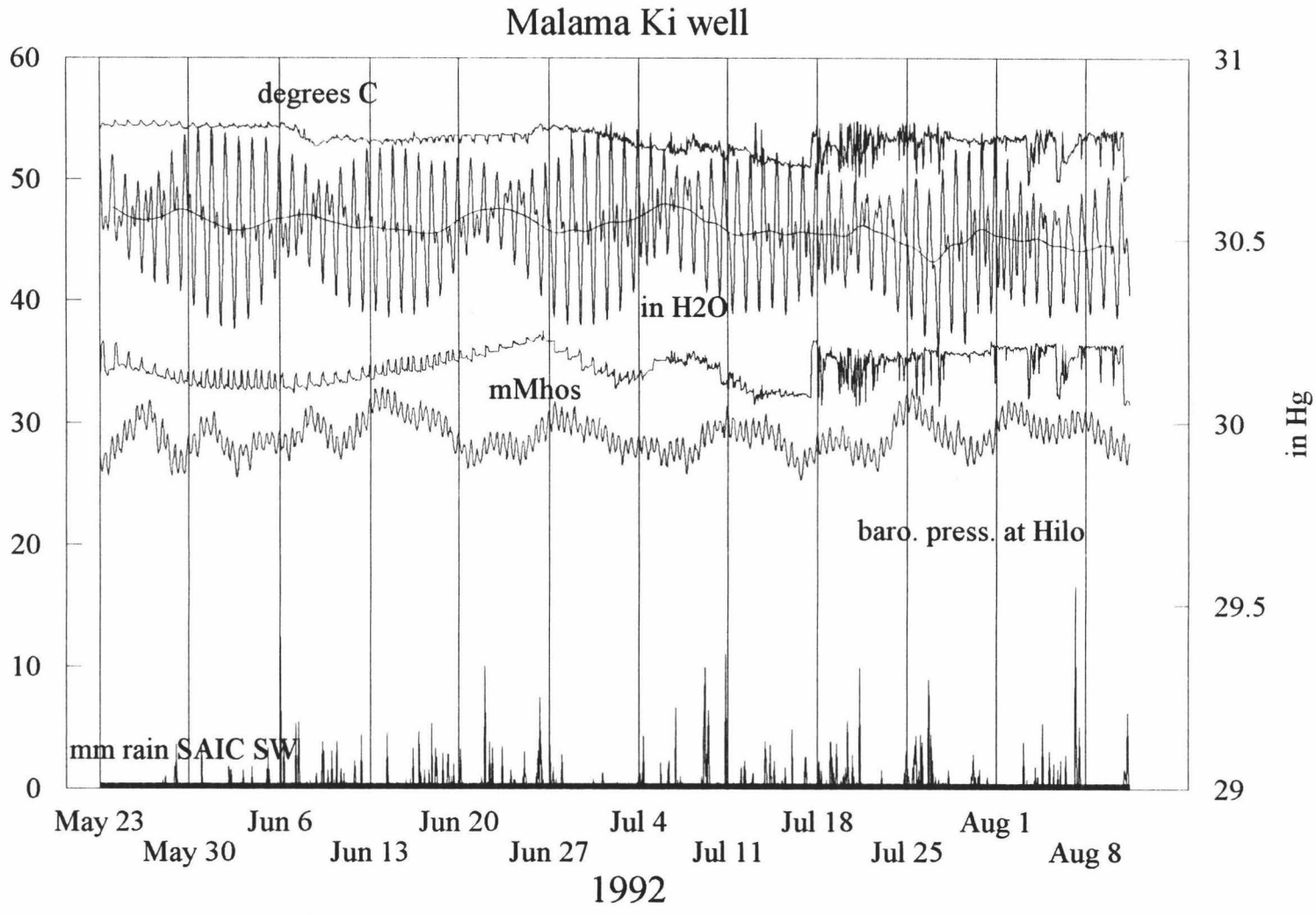

Figure 42. Malama Ki well hourly hydrological data 5/92 - 8/92.

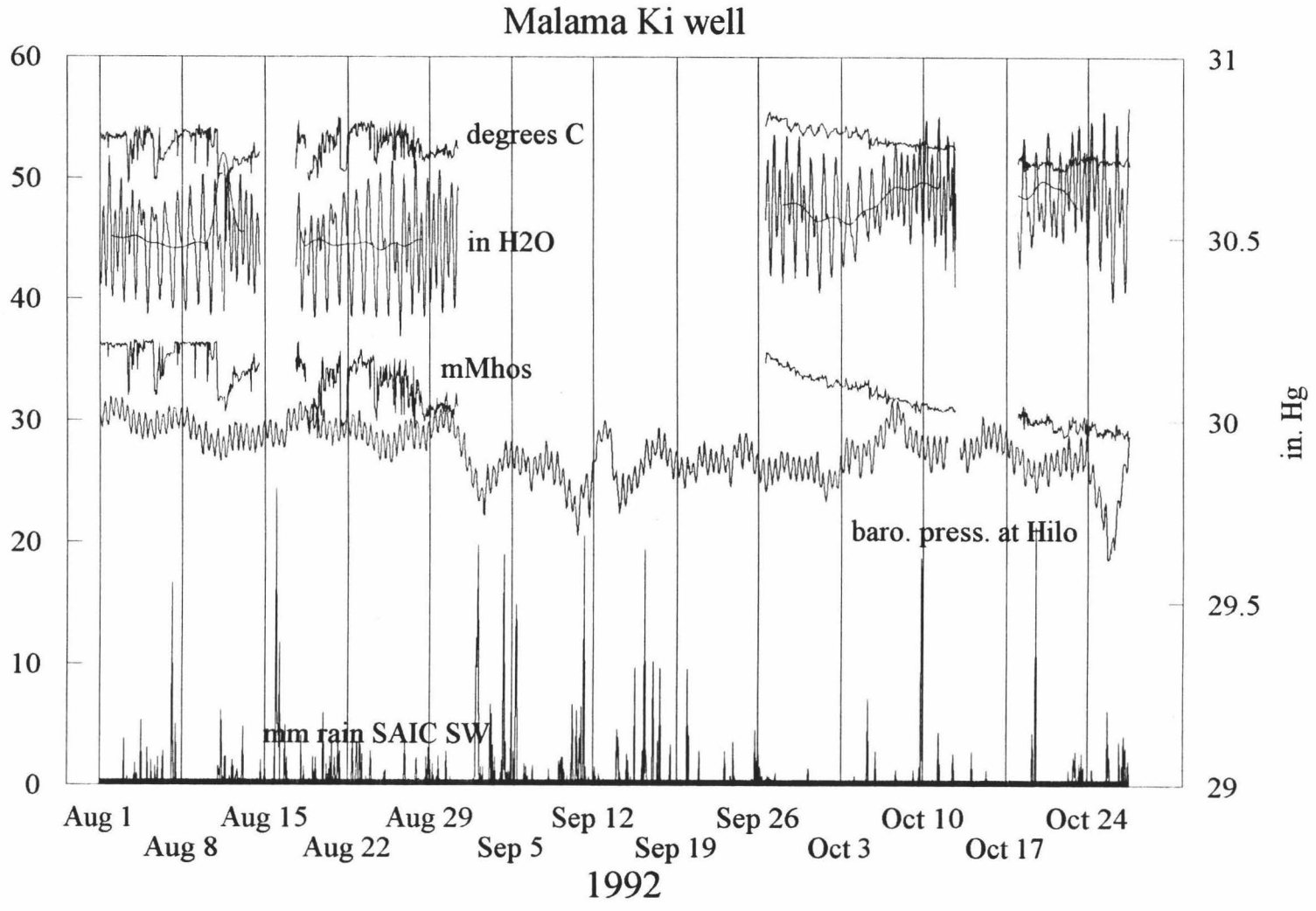

Figure 43. Malama Ki well hourly hydrological data 8/92 - 10/92.

Hydraulic Conductivity

With the addition of appropriate time lags for each well, hourly water level data from the Paradise Park reference well, Kapoho Airstrip well, Allison well, and Malama Ki well, and hourly tidal data recorded at Hilo, Hawaii, had higher than r = .90 correlation coefficients. This close correlation suggests a cause and effect relationship between ocean tides and water level fluctuations in these wells. Hence, water level data from them and recorded tidal data can be used to estimate hydraulic conductivity in the unconfined aquifer between the well and the coast by the Werner and Noren (1951) tidal decomposition method. This method was perfected in Hawaii by Kanehiro and Peterson (1977). The following treatment closely follows their methodology.

The method assumes that the ocean tidal signal, and the resulting water level fluctuations in the well, are a complex wave composed of sine waves generated by the gravitational forces of the sun and moon acting on the earth. The elevation of the tide above MSL at any given point may be expressed as:

$$H(t) = \sum_{i=1}^{n} H_i \cos(\omega_i t + \phi_i) \qquad 11.$$

where $H(t)$ = elevation of the tide as a function of time

H_i = coefficient representing the amplitude of the ith tidal constituent

ω = angular velocity

t = time

ϕ = tidal phase

n = number of tidal constituents being considered

While this expression for the tide seems relatively simple, there are over 200 constituents of tidal force. Fortunately, only seven of these constituents are large enough to be of general geophysical interest. They are listed in Table 12 below (after Kanehiro and Peterson 1977).

TABLE 12. TIDAL CONSTITUENTS

Symbol	Name	Species	Angular Velocity (rad/hr)
K_1	Lunisolar	Diurnal	0.262516
O_1	Larger Lunar	Diurnal	0.243352
P_1	Larger Solar	Diurnal	0.261083
M_2	Principal Lunar	Semidiurnal	0.505868
S_2	Principal Solar	Semidiurnal	0.523599
N_2	Larger Lunar Elliptic	Semidiurnal	0.496367
K_2	Lunisolar	Semidiurnal	0.525032

The Werner and Noren method treats the unconfined coastal aquifer as a filter. If a simple input signal, such as a tidal constituent cosine wave, with known amplitude and period is fed into it, the resulting output signal, a well water level constituent cosine wave, may be analyzed. The filter characteristics of the aquifer may be determined from the attenuation and phase lag imparted to the output signal, and if the governing equations for the aquifer are known, the coefficients of these equations may be found.

The general differential equations governing flow through porous media are the continuity equation;

$$-\nabla \cdot \rho q_i = \frac{\partial(n\rho)}{\partial t} \qquad 12.$$

and Darcy's law;

$$q_i = -K_{ij}\frac{\partial h}{\partial x_j} \qquad 13.$$

where ρ = density of water

n = porosity of the aquifer

q_i = specific discharge

K_{ij} = hydraulic conductivity tensor

h = piezometric head

x_j = space variable

Although Hawaiian basaltic aquifers are not isotropic and homogenous, difficulties in measuring and quantitatively describing their anisotropy and inhomogeneity require the following simplifying assumptions.

1. The aquifer is homogenous, isotropic, of large areal extent, and of uniform thickness.
2. The fluid is incompressible.
3. The problem is treated in one horizontal dimension which is perpendicular to the coast.

With these simplifying assumptions, the governing equation for an unconfined aquifer is written as;

$$\frac{\partial^2 h}{\partial x^2} = \frac{n'}{Kz}\frac{\partial h}{\partial x} \qquad 14.$$

where n' = apparent porosity

K = hydraulic conductivity

z = average saturated depth of the aquifer

Werner and Noren write the solution to the problem as:

$$h'(x,t) = \frac{h_o'}{4}\frac{A+B+C+D}{\sin h^2(n'\omega/2Kz)^{.5}+\cos^2[(n'\omega/2Kz)^{.5}L]} \qquad 15.$$

where $A = \exp[\sqrt{\frac{n'\omega}{2Kz}}(x+L)]\sin[n'\omega/2Kz)^{.5}(x-L)+\omega t]$

$B = \exp[\sqrt{\frac{n'\omega}{2Kz}}(x-L)]\sin[n'\omega/2Kz)^{.5}(x+L)+\omega t]$

$C = \exp[-\sqrt{\frac{n'\omega}{2Kz}}(x-L)]\sin\{-[n'/2Kz)^{.5}(x+L)+\omega t]\}$

$D = \exp[-\sqrt{\frac{n'\omega}{2Kz}}(x+L)]\sin\{-[(n'/2Kz)^{.5}(x-L)-\omega t]\}$

L = the horizontal width of the aquifer

x = a portion of the horizontal width of the aquifer

In the case at hand where $\sqrt{\frac{n'\omega}{2Kz}}L$ is large the solution simplifies to;

$$h'(x,t) = h'_o\exp[-\sqrt{\frac{n'\omega}{2Kz}}(L-x)]\sin[\omega t-(n'\omega/2Kz)^{.5}(L-x)] \qquad 16.$$

The above solutions essentially define wave motion whose amplitude is being damped exponentially. The general form of a cosine wave without damping may be written as;

$$y = y_m\cos(\tfrac{2\pi}{\lambda}x - \tfrac{2\pi}{\lambda}vt) \qquad 17.$$

where λ = wavelength

v = phase velocity

By comparison it may be seen that the solution in terms of the exponential decrease may be written as;

$$h'(x,t) = h'_o\exp(-\sqrt{\frac{n'\omega}{2Kz}}\,l) \qquad 18.$$

where $h'(x,t)$ = the amplitude of the tidal signal at the well, as a function of distance and time

h_o' = the amplitude of the tidal signal at the coast

l = the distance between the well and the coast (L - x)

Solving for the aquifer characteristics, apparent porosity, n', and hydraulic conductivity, K, the equation becomes;

$$\frac{n'}{Kz} = \frac{1}{l^2}\frac{2}{\omega}(\ln\frac{h'}{h_o})^2 \qquad 19.$$

Notide, a computer program modified by Michael L. Niederer from FITWAV1 was used to decompose both the ocean and well tidal signals. One calendar month, which encompasses one lunar cycle, of hourly recorded tidal data and hourly well water level data were used as the input signals. Because of equipment malfunctions, different months were used for each well except for Kapoho Airstrip well and Malama Ki well, which use the same month of hourly recorded ocean tidal data. The angular velocity of each of the constituent signals remained constant between the ocean and the well and has been presented in Table 12. The amplitudes, in the ocean and the well, of four of the seven geophysically significant tidal constituents used in this study are presented in Table 13.

TABLE 13. TIDAL CONSTITUENT AMPLITUDES

	O_1 (ft.)	P_1 (ft.)	K_1 (ft.)	M_2 (ft.)
Paradise Park well (08/01/93 - 08/31/93)	.06540	.01980	.12019	.08749
Kapoho Airstrip well (06/01/92 - 06/30/92)	.10535	.07906	.15915	.13660
Allison well (12/01/93 - 12/31/93)	.21195	.15446	.34455	.51932
Malama Ki well (06/01/92 - 06/30/92)	.13400	.06308	.24233	.22100
Ocean tide (6/01/92 - 06/30/92)	.29828	.17971	.53247	.71221
Ocean tide (08/01/93 - 08/31/93)	.27839	.17156	.47569	.73526
Ocean tide (12/01/93 - 12/31/93)	.27254	.16365	.51496	.69435

The distance between each well and the coast was measured using the distance function in the computer mapping program MapInfo. Apparent porosity, n', was assumed to be 10%, which is a reasonable value for Hawaiian basaltic aquifers (Kanehiro and Petereson, 1977). The average saturated depth of the aquifer, z, was determined from cuttings and cores recovered from SOH#2, a geothermal exploration hole drilled approximately 100 m south of Kapoho Airstrip well. Unaltered subaerial basalt cuttings were recovered from this hole at 515 m, there were no returns between this depth and 582 m where altered hyaloclastite and submarine pillow basalt cores were recovered to a depth of 607 m (Novak, et al, 1991). The palagonized hyaloclastites recovered from this depth interval are an effective aquitard; therefore an average saturated aquifer depth of 500 m (600 m minus 100 m of vadose zone above sea level) was used for this study. The resulting average values of hydraulic conductivity between each well and the coast and previous workers estimates of hydraulic conductivity are presented in Table 14.

TABLE 14. HYDRAULIC CONDUCTIVITY

Druecker and Fan (1976)	Puna			
	3,338 - 4,173 m/day			
Imada (1984)	non-rift	LERZ		
	4,337 - 8,277 m/day	881 - 2,356 m/day		
Takasaki (1992)	north flank	LERZ	south flank	
	1,954 m/day	2,164 m/day	2,033 m/day	

Werner and Noren Method

	Paradise Park	Kapoho Airstrip	Allison	Malama Ki
K avg.	2,521 m/day	13,032 m/day	177,751 m/day	4,865 m/day
Std. Dev.	726	4,494	255,633	954

The hydraulic conductivity values obtained by the Werner and Noren method are higher than those estimated by other workers. Hydraulic conductivities for the Paradise Park and Malama Ki wells, although high, are not too dissimilar to previous estimates. Hydraulic conductivity for Kapoho Airstrip well may be reduced to a reasonable value by assuming a lower apparent porosity for the LERZ than for the north and south flanks. When apparent porosity is reduced from 10 % to 2%, hydraulic conductivity for Kapoho Airstrip well becomes 2,353 m/day. However, it is unlikely that apparent porosity in this area of the LERZ is significantly less than that of the adjacent flank areas for the following reasons. High water in Kapoho Airstrip well and Malama Ki well follows high tide by similar time lags, 18.5 and 17.9 hours, respectively. Tidal efficiency in Kapoho Airstrip well is 33%, and tidal efficiency in Malama Ki well, half as far from the coast, is 46%. Unusually high hydraulic conductivity in Kapoho Airstrip well may be a result of its structural setting. The well is located near the subaerial terminus of the LERZ in a shallow graben. The unbuttressed condition of the LERZ at this point and the faults of the graben may have caused unusually dense fracturing which would account for its unusually high hydraulic conductivity.

The incredibly high hydraulic conductivity and very large standard deviation estimated for Allison well result from one tidal constituent, P_1, yielding an extremely large K value. With P_1 removed, the hydraulic conductivity for Allison well becomes 30,331 m/day, while this value is extremely large, it is not absurd. As in Kapoho Airstrip well, unusually high hydraulic conductivity in Allison well may be a result of its structural setting. The well is located near the coast on the LSF in an area which has experienced

noticeable subsidence since the 1975 earthquake, here also, unusually dense fracturing may account for unusually high hydraulic conductivity.

Discussion

All the wells used in this study, both the thermal wells and the non-geothermal reference well, respond in much the same manner to natural stresses placed upon their aquifers. All but MW-2 show a daily tidal water level fluctuation proportionate to the permeability of the geologic units between the well and the coast. All but Allison well show an inverse response to barometric pressure variations. All but Allison well show a long term rise or fall in water level in response to seasonal changes in rainfall.

An examination of the magnitude of seasonal water level change in each well reveals a basic relation between permeability and available recharge. Since data sets of differing length made comparison difficult, it was assumed that the December to June change in water level observed in the Paradise Park reference well represented the wet to dry season change in water level. Data sets of lesser duration from the other wells were normalized to it. The data is summarized in the following table.

TABLE 15. SEASONAL RECHARGE

Well	Data set length	Change in water level	Change in water level norm. to 5 mos.
Malama Ki	2.5 mos.	16.54 cm	33.07 cm
MW-2	4 mos.	34.21 cm	42.54 cm
Kapoho Airstrip	4.5 mos.	40.33 cm	44.81 cm
Paradise Park	5 mos.	51.23 cm	51.23 cm

Malama Ki well shows the least seasonal change in water level using this method; this is a function of the high permeability and restricted recharge available to the LSF. Despite their differences in well water level response to tidal fluctuations, Kapoho Airstrip well and MW-2 have similar seasonal water level changes. This is an indication that recharge to both wells flows down the LERZ from west to east, channeled by the dike structure. The magnitude of seasonal water level change in these LERZ wells is midway between that of Malama Ki well and Paradise Park well, reflecting the larger amount of recharge available to the LERZ than to the LSF. The Paradise Park reference well shows the largest seasonal water level change. This is a function of its somewhat restricted permeability and the extremely large amount of recharge available to the LNF.

Medium term changes in well water levels appear to be a result of sea level fluctuations caused by changes in barometric pressure. All the wells except Allison well have negative water level - barometric pressure correlation coefficients between $r = -0.27$ and $r = -0.47$ which is evidence that they respond in a more or less similar manner to barometric pressure changes. Correlation between well water level changes in Kapoho Airstrip well and the other continuous monitoring study wells is presented in Table 16.

TABLE 16. CORRELATION BETWEEN WELL WATER LEVELS

Well	Time Period	r
Malama Ki	05/22/92 - 09/15/92	0.55943
Paradise Park	05/26/93 - 09/29/93	0.03884
MW-2	05/26/93 - 09/29/93	0.23267
Allison	11/01/93 - 12/31/94	0.80258

The high correlation coefficients between water level fluctuations in Kapoho Airstrip well and the LSF wells, Malama Ki and Allison, are an indication that these wells belong to the same groundwater province and may have similar transmissivities. MW-2 shows only weak correlation with Kapoho Airstrip because its waters are shielded from lower LERZ and LSF groundwater flow by dikes. The very low correlation coefficient between Kapoho Airstrip well and the Paradise Park reference well indicates it belongs to a different groundwater province.

All the wells show a temperature gradient from warmer to cooler water with increasing depth. In the Paradise Park reference well relatively warm low conductivity water is introduced at the top of the water table by vertical infiltration, where it floats on the slightly cooler higher conductivity groundwater that enters the ground at higher elevations. In the thermal wells, hot high conductivity water is introduced at the bottom of the water table by hydrothermal upflow. It rises to the top of the water table by being slightly more buoyant than the slightly cooler lower conductivity water it passes through. At the same time, vertical infiltration which is cold compared to thermal water, descends through the thermal layer at the top of the water table until it equilibrates with water deeper in the aquifer, creating the slightly cooler lower conductivity layer beneath. The laminar nature of groundwater flow aids in maintaining this stratification (Fetter, 1980).

The effects of vertical infiltration are visible in the Paradise Park reference well and to some extent in Allison well. Although one is a reference well and the other is a warm mixed water well, they are the two shallowest wells in this study, 41.78 m and 37.82 m deep respectively. Vertical infiltration effects are not visible in any of the deeper wells

perhaps because, as an infiltration front travels greater distances, it becomes more vertically dispersed. When an attenuated infiltration front arrives at the top of the deep water table its effects on water level are easily overwhelmed by daily tidal fluctuations.

CHAPTER V.

CONCLUSIONS

Hydrological

The aquifers which comprise the LNF, LERZ, and LSF groundwater systems are open systems in a state of dynamic equilibrium, and are constantly adjusting in response to meteorological inputs. Groundwater in the lower LERZ and LSF (Kapoho Airstrip, Allison, and Malama Ki wells) appears to comprise an aquifer which responds to these inputs as a single unit, but dike confined groundwater at higher elevations on the LERZ (MW-1, MW-2, MW-3, and GTW-3 wells) is in only partial communication with this system. The LNF aquifer (Paradise Park reference well) comprises a separate groundwater system.

Groundwater levels are affected by three primary meteorological inputs. Daily ocean tidal fluctuations produce the most significant, and shortest term, variation in well water levels. Synoptic changes in barometric pressure cause variations in water levels which have a duration of several weeks. Seasonal changes in rainfall cause changes in water levels over a period of approximately six months. Changes in rainfall of several years duration cause long term changes in water levels. Variations in rainfall make greater or lesser amounts of cold groundwater available to mix with thermal brackish water in the warm mixed water wells. This causes variations in the chemistry and temperature of the mixed water wells. Concentrations of total dissolved solids

(conductivity) and temperatures in well waters rise during periods of low rainfall, and fall when rainfall increases.

Hydrogeochemical

Water chemistry in LERZ and LSF thermal wells and shoreline warm springs is diverse, but not without order. When analyses from all the wells and springs are plotted on Giggenbach's ternary "maturity" diagram (Figure 26), all fall in the lower right corner of the diagram between "immature" average Hawaii groundwater on the basalt dissolution line and seawater in the "partially mature" field. This grouping is evidence that the two end member waters which mix to create the water in these wells are groundwater and slightly thermally altered seawater. Geothermal reservoir fluids, which plot far to the left of this group, do not appear to make a significant contribution to lower Puna groundwaters.

The thermal wells can then be divided into low, medium, and high chloride wells. All the low chloride wells, KS-3, KS-4, KS-10, MW-1, and MW-3, are located in the LERZ on Puna Geothermal Venture's Pohoiki lease. Water in all these wells shows enrichment in sulfate which is indicative of steam heating.

Except for Allison well on the LSF, all the medium chloride wells, KS-7, KS-8, KS-9, MW-2, and Kapoho Airstrip well, are located within the LERZ. All show evidence of containing a fraction of thermally altered brackish water characterized by an enrichment in Ca^{2+} and depletion in Mg^{2+} compared to SMOW, and all but MW-2 show evidence of steam heating.

The two high chloride wells, GTW-3 and Malama Ki well, are located in the LERZ and LSF respectively. Along with the shoreline warm springs, Kapoho Bay, Campbell, Pualaa, and Isaac Hale, they show enrichment in Ca^{2+} and depletion in Mg^{2+} and SO_4^{2-}, which is characteristic of thermally altered brackish water.

On this basis, the low chloride wells may also be classified as steam heated groundwater wells, the medium chloride wells as steam heated groundwater and thermally altered brackish water mixed wells; and the high chloride wells and shoreline warm springs as thermally altered brackish water mixed wells and springs.

Contact with a thermal source has further altered the water chemistry of all the LERZ and LSF wells and springs. All, except Allison well, have silica concentrations higher than average Hawaii groundwater. Silica content offers a quantitative method for assessing the fractions of thermal water in these wells and the temperatures of the thermal sources these waters have contacted. Once the thermal fraction of water in each well is determined, the original concentration of chlorides in that fraction may be calculated. The thermal water fraction of all the wells has a chloride concentration less than that of seawater.

Water in two of the shoreline warm springs, Pualaa and Campbell, appears to have contacted the highest temperature thermal source. The silica geothermometer yields a temperature for the thermal water fraction of the springs as 222.6 ^{0} C and 214.7 ^{0} C respectively. KS-3 and MW-2 yield the coolest thermal water fraction temperature, about 100 ^{0} C. The unusually low silica concentration of Allison well, 31.5 mg/l, does not allow

the silica geothermometer to be applied. The thermal water fraction temperatures of all the other wells and springs average 181.5 ^{0} C, with a standard deviation of 15.1 ^{0} C.

Hot fraction water temperatures produced from the silica geothermometer agree well with the degree of alteration in well water to SMOW ion ratios. All the wells with appreciable chloride contents show Ca^{2+} enrichment and Mg^{2+} depletion compared to SMOW. However, none of them show alteration ratios above those produced from seawater-basalt reactions at 200 ^{0} C.

When calculated silica geothermometer temperatures for water samples from KS-3, KS-8, KS-9, and KS-10 are plotted on static temperature surveys taken in these wells after drilling and before production, they fall at the beginning or in the middle of the steep temperature gradient identified by Puna Geothermal Venture (PGV) geologists as the "impermeable zone" between the unconfined groundwater aquifer and deep geothermal aquifers (Figures 44 through 47). Therefore, the thermal water portion of the KS series wells must originate at the bottom of the unconfined aquifer where it is heated by conduction and steam infiltration from the "impermeable zone". Unfortunately deep temperature logs cannot exist for shallow groundwater wells, so this correlation cannot be applied to the other LERZ and LSF wells.

The several lines of evidence discussed above strongly suggest that thermal water in LERZ and LSF wells and springs does not originate in the 350^{0} C geothermal reservoir tapped by commercial production. The thermal fraction of all the LERZ and LSF wells and springs very probably originates at the bottom of the unconfined aquifer. Whether this water is fresh or brackish is a function of local small scale geology.

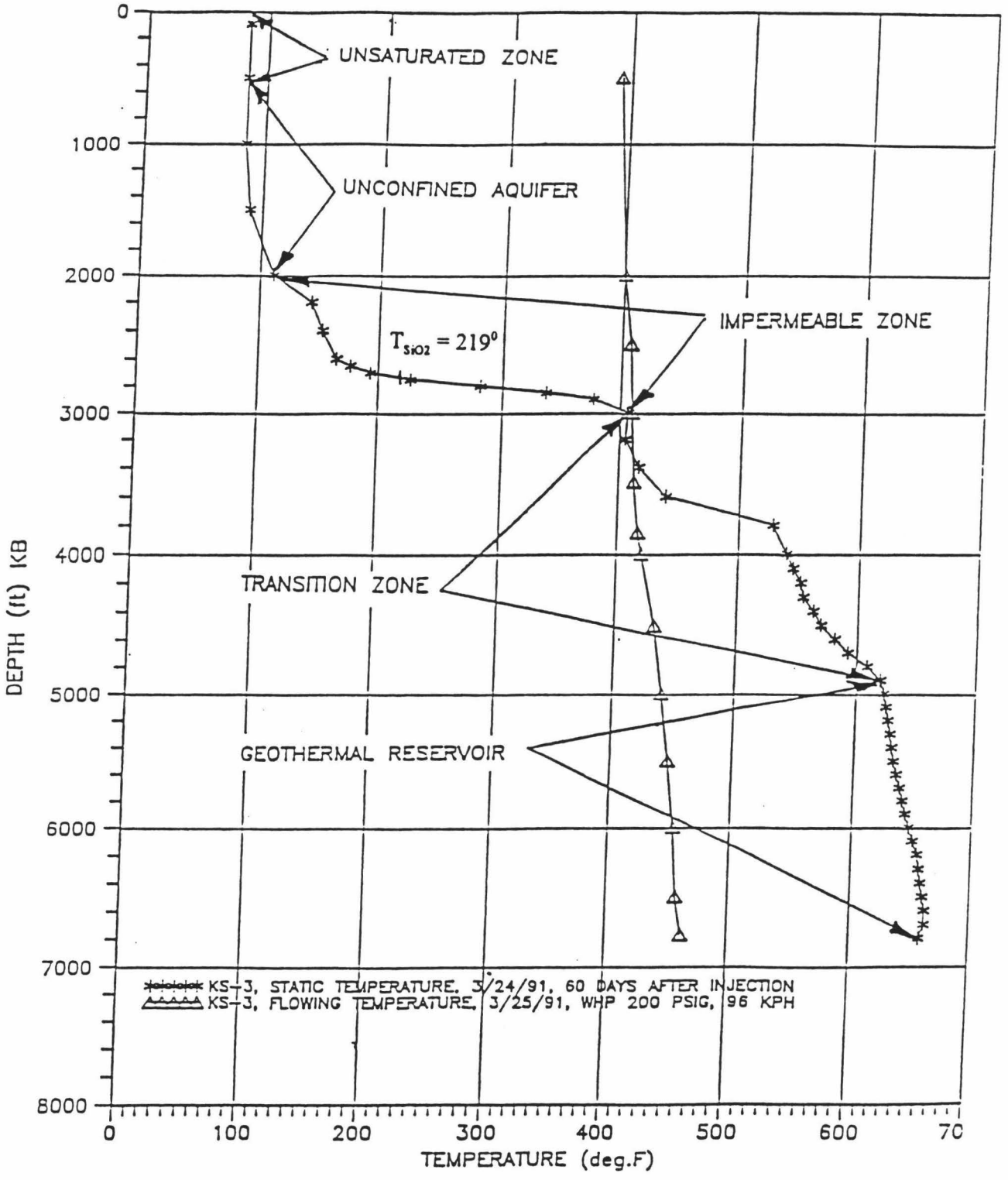

Figure 44. KS-3 static and flowing temperature surveys.

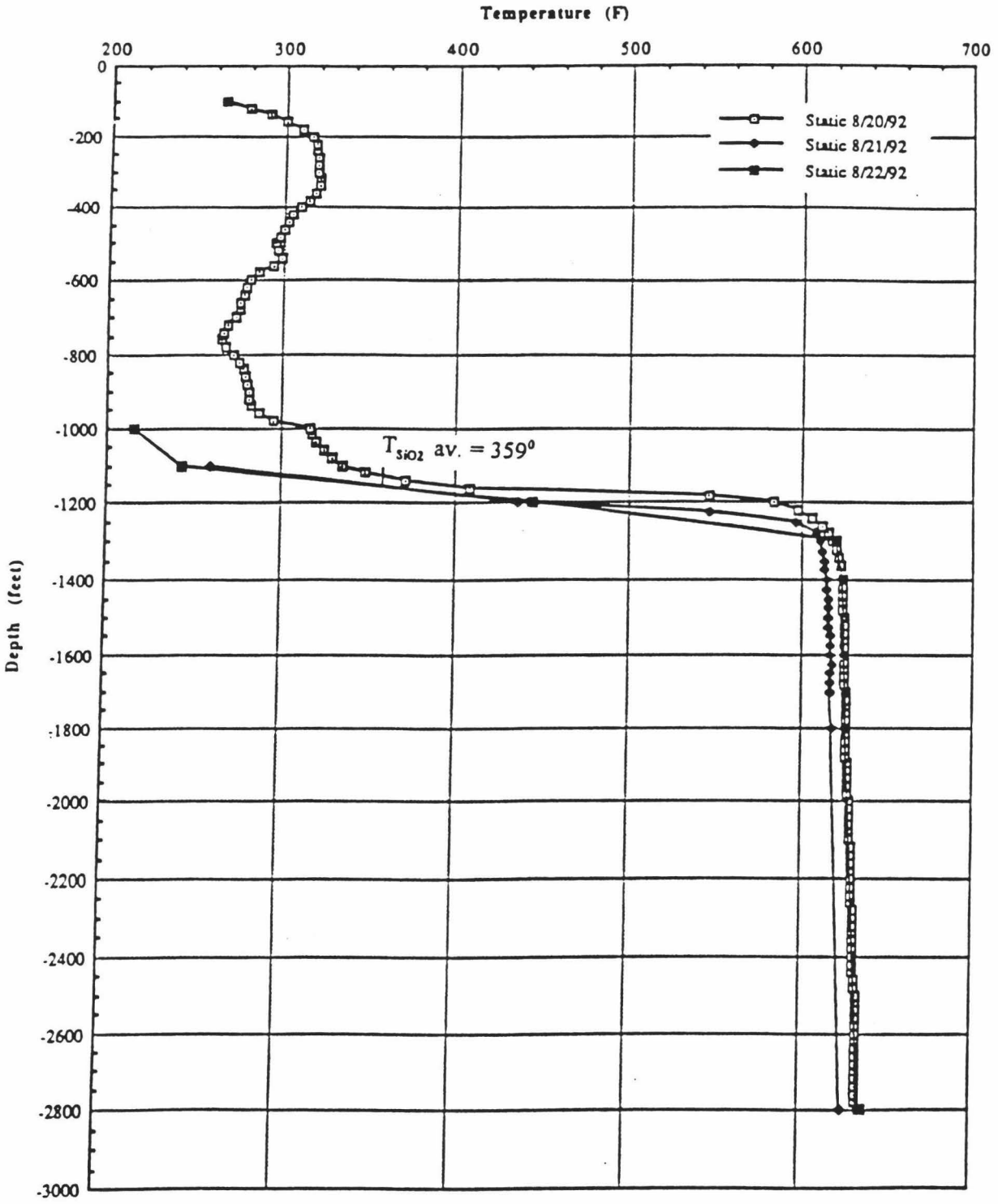

Figure 45. KS-8 static temperature survey.

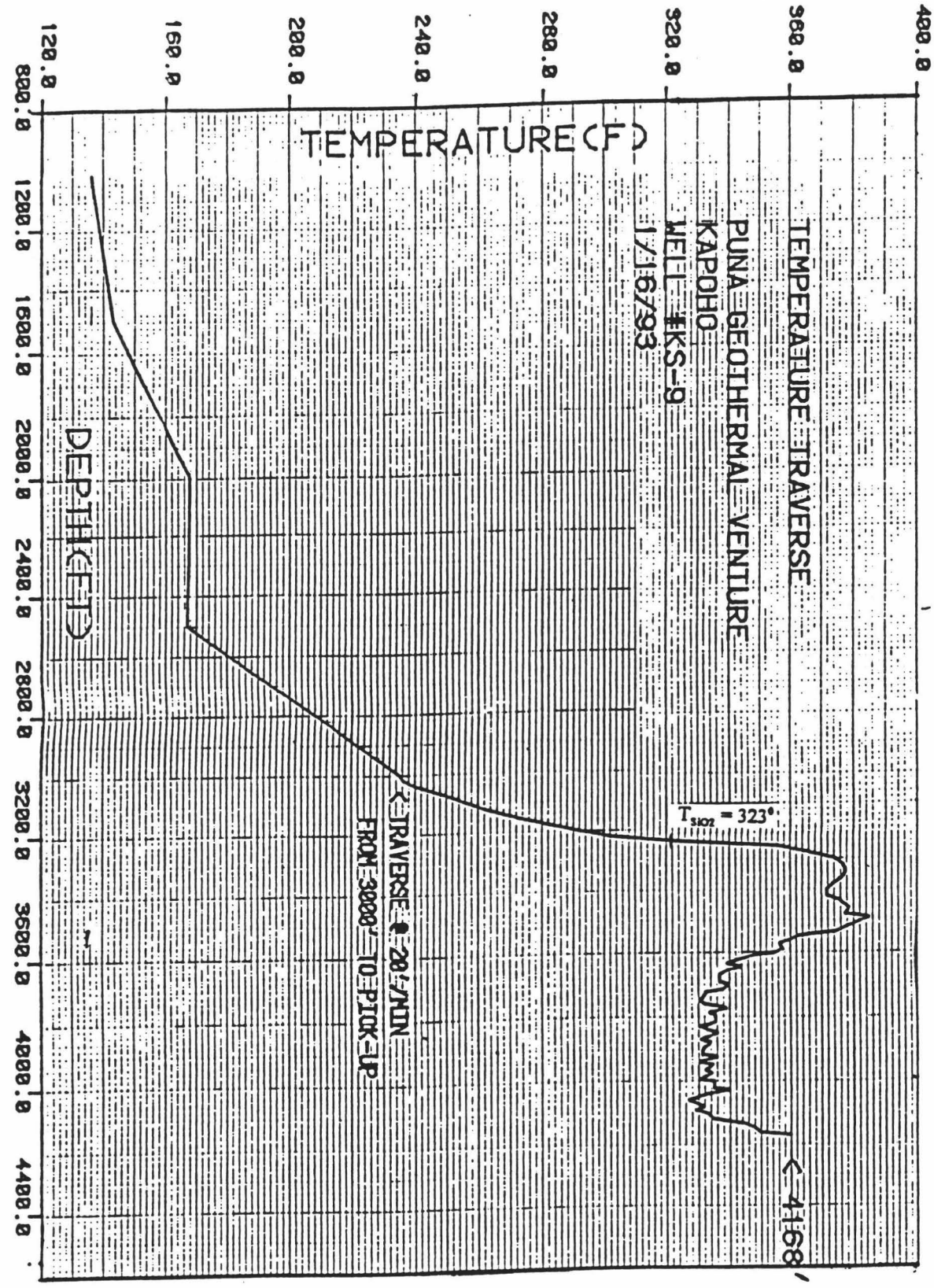

Figure 46. KS-9 static temperature survey.

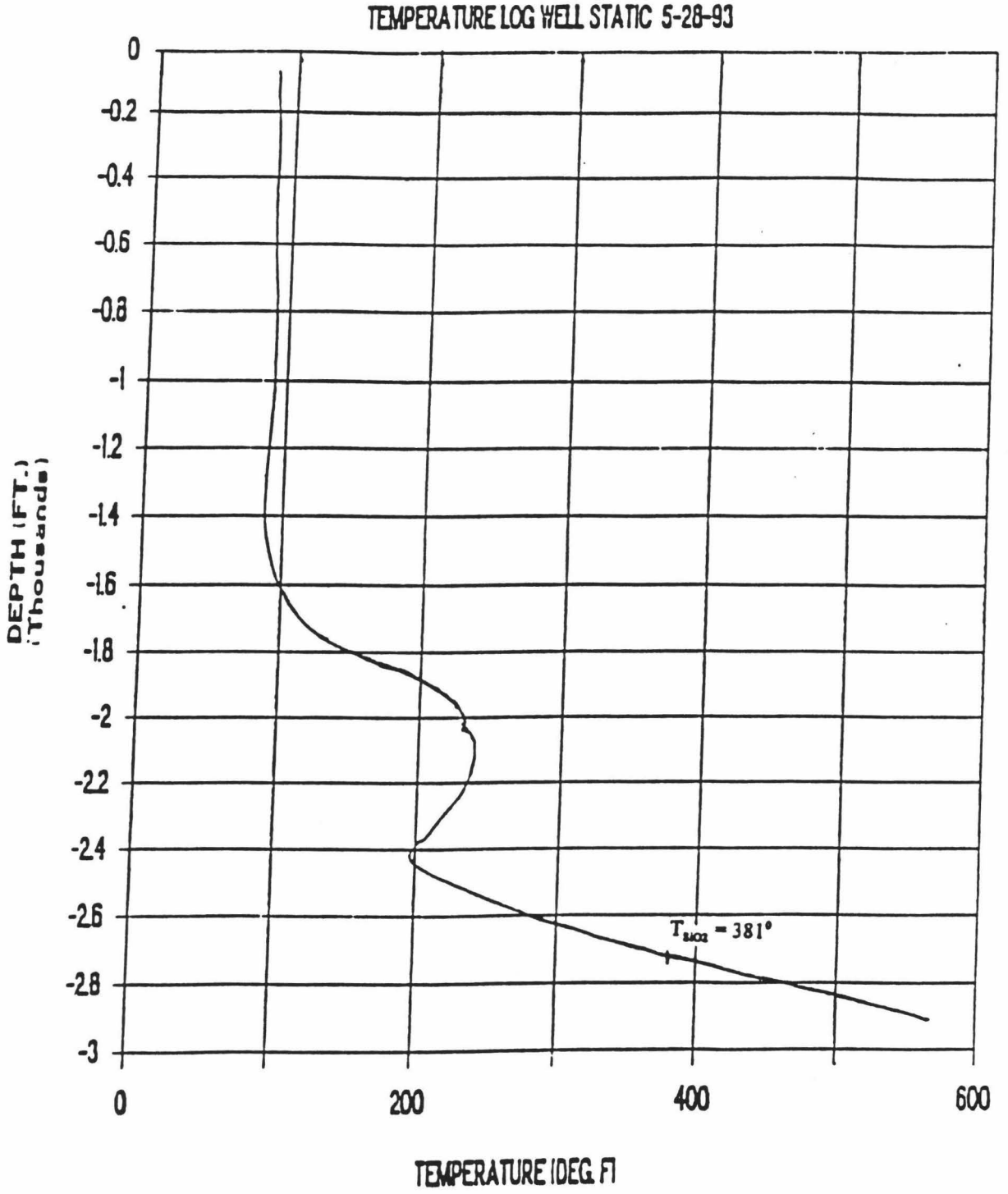

Figure 47. KS-10 Static temperature survey.

A Conceptual Model of Shallow Groundwater Flow in the LERZ and LSF

Previous models have regarded the disparate chemistry of LERZ well waters as evidence that they originated from separate aquifers. However, beneath this apparent diversity lies a discernible pattern governed by the geologic structure of the LERZ.

A technique developed by A. H. Truesdell and R. O. Fournier (1977), the silica versus enthalpy diagram (Figure 48), can be useful in detecting this pattern. The diagram uses the principal of conservation of enthalpy and mass to establish a linear relationship between thermal waters whose enthalpy and silica concentration have changed by dilution with ambient groundwater. Enthalpy in calories per gram and silica concentration in mg per liter of ambient groundwater and thermal well waters are plotted on the diagram. Thermal waters which can be connected by a straight line to ambient groundwater are related to each other by dilution. Hence, they lie on the same flow path within the aquifer (Figure 48). This method, together with a stable isotope study by M. Scholl, et al. (1992), which identified possible recharge elevations for LERZ and LSF wells and springs will be used to delineate probable flow paths within the LERZ and LSF groundwater aquifers.

The temperature and chemistry of a water sample from the farthest uprift PGV well, KS-4, show evidence of steam heating. How far this thermal signature extends uprift will probably never be known since this well is close to the uprift border of the PGV Pohoiki lease. However, for this study, it and the proven producer, HGP-A well, will define the uprift boundary of the Pohoiki geothermal field (Figure 49). Since MW-3 shows strong evidence of steam heating, it will represent the north boundary of the field.

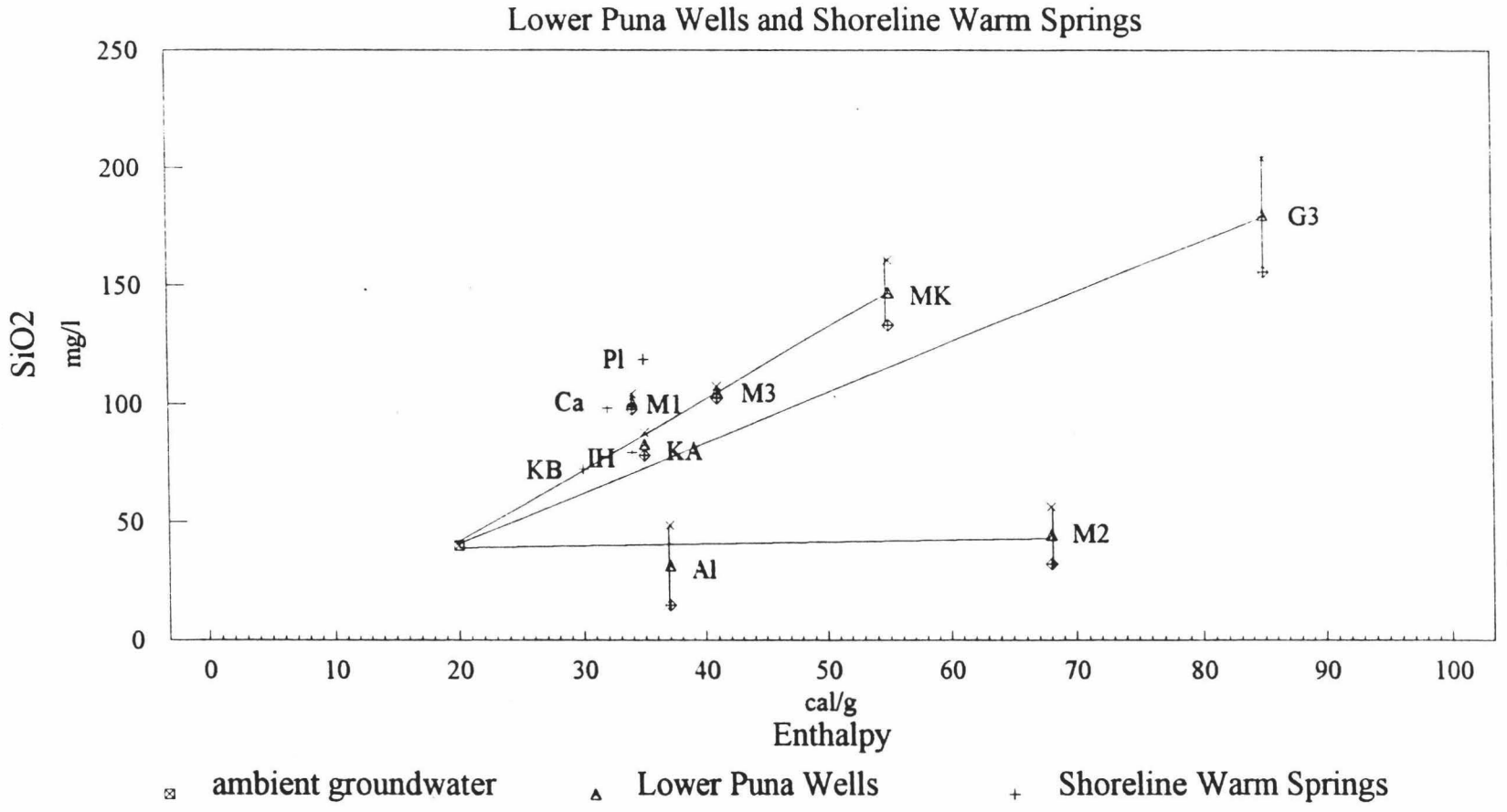

Figure 48. Silica versus enthalpy.

The south boundary of the field lies between KS-7 and Lanipuna-1 & -6 wells (Appendix A). All the wells within this roughly triangular area (Figure 49), show evidence of steam heating (Figure 50). Heads vary in them by as much as 3 m over a horizontal distance of less than 30 m and there is no coherent spatial variation in head in these wells in any direction (Table 1). Nor, other than their common enrichment in sulfate, is their chemistry coherent. Though generally low, chloride varies by an order of magnitude in them.

These wells tap rift crest, dike confined, micro-aquifers which receive up gradient recharge as it pours down rift from dike compartment to dike compartment. Dikes channel and dam groundwater at the top of the water table and help to shield these partitions from shallow seawater incursion. Secondary mineral precipitation and groundmass alteration created by hydrothermal circulation in the geothermal reservoir further seal them at depth. Conduction and steam seepage through this seal keeps micro-aquifer waters well mixed by convection.

Puu Honuaula, the large cinder cone which bisects the Pohoiki geothermal field parallel to the LERZ axis, also appears to act as a barrier to groundwater flow within the LERZ. At least a portion of the groundwater which flows down rift north of Puu Honuaula remains north of the LERZ axis. This is apparent in the silica versus enthalpy diagram, a dilution line runs from MW-3 to Kapoho Airstrip well to Kapoho Bay spring (Figure 48). This relationship may account for the fact that Kapoho Airstrip well is the only well outside the Pohoiki geothermal field which shows significant sulfate enrichment (Figure 50).

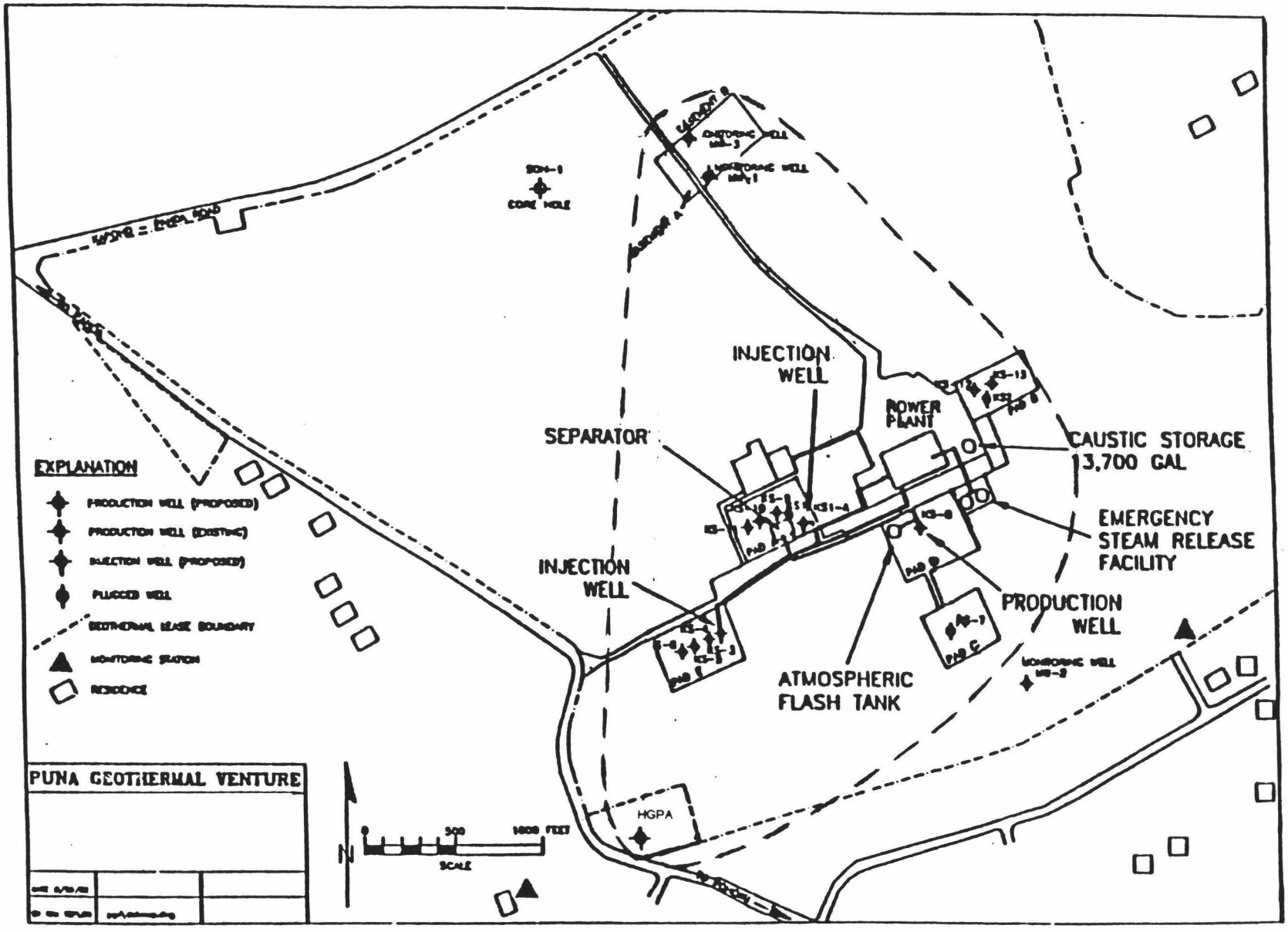

Figure 49. Pohoiki Geothermal Field.

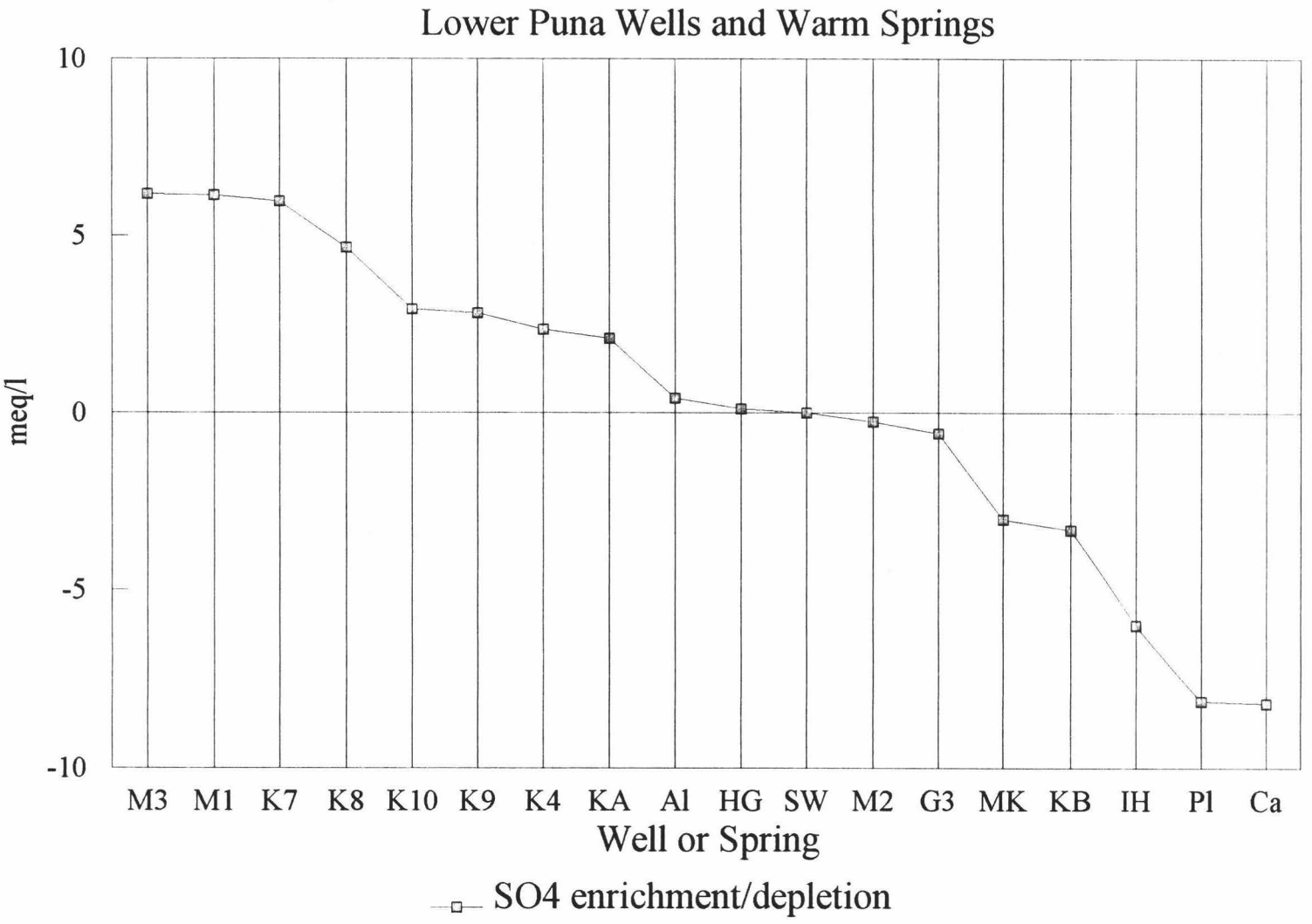

Figure 50. Sulfate enrichment or depletion compared to SMOW. Well name abbreviations in Table 1.

Groundwater which passes south of Puu Honuaula finds its way through the LERZ at the eastern boundary of the Pohoiki geothermal field and streams down the south flank. Two lines of evidence support this conclusion. First, the two unusually low silica wells, MW-2 and Allison, form a dilution line on the silica versus enthalpy diagram (Figure 48). Second, Scholl's (1992) deuterium study identified possible recharge elevations for MW-2, Campbell, and Pualaa springs as up to 1,500 ft. The LERZ does not attain these elevations directly upgradient from these springs Meteoric recharge to them must travel down rift, mix with thermal discharge around the 200 m elevation of MW-2, then flow down the LSF groundwater gradient to the springs.

The eastern boundary of the Pohoiki geothermal field is undiscovered, however, it must lie east of KS-2 (Appendix A) and west of GTW-3 (Figure 49), since water chemistry changes abruptly across this boundary. As discussed above, MW-3 and KS-7 are steam heated, low chloride wells. GTW-3 shows no evidence of steam heating (Figure 50) and its chloride content is ~28% that of SMOW.

Hydrothermal processes which cause secondary mineral crystallization in voids and groundmass alteration of basalts to smectite clays (Facca, 1967) have formed a seal around the Pohoiki geothermal reservoir, effectively excluding the influx of seawater into the bottom of the groundwater aquifer which overlies it. Beyond the "sides" of the reservoir, where temperatures are relatively cooler, less alteration has taken place and this seal does not exist. Heat conduction through the seal sets convection cells in motion which tap brackish water available at the bottom of the unshielded groundwater aquifer.

This is the structural setting tapped by MW-2 and GTW-3. Both are dike confined LERZ wells with medium and high chloride concentrations respectively, but neither shows evidence of steam heating (Figure 50). It is a reasonable assumption therefore, that hydrothermal alteration is the effective seal against seawater intrusion at the bottom of the groundwater aquifer directly above the Pohoiki geothermal reservoir. Dikes may compartmentalize and channel groundwater within the LERZ but they cannot exclude the influx of seawater at depth. It may further be assumed that the medium chloride well MW-2 is at the very edge of the field. GTW-3 is beyond the edge, closely downgradient from the upflow zone of a powerful convection cell. GTW-3's high chloride concentration, high temperature, and reverse temperature profile (Thomas, et al., 1979) all bear evidence of this.

Water in Malama Ki well, on the LSF, shows a resemblance to that of GTW-3. Its chloride concentration is ~28% that of SMOW, it is hotter than the study area average well temperature of 40.3^0 C, and it also has a reverse temperature profile (Thomas, et al., 1979). However, it is located cross gradient from GTW-3, so it is unlikely the two wells are related to each other by dilution. Malama Ki well does lie downgradient of Puu Lena, a large tuff crater on the southern edge of the LERZ. The thermal portion of Malama Ki well water very probably has the same structural origin as that of GTW-3. A convection cell must exist on the LERZ near Puu Lena. Thermal water from it mixes with groundwater as it flows down the LSF gradient where it is intersected by Malama Ki well. This water may be traced farther down gradient to the coast by a dilution line from Malama Ki well to Isaac Hale spring on the silica versus enthalpy diagram (Figure 48).

If a powerful convection cell analogous to that which supplies the thermal portion of GTW-3 well water exists in the vicinity of Puu Lena, then it follows by analogy that a hydrothermal system must also exist in this area. Further evidence of the existence of this system is Puu Lena itself, created by a large prehistoric phreatomagmatic eruption. Unfortunately, this system will probably never be fully explored since the land around Puu Lena comprises the Leilani Estates subdivision.

Pualaa and Campbell, the two hottest shoreline springs with the highest silica concentration on the LSF, do not form a dilution line with any of the LERZ wells. However, they do lie directly down gradient from the Pohoiki geothermal field and are bracketed (in map space) by flow lines from MW-3 - Kapoho Airstrip well - Kapoho Bay spring and MW-2 - Allison well. Their location and sulfate depletion (Figure 50) makes it a reasonable assumption, therefore, that their waters represent outflow from a convection cell just beyond the boundary of the field, much like GTW-3.

In summary, the LERZ - LSF groundwater system is controlled by the Pohoiki geothermal reservoir and the hydrothermal system present in the vicinity of Puu Lena, but the input from these reservoirs is enthalpic, not a direct fluid contribution. Steam heated, low chloride, groundwater lies directly above the Pohoiki reservoir. An aureole of high temperature, high chloride, groundwater borders the Puu Lena system to the south and the Pohoiki field to the east and south, but does not appear to be present north of the LERZ axis. This water flows down the LSF groundwater gradient to surface in the LSF shoreline warm springs.

CHAPTER VI.

RECOMMENDATIONS FOR FUTURE WORK

A more detailed understanding of the LERZ - LSF groundwater system will only be gained as more wells are drilled to provide more groundwater sampling points. However, since groundwater in this area has not proved potable or even suitable for irrigation, it seems unlikely that more water wells will be drilled. Renewed geothermal well drilling at PGV, scheduled for the summer of 1995, will provide another opportunity to sample groundwater in the Pohoiki geothermal field. More accurate analyses will be available from these wells than those previously drilled because University of Hawaii personnel will be on hand to collect and analyze these samples.

The monitoring program should be expanded to include the MSF. At least one new water well has been drilled in this area. Near shore, old Hawaiian dug wells and shoreline springs also exist. Locating and sampling these wells and springs may give insight into the possible existence of MERZ hydrothermal systems.

Data from the continuous monitoring project are being used to develop a baseline for analysis of trends in water level, temperature, and conductivity. This baseline will be used to identify and assess the impacts, if any, of geothermal development on the LERZ - LSF groundwater system. However, since the Terra Systems sensors did not function reliably in the high temperature wells, most of these data are from the medium temperature wells which lie far down gradient from the Pohoiki geothermal field. The continuous monitoring project should be refocused on the high temperature wells, and an effort

should be made to obtain reliable high temperature sensors to be installed in GTW-3 and MW-2. These are the closest down gradient wells to the Pohoiki geothermal field, any perturbations to the LERZ - LSF groundwater system caused by geothermal production and/or reinjection will first appear in them.

APPENDIX A

A CHRONOLOGY OF GEOTHERMAL EXPLORATION AND PRODUCTION

IN THE KILAUEA EAST RIFT ZONE

NAME	OPERATOR	YEAR DRILLED	DEPTH FT	T MAX F^0	DATA SOURCE
HGPA	State of Hawaii	1976	5,210	680	1
Pohoiki Field discovery well, produced 3 MW from 1982 to 1989, currently shut in, used as monitor well.					
Ashida 1	Barnwell-WRI	1981	8,300	550	1
Exploratory, dry, plugged.					
Lanipuna 1	Barnwell-WRI	1981	8,389	685+	1
Production test, dry, may be hottest well in field, plugged.					
KS-1	Thermal Power	1981	7,290	650	1
Production test, tested at 3.2 MW, casing damaged, plugged.					
KS-2	Thermal Power	1982	8,005	670	1
Production test, tested at 2 MW, casing damaged, plugged.					
Lanipuna 1-ST	Barnwell-WRI	1983	6,271	429	1
Side track from Lanipuna 1, production test, probably outside of reservoir, plugged.					
Lanipuna 6	Barnwell-WRI	1984	4,956	335	1
Production test, coolest hole, probably outside the reservoir, possible injection well, suspended.					
KS-1A	Thermal Power	1985	6,505	670	1
Production test, tested at 3 MW, damaged, reworked by PGV, currently used as injection well.					
SOH-4	State of Hawaii	1990	6,562	576	3
Scientific observation core hole, may have entered KMERZ reservoir, currently used as monitoring well.					

NAME	OPERATOR	YEAR DRILLED	DEPTH FT	T MAX F^0	DATA SOURCE
KMERZ A-1	True/Mid Pacific Geothermal	1990	8,651	635	1
KMERZ A-1 ST			8,741		1

Exploratory on KMERZ, original hole plus sidetrack and 3 redrills, logged and tested, deepest hole in rift zone, steam entries reported, suspended.

KS-3	Puna Geothermal Venture	1990	7,406	664+	2

Production test, tested at 3.2 MW, currently used as injection well.

SOH-1	State of Hawaii	1991	5,526	408	3

Scientific observation core hole, probably outside of reservoir, currently used as monitoring well.

SOH-2	State of Hawaii	1991	6,802	661	3

Scientific observation core hole, may have entered Kapoho reservoir, currently used as monitoring well.

KS-7	PGV	1991	1,678	500+	2

Steam/gas kick, injection test, plugged.

KS-8	PGV	1991	3,488	630+	2

Slant drilled, 30 hour steam/gas blowout, production test, potentially large producer (14 MW), reworked 1992, produced 5 MW, casing damaged when well was shut in after lightening strike to power line, plugged.

KS-4	Puna Geothermal Venture	1992	6,713		2

Drilled, and currently used as an injection well.

KS-9	PGV	1992	4,427		2

Slant drilled, production test, potentially large producer, producing 9 MW with no pressure drawdown as of 4/24/93.

KS-10	PGV	1993	5,083		2

Slant drilled, potentially large producer.

Data sources:

1. Geothermex Draft Annual Report, July 1992, for Hawaii Department of Business and Economic Development

2. Puna Geothermal Venture Drilling Reports

3. Scientific Observation Project Drilling Reports

APPENDIX B

WELL CASING SCHEMATICS

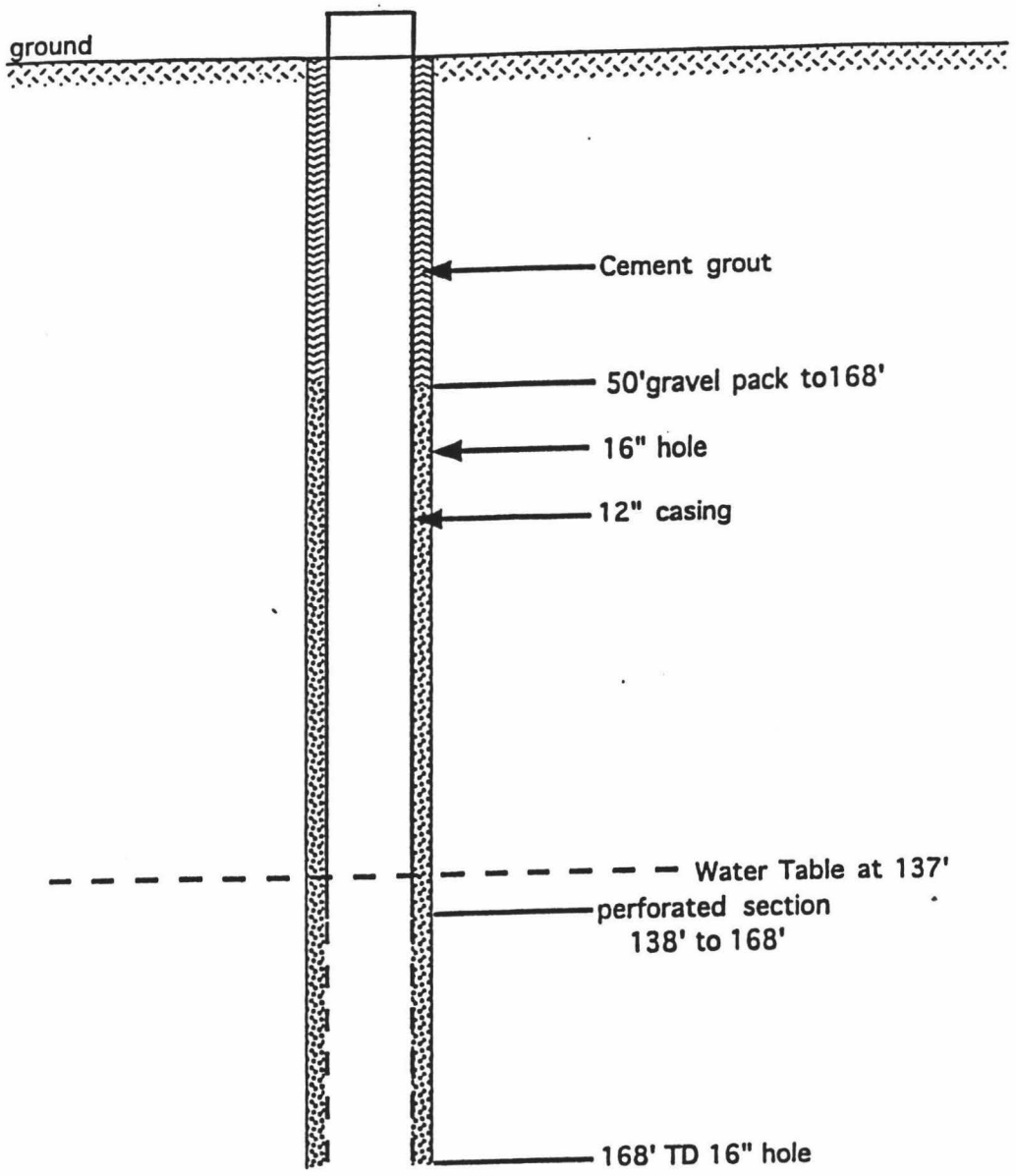

HAWAIIAN PARADISE WELL #1

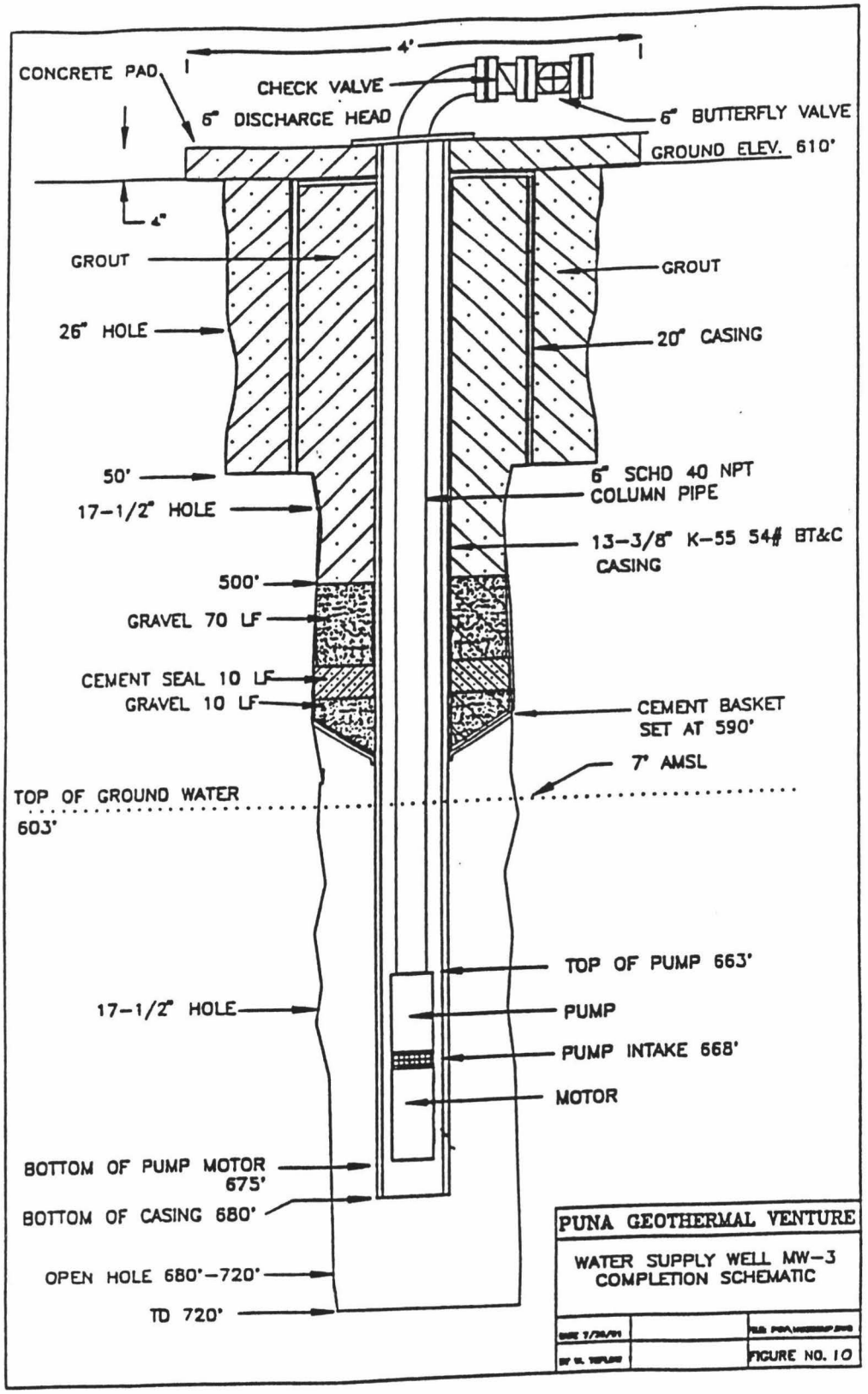
4'
CONCRETE PAD
CHECK VALVE
6" DISCHARGE HEAD
6" BUTTERFLY VALVE
GROUND ELEV. 610'
4"
GROUT
GROUT
26" HOLE
20" CASING
50'
6" SCHD 40 NPT
COLUMN PIPE
17-1/2" HOLE
13-3/8" K-55 54# BT&C
CASING
500'
GRAVEL 70 LF
CEMENT SEAL 10 LF
GRAVEL 10 LF
CEMENT BASKET
SET AT 590'
7' AMSL
TOP OF GROUND WATER
603'
TOP OF PUMP 663'
17-1/2" HOLE
PUMP
PUMP INTAKE 668'
MOTOR
BOTTOM OF PUMP MOTOR
675'
BOTTOM OF CASING 680'
OPEN HOLE 680'-720'
TD 720'
PUNA GEOTHERMAL VENTURE
WATER SUPPLY WELL MW-3
COMPLETION SCHEMATIC
FIGURE NO. 10

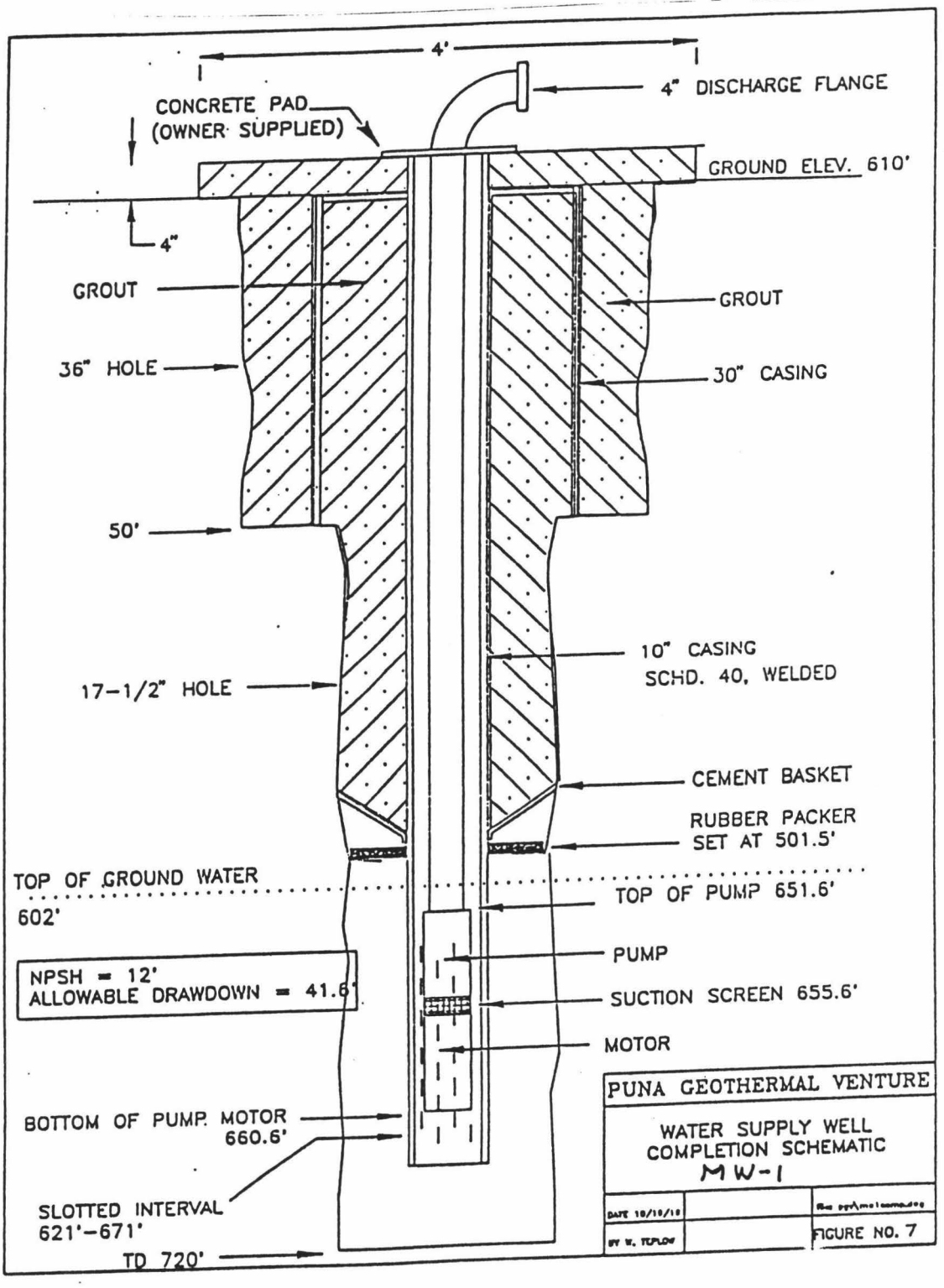
4'
4" DISCHARGE FLANGE
CONCRETE PAD
(OWNER SUPPLIED)
GROUND ELEV. 610'
4"
GROUT
GROUT
36" HOLE
30" CASING
50'
10" CASING
SCHD. 40, WELDED
17-1/2" HOLE
CEMENT BASKET
RUBBER PACKER
SET AT 501.5'
TOP OF GROUND WATER
602'
TOP OF PUMP 651.6'
NPSH = 12'
ALLOWABLE DRAWDOWN = 41.6'
PUMP
SUCTION SCREEN 655.6'
MOTOR
BOTTOM OF PUMP MOTOR
660.6'
SLOTTED INTERVAL
621'-671'
TD 720'
PUNA GEOTHERMAL VENTURE
WATER SUPPLY WELL
COMPLETION SCHEMATIC
MW-1
FIGURE NO. 7

Kapoho Airstrip Well

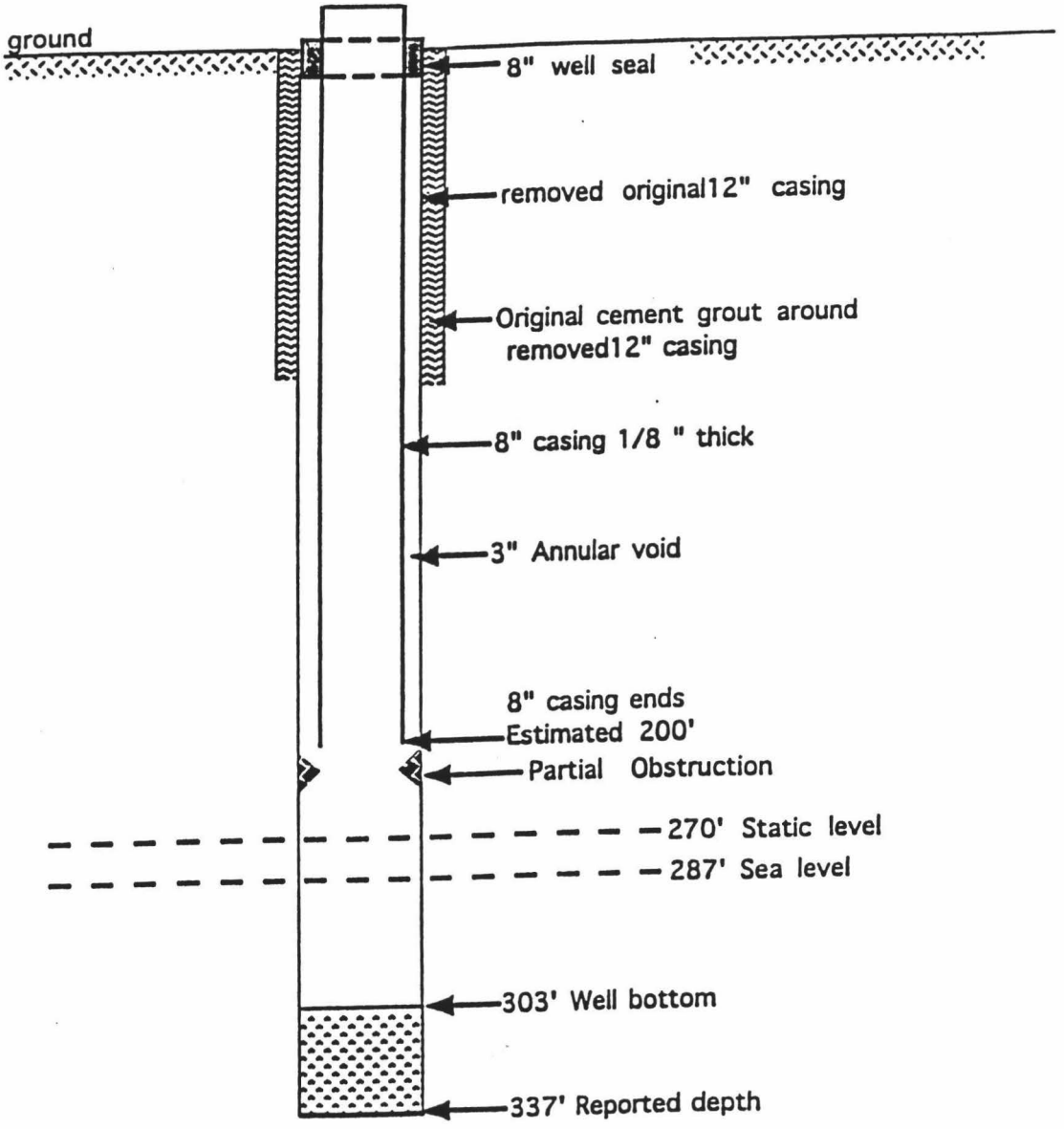

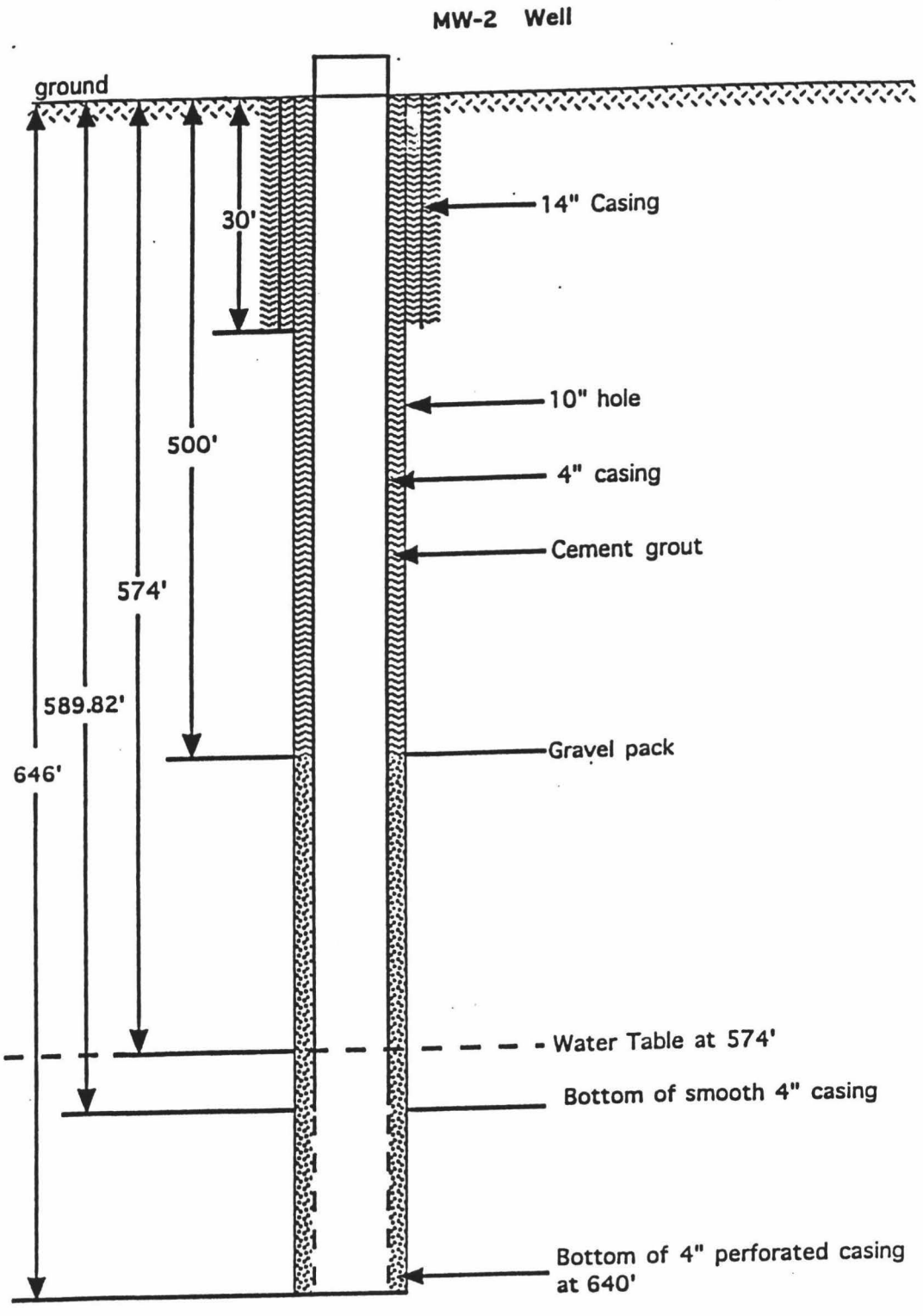
MW-2 Well
ground
30'
500'
574'
589.82'
646'
14" Casing
10" hole
4" casing
Cement grout
Gravel pack
Water Table at 574'
Bottom of smooth 4" casing
Bottom of 4" perforated casing at 640'

POHOIKI WELL NO. 2881-01

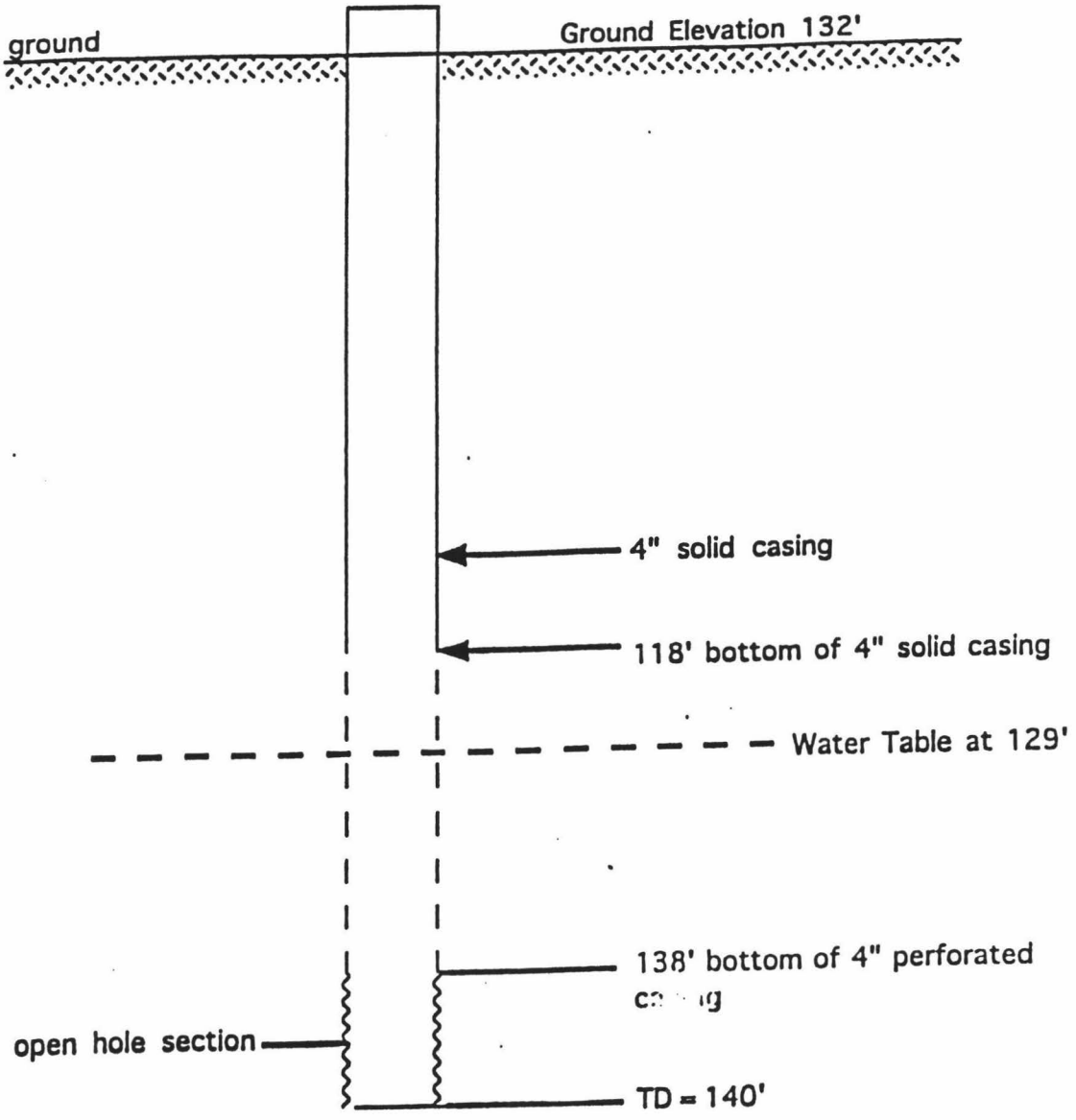

MALAMA-KI EXPLORATORY WELL

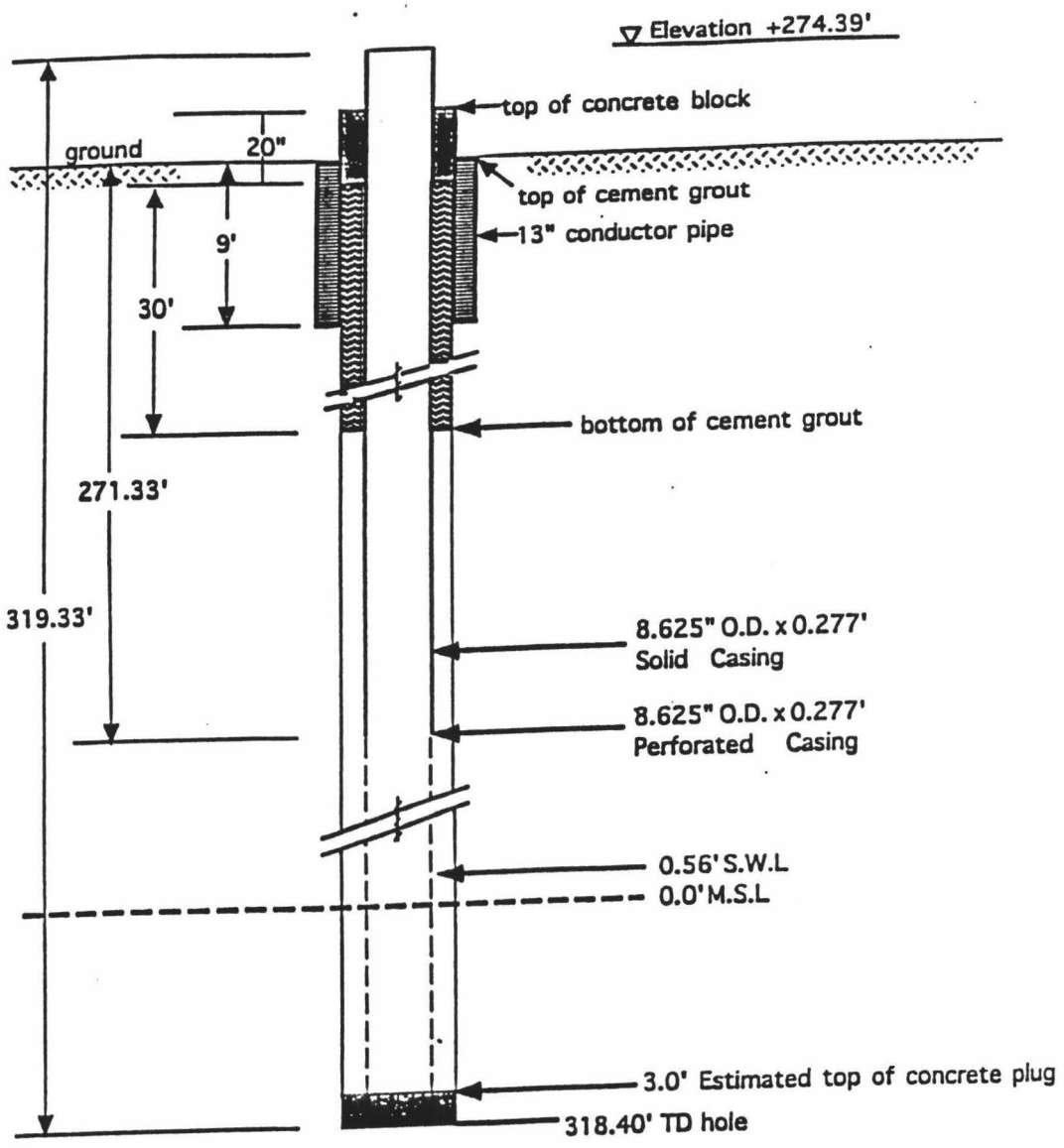

References

Anonymous, 1990, MW-1 Well Completion Report, unpublished technical report, Puna Geothermal Venture, 3 pp.

Anonymous, 1990, MW-2 Well Completion Report, unpublished technical report, Puna Geothermal Venture, 3 pp.

Anonymous, 1990, MW-3 Well Completion Report, unpublished technical report, Puna Geothermal Venture, 3 pp.

Anonymous, 1991, KS-3 Engineering and Geological Report, unpublished technical report, Puna Geothermal Venture, 6 pp.

Anonymous, 1991, KS-4 Engineering and Geological Report, unpublished technical report, Puna Geothermal Venture, 6 pp.

Anonymous, 1991, KS-7 Weekly Drilling Reports, unpublished technical report, Puna Geothermal Venture

Anonymous, 1992, KS-8 Well Completion Report, unpublished technical report, Puna Geothermal Venture, 49 pp.

Anonymous, 1992, Draft Annual Report: Geothermal Resources Assessment, Geothermex, Inc., for Department of Business, Economic Development and Tourism, State of Hawaii, 130 pp.

Anonymous, 1993, KS-9 Well Completion Report, unpublished technical report, Puna Geothermal Venture, 12 pp.

Anonymous, 1993, KS-10 Well Completion Report, unpublished technical report, Puna Geothermal Venture, 12 pp.

Armstead, H. C. H., 1978, Geothermal Energy: Its past, present, and future contributions to the energy needs of man. John Wiley & Sons, New York, 357 pp.

Arnorsson, S., Gronvold, K., and Sigurdsson, S., 1978, Aquifer chemistry of four high-temperature geothermal systems in Iceland, Geochimica et Cosmochimica Acta, vol. 42, p 523 - 536.

Bischoff, J. L. and Seyfried, W. E., 1978, Hydrothermal chemistry of seawater from 25 to 350 C. American Journal of Science, vol. 278, no. 6, p 838-860.

Broyles, M. L., Sugenaga, W. and Furumoto, A. S., 1978, Structure of the lower East Rift Zone of Kilauea volcano, Hawaii, from seismic and gravity data, Journal of Volcanology and Geothermal Research, 5, p 317-336.

Casadevall, T. J. and Hazlett, R. W., 1982, Thermal Areas on Kilauea and Mauna Loa Volcanoes, Hawaii, Journal of Volcanology and Geothermal Research, p 173-188.

Clague, D. A. and Dalrymple, G. B., 1987, The Hawaiian-Emperor Volcanic Chain, Part 1, Geologic Evolution, U.S. Geological Survey Professional Paper 1350, p 5-43.

Cox, M. E. and Thomas, D. M, 1979, Cl/Mg ratio of Hawaiian groundwaters as a regional geothermal indicator in Hawaii, Hawaii Institute of Geophysics Technical Report, HIG-79-9, 51 pp.

Davis, D. A., and Yamanaga, G., 1973, Water resources summary Island of Hawaii, DOWALD, Department of Land and Natural Resources Circular C45, 38 pp.

Delanoy, G., 1993, Analyses of lower Puna well water samples, unpublished technical report for University of Hawaii and DOWALD, Department of Land and Natural Resources, State of Hawaii.

Deymonaz, J., 1991, SOH#4 Summary Report of Drilling Operations, unpublished technical report, 11 pp.

Deymonaz, J., 1991, SOH#1 Summary Report of Drilling Operations, unpublished technical report, 10 pp.

Deymonaz, J., 1992, SOH#2 Summary Report of Drilling Operations, unpublished technical report, 20 pp.

Domenico, P. A., and Schwartz, F. W., 1990, Physical and Chemical Hydrogeology. John Wiley and Sons, New York, p 130.

Druecker, M. and Fan, P. F., 1976, Hydrology and Chemistry of Groundwater in Puna, Hawaii, Groundwater, 14(5), p 328-338.

Eaton, J. P. and Murata, K. J., 1972, in Natural History of Hawaii, How Volcanoes Grow, University of Hawaii Press, Honolulu, Hawaii, 178 pp.

Ellis, A. J., 1970, Quantitative Interpretation of Chemical Characteristics of Hydrothermal Systems, U. N. Symposium on the Development of Geothermal Resources, Vol. 2, p 516-528.

Ellis, A. J. and Mahon, W. A. J., 1964, Natural hydrothermal systems and experimental hot-water/rock interactions, Geochimica et Cosmochimica Acta, Vol. 28, p 1323-1357.

Epp, D., and Halunen, A. J. Jr., 1979, Temperature profiles in wells on the island of Hawaii: Geothermal Resources Exploration in Hawaii, # 7, Prepared for the National Science Foundation, Grant GI-38319, 31 pp.

Facca, G., 1967, The self-sealing geothermal field, Bulletin Volcanologique, Vol. 30, p 271-273.

Fetter, C. W., 1988, Applied Hydrogeology, Merrill Publishing, New York, 592 pp.

Flanigan, V. J. and Long, C. L., 1987, Aeromagnetic and near-surface electrical expression of the Kilauea and Mauna Loa volcanic rift system: in Volcanism in Hawaii: USGS Professional Paper 1350, p 935-946.

Fournier, R. O. and Truesdell, A. H. , 1973, An empirical Na - K - Ca geothermometer for natural waters, Geochimica et Cosmochimica Acta, Vol. #37, p 1255-1275.

Fournier, R. O., White, D. E., and Truesdell, A. H., 1974, Geochemical Indicators of Subsurface Temperature, Part 1, Basic Assumptions, Journal Research U. S. Geological Survey, Vol. 2, # 3, p 259-262.

Fournier, R. O. and Truesdell, A. H., 1974, Geochemical Indicators of Subsurface Temperature, Part 2, Estimation of Temperature and Fraction of Hot Water Mixed with Cold Water, Journal Research U. S. Geological Survey, Vol. 2, # 3, p 263-270.

Furumoto, A. S., 1978, Nature of the magma conduit under the East Rift Zone of Kilauea Volcano, Hawaii, Bulletin of Volcanology, 41, p 435-453.

Giggenbach, W. F., 1987, Geothermal solute equilibria. Derivation of Na-K-Mg-Ca geoindicators, Geochimica et Cosmochimica Acta, Vol. 52, p 2749-2765.

Henderson, P., 1982, Inorganic Geochemistry, Pergamon Press, New York, p 280.

Holcomb, R. T., 1987, Eruptive History and Long-Term Behavior of Kilauea Volcano, U. S. Geological Survey Professional Paper 1350, p 261-350.

Imada, J. A., 1984, Numerical modeling of groundwater in the East Rift Zone of Kilauea Volcano, Hawaii, Unpublished M.S. thesis, University of Hawaii, Honolulu, 102 pp.

Ingebritsen, S. E. and Scholl, M. A., 1993, The Hydrogeology of Kilauea Volcano, Geothermics, vol. 22, No. 4 p 255-270.

Iovenetti, J. L.,. 1990, Shallow Groundwater Mapping in the Lower East Rift Zone Kilauea Volcano, Hawaii, Geothermal Resources Council Transactions, vol. 14, p 699-703.

Juvik, J. O., Singleton, D. C., and Clarke, G. C., 1978, Climate and water balance on the Island of Hawaii. In Mauna Loa Observatory: A 20th Anniversary Report, J. Miller ed. U.S. Dept. of Commerce, NOAA Special Report, p 129-139.

Kanehiro, B. Y. and Peterson, F. L., 1977, Groundwater recharge and coastal discharge for the northwest coast of the island of Hawaii: A computerized water budget approach. Technical Report No. 110, Water Resources Research Center, University of Hawaii, 83 pp.

Keenan, J. H., Keyes, F. G., Hill, P. G., and Moore, J. G., 1969, Steam Tables, Wiley, New York, 162 pp.

Keller, G. V., Grose, L. T., Murray, J. C., and Skokan, C. K., 1979, Results of an experimental drill hole at the summit of Kilauea volcano, Hawaii. Journal of Volcanology and Geothermal Research, vol. 5, p 345-385.

Kestin, J. ed. in chief, 1980, Sourcebook on the Production of Electricity from Geothermal Energy, U.S. Dept. of Energy, Washington D. C., 997 pp.

Kroopnik, P. M., Buddemeier, R. W., Thomas, D., Lau, L. S. and Bills, D., 1978, Hydrology and Geochemistry of a Hawaiian Geothermal System: HGP-A, 64 pp.

Macdonald, G. A. and Abbott, A. T., 1970, Volcanoes in the Sea, University of Hawaii Press, Honolulu, 441 pp.

Macdonald, G. A., Abbott, A. T. and Peterson, F. L., 1983, Volcanoes in the Sea, 2nd ed., University of Hawaii Press, Honolulu, p 238-241.

Mahon, W. A. J., 1975, Review of Hydrogeochemistry of Geothermal Systems-Prospecting, Development, and Use, Second U. N. Symposium on Development and Utilization of Geothermal Resources, Vol. 1, p 775-783.

McDougal, I. and Swanson, P. A., 1972, Potassium-argon ages of lavas from the Hawi and Pololu Volcanic Series, Kohala Volcano, Hawaii, Geological Society of America Bulletin, Vol. 75, p 107-128.

McMurtry, G. M., Fan, P. F. and Copelen, T. B., 1977, Chemical and Isotopic Investigations of Groundwater in Potential Geothermal Areas in Hawaii, American Journal of Science, vol. 277, p 438-458.

Mink, J. F., 1961, Some geochemical aspects of sea water intrusion in an island aquifer. Internat. Assoc. Sci. Hydrology Comm. Subterranean Waters Pub. 52, p 424-439.

Moore, R. B., D. A. Clague, M. Rubin, and W. A. Bohrson, 1987, Volcanism in Hawaii. Hualalai Volcano: a preliminary summary of geologic, petrologic, and geophysical data. U.S. Geol. Surv. Prof. Pap. 1350, p 571-585.

Moore, J. G. and Reed, R. K., 1963, Pillow structure of submarine basalts east of Hawaii, U. S. Geol. Surv. Professional Paper 475-B, p B153-B 157.

Mottl, M. J., and Holland, H. D., 1978, Chemical exchange during hydrothermal alteration of basalt by seawater-I: Experimental results for major and minor components of seawater. Geochimica et Cosmochimica Acta, vol. 42, p 1103-1115.

Mottl, M. J. and Seyfried, W. E., 1980, Subseafloor hydrothermal systems: rock vs. seawater dominated, in Rona, P. A. and Lowell, R. P., eds., Seafloor spreading centers: Hydrothermal Systems: Stroudsberg, Pa., Dowden, Hutchison, and Ross, Inc. 424 pp.

Novak, E. A. and Evans, S. R., 1990, Preliminary Results from Two Scientific Observation Holes on the Kilauea East Rift Zone, Transactions, Geothermal Resources Council, vol. 15, p 187-193.

Novak, E. A., Trusdell, F. A. and Evans, S. R., 1991, Scientific Observation Holes #4, #1, and #2 Core Logs, unpublished data, 2000 pp.

Peterson, D. W., and Moore, R. B., 1987, Geologic History and Evolution of Geologic Concepts, Island of Hawaii, U. S. Geological Survey Professional Paper 1350, p 149-186.

Porter, S. C., 1979, Quaternary stratigraphy and chronology of Mauna Kea, Hawaii: a 380,000-yr record of mid-Pacific volcanism and ice-cap glaciation. Geol. Soc. Am. Bull. 90, p 980-1093.

Ruffner, J. A., 1980, Climates of the States, NOAA Narrative Summaries, Tables and Maps for Each State, Gale Research Co., vol. 1, p 181-206.

Schofield, J. C., 1956, Methods of distinguishing sea-groundwater from hydrothermal water, New Zealand Journal of Science and Technology, vol. 37, #5, p 597 - 602.

Scholl, M., Ingebritsen, S., Janik, C., Fahlquist, L., Kauahikaua, J., and Trusdell, F., 1992, Geochemical and stable isotope and chemical composition of surface water, groundwater, and precipitation - Kilauea Volcano area, Hawaii--preliminary results (abstr.), Eos, Transactions of the American Geophysical Union, Fall Meeting Supplement, p 161.

Seyfried, W. E. and Bischoff, J. L., 1979, Low temperature basalt alteration by seawater, an experimental study at 70 C and 150 C. Geochimica et Cosmochimica Acta, vol. 43, p 1937-1947.

Sorey, M. L., and Colvard, E. M., 1993, Potential for impacts from the Hawaii Geothermal Project on ground-water resources, U.S.G.S. Water Resources Investigations Report 93-XXXX, 22 pp.

Stearns, H. T. and Macdonald, G. A., 1946, Geology and groundwater resources of the island of Hawaii: Honolulu, Hawaii Div. of Hydrography Bull. 9, 363 p.

Swain, L. A., 1973, Chemical quality of ground water in Hawaii: U. S. Geological Survey Report R48, prepared in cooperation with the Hawaii Division of Water and Land Development, Dept. of Land and Natural Resources, 54 pp.

Takasaki, K. J., 1978, Summary appraisals of the Nation's groundwater resources -- Hawaii region, Department of the Interior, Geologic Survey Professional Paper 813-M, 29 pp.

Thomas, D. M., 1985, Characteristics of the geothermal resource associated with the volcanic systems in Hawaii, Geothermal Resources Council Transactions, vol. 9 - Part II, p 417-422.

Thomas, D. M., 1986, Geothermal Resource Assessment in Hawaii, Geothermics, Vol. 15, #4, p 435-514.

Thomas, D. M.,1987, A Geochemical Model of the Kilauea East Rift Zone, U. S. Geological Survey Professional Paper 1350, p 1507-1525.

Thomas, D. M., Cox, M., Erlandson, D., and Kajiwara, L., 1979, Potential Geothermal Resources in Hawaii: a Preliminary Regional Survey, Hawaii Institute of Geophysics, 31 pp.

Thomas, D. M., manuscript, The Hydrogeochemistry of Kilauea Volcano, 50 pp.

Tomasson, J., and Kristmannsdottir, H., 1972, High temperature alteration minerals and thermal brines, Rekjanes, Iceland, Contributions to Mineralogy and Petrology, 36, p 123-134.

Truesdell, A. H., and Fournier, R. O., 1975, Calculation of Deep Temperatures in Geothermal Systems from the Chemistry of Boiling Spring Waters of Mixed Origin, Second U. N. Symposium Proceedings, Vol. 1, p 837-844.

Truesdell, A. H., and Fournier, R. O., 1977, Procedure for Estimating the Temperature of a Hot-Water Component in a Mixed Water by Using a Plot of Dissolved Silica Versus Enthalpy, Journal Research U. S. Geological Survey, Vol. 5 # 1, p 49-52.

Walker, G. P. L., 1990, Geology and Volcanology of the Hawaiian Islands, Pacific Science, Vol. 44, # 4, p 315-347.

Werner, P. W., and Noren, D., 1951, Progressive waves in nonartesian aquifers. Transactions of the American Geophysical Union, 32 (2), p 238-244.

Zablocki, C. J., 1978, Streaming Potentials Resulting from the Descent of Meteoric Water--A Possible Source Mechanism for Kilauean Self-Potential Anomalies, Geothermal Resources Council Transactions, Vol. 2, p 747 - 748.